

Assessing tRNA sequence flexibility using
semi *de novo* designed nonsense suppressor tRNAs

DISSERTATION

Zur Erlangung des akademischen Grades

“Doctor rerum naturalium“

Dr. rer. nat.

Eingereicht an der

Fakultät für Mathematik, Informatik

und Naturwissenschaften der Universität Hamburg

Vorgelegt von

Suki Albers, M.Sc.

Hamburg

Juni 2019

Die vorgelegte Arbeit wurde von Mai 2015 bis März 2019 am Institut für Biochemie und Molekularbiologie der Universität Hamburg unter Anleitung von Frau Prof. Dr. Zoya Ignatova durchgeführt.

Datum der Freigabe der Dissertation zur Veröffentlichung: 20.09.2019

Gutachter: Prof. Dr. Zoya Ignatova

Prof. Dr. Mario Mörl

CONTENTS

LIST OF ABBREVIATIONS	XIII
1 SUMMARY	1
2 ZUSAMMENFASSUNG	3
3 INTRODUCTION	5
3.1 Translation in prokaryotes.....	5
3.2 Transfer RNAs and their structure	7
3.3 Aminoacylation of tRNAs by aminoacyl-tRNA synthetases and their recognition elements.....	12
3.4 EF-Tu binding affinity is mediated by the tRNA sequence and its esterified amino acid	13
3.5 The role of EF-P in translation.....	16
3.6 Nonsense suppressor tRNAs	16
3.6.1 Nonsense suppressor tRNA designs	18
3.6.2 Applications of nonsense suppressor tRNAs.....	19
3.7 Factors modulating nonsense suppression efficiency	21
4 AIM OF THE THESIS	27
5 RESULTS	28
5.1 Nonsense suppressor tRNA designs.....	28
5.2 <i>In vitro</i> aminoacylation levels vary between the designed tRNAs	30
5.3 Editing of the tRNA anticodon region barely influences aminoacylation levels	34
5.4 Assessing tRNA functionality by GFP read-through assay	35
5.5 <i>In vitro</i> translation reactions show the importance of tRNA modifications	37
5.6 0.05% (v/v) L-arabinose induces maximal GFP expression of pBAD33 vectors expressed in XL1-blue cells	38

5.7	The natural read-through of termination codons in XL1-blue cells decreases in the order TAG>TGA~TAA	39
5.8	tRNA expression reduces cell growth	41
5.9	Nonsense suppressor tRNAs derived from native tRNA ^{Ala} promote read-through of PTCs.....	43
5.10	Anticodon-edited tRNAs do not promote nonsense suppression.....	44
5.11	The TΨC-stem is the main determinant of nonsense suppression	46
5.12	Incorporation of A37 and variable loop extensions reduce nonsense suppression levels.....	49
5.13	Design DTS2 is the most active nonsense suppressor tRNA.....	52
6	DISCUSSION	56
6.1	3'-Heterogeneity and dimerization reduces tRNA aminoacylation levels	56
6.2	Natural nonsense suppressor tRNAs read through stop codons.....	58
6.3	Nonsense suppression levels are strongly influenced by codon context.....	58
6.4	Post-transcriptional modifications are important for tRNA's nonsense suppressor functionality	60
6.5	The anticodon stem-loop is not the main determinant of nonsense suppression efficiency.....	60
6.6	The TΨC-stem is the main determinant of nonsense suppression	63
6.7	Incorporation of A37 and variable loop extensions reduce nonsense suppression.	65
6.8	Additional base substitutions could further increase nonsense suppression efficiency.....	67
6.9	Application of designed nonsense suppressor tRNAs.....	68
7	CONCLUSION	70
8	MATERIALS AND METHODS	71
8.1	Materials.....	71
8.1.1	Enzymes	71
8.1.2	Kits	71

8.1.3	Reagents	72
8.1.4	Antibodies.....	72
8.1.5	Vectors.....	72
8.1.6	<i>E. coli</i> cell strains	73
8.1.7	Oligonucleotides.....	73
8.1.8	Buffers	77
8.2	Methods.....	82
8.2.1	Cloning and transformation.....	82
8.2.2	Growth curves	82
8.2.3	tRNA design.....	83
8.2.4	<i>In vitro</i> T7 transcription.....	83
8.2.5	tRNA folding.....	84
8.2.6	Fluorescent labeling of tRNAs	84
8.2.7	<i>In vitro</i> aminoacylation.....	84
8.2.8	Purification and enrichment of His-tagged <i>E. coli</i> Alanyl-tRNA synthetase	84
8.2.9	Preparation of <i>E. coli</i> S30 cell-free expression system	85
8.2.10	<i>In vitro</i> translation	86
8.2.11	Immunoblotting	86
8.2.12	Northern blotting	86
8.2.13	Fluorescence intensity measurements	87
8.2.14	FACS.....	87
9	REFERENCES	88
10	SUPPLEMENTARY INFORMATION	111
10.1	Supplementary Figures.....	111
10.2	List of substances used in this study	113
11	ACKNOWLEDGEMENTS	117
12	EIDESSTATTLICHE VERSICHERUNG	118

LIST OF ABBREVIATIONS

30S IC	30S initiation complex
A	Adenine
aaRS	Aminoacyl-tRNA synthetase
aa-tRNA	Aminoacyl-tRNA
AlaRS	Alanyl-tRNA synthetase
A-site	Aminoacyl site
ASL	Anticodon stem-loop
bp	Base pair
C	Cytosine
EF	Elongation factor
EF-P	Elongation factor P
EF-Tu	Elongation factor thermo unstable
eGFP	Enhanced green fluorescent protein
E-site	Exit site
G	Guanine
GFP	Green fluorescent protein
GTP	Guanosine triphosphate
IF	Initiation factor
LB medium	Luria-Bertani medium
<i>Mj</i>	<i>Methanocaldococcus jannaschii</i>
mRNA	Messenger RNA

ncAA	Non-canonical amino acid
nt	nucleotide
PAGE	Polyacrylamid gel electrophoresis
P-site	Peptidyl site
PTC	Premature termination codon
PTMs	Post-transcriptional modifications
RF	Release factor
RNA	Ribonucleic acid
rRNA	Ribosomal RNA
T	Thymine
tRNA	Transfer RNA
U	Uracil

1 SUMMARY

Nonsense suppressor tRNAs are useful tools in understanding tRNA functionality and evolutionary constraints of this commonly shaped molecule. In contrast to native elongator tRNAs, competition with other tRNA isodecoders is abolished in cells lacking natural nonsense suppressor tRNAs. Thus, evaluation of single nucleotide as well as whole motif swaps on the performance of tRNA in translation is facilitated. This study aims at identifying nucleotides or regions that are major determinants of the functionality of nonsense suppressor tRNAs. Nonsense suppressor tRNA construction started with a semi *de novo* design, which preserved recognition elements for *E. coli* Alanyl-tRNA synthetase, bases involved in tertiary interactions defined from the crystal structure of unmodified *E. coli* tRNA^{Phe} and a stop anticodon. The other bases were chosen to match the highest probability to form the cloverleaf secondary structure. The resulting designs n1-n6, even though aminoacylated, except n2, proved to be non-functional. Interestingly, n2 contained the G3-U70 wobble base pair, which serves as main identity element of tRNA^{Ala}, but could not be charged with Ala. Exchange of the 6-67 and/or 7-68 base pair of n2 reestablished recognition by AlaRS.

An investigation of the anticodon loop of native elongator tRNAs from different species has shown that nucleotides surrounding the anticodon triplet are rather conserved. Subsequent nucleotide exchanges of the anticodon loop according to the most frequent bases occurring in these positions, led to the designs n1A1-n1A3 and n3A1-n3A3. However, the resulting nonsense suppressor tRNA designs did also not promote stop codon read-through. In contrast, tRNA^{Ala}(UCA(U)), generated by replacing the anticodon triplet of a native tRNA^{Ala}(UGC) isoacceptor by the opal stop anticodon, promoted GFP expression. This suggested that the anticodon context of tRNA^{Ala}(UCA(U)) might be more suitable for nonsense suppression. Thus, designs n1A3_A37-n1A5 were produced by exchanging the anticodon loop of n1A3 with that found in tRNA^{Ala}(UCA(U)). Again, nonsense suppression levels were close to background values. All attempts to increase nonsense suppression by anticodon loop exchanges

were unsuccessful. This suggested that other tRNA regions than the anticodon were responsible for the lack of functionality.

During translation elongation, tRNAs are delivered to the ribosomal A-site as a ternary complex with EF-Tu and GTP. EF-Tu binding is finely tuned for a specified tRNA body and its esterified amino acid in order to achieve uniform binding of elongator tRNAs. The binding affinity of tRNAs to EF-Tu is mainly determined by the three T Ψ C-stem base pairs 49-65, 50-64, 51-63. Because all designs contained recognition elements of Alanyl-tRNA synthetase and thus, should be aminoacylated with Ala, the T Ψ C-stem base pairs of native tRNA^{Ala}(UGC) were inserted into n1A3. Interestingly, the resulting design TS1 did not promote nonsense suppression. A further increase in EF-Tu binding affinity was achieved by substituting the T Ψ C-stem base pairs with that found in tRNA^{GluE2}. Design TS2 served as active nonsense suppressor tRNA, reaching $8.7 \pm 0.9\%$ suppression, as compared to the wildtype GFP. Combinatorial insertion of the D-region and T Ψ C-stem base pairs of tRNA^{Pro1} and tRNA^{GluE2}, respectively, increased read-through levels to $15.2 \pm 2.4\%$, which were higher than those observed for tRNA^{Ala}(UCA(U)) with $12.3 \pm 3.4\%$. Incorporation of only the D-region of tRNA^{Pro1} into n1A3, design D1, showed nonsense suppression near to the background level. Increase of the variable region of TS2 and DTS2, e.g. similar to that found in *E. coli* tRNA^{Sec}, abolished nonsense suppression, while substitution of G37 by A37 was lethal to *E. coli* cells.

Taken together, the results show that incorporation of the T Ψ C-stem base pairs of tRNA^{GluE2} and therefore high EF-Tu binding affinity promoted PTC read-through of the semi *de novo* designed nonsense suppressor designs used in this study. In contrast to previous studies, editing of the anticodon region or extension of the variable region did not stimulate nonsense suppression. Thus, the T Ψ C-stem exhibited the largest effect on the nonsense suppression efficiency, while other tRNA regions, such as the D-region, rather fine-tuned the read-through levels.

2 ZUSAMMENFASSUNG

Nonsense Suppressor tRNAs sind wertvolle Werkzeuge, um die Funktionalität und evolutionäre Antriebskraft zur Ausbildung der L-Struktur von tRNAs zu untersuchen. Im Gegensatz zu natürlichen Elongator tRNAs besteht in Zellen, die keine natürlichen Suppressor tRNAs exprimieren, keine Konkurrenz zu anderen tRNA Isodekodern. Dies erleichtert es, den Einfluss des Austausches einzelner Nukleotide sowie ganzer Motive auf die Partizipation von tRNAs in der Proteinbiosynthese zu evaluieren. Das Ziel dieser Studie ist es, Nukleotide oder Regionen, welche die Funktionalität von Nonsense Suppressor tRNAs maßgeblich beeinflussen, zu identifizieren. Die Konzeption der Nonsense Suppressor tRNAs begann mit einem semi *de novo* Design. Dies beinhaltete Erkennungselemente von *E. coli* Alanyl-tRNA Synthetase, Basen, die in tertiären Interaktionen involviert sind und anhand der Kristallstruktur der unmodifizierten *E. coli* tRNA^{Phe} identifiziert wurden, sowie das Stop Anticodon. Die verbliebenen Basen wurden entsprechend der höchsten Wahrscheinlichkeit zur Ausbildung der Kleeblatt tRNA Sekundärstruktur ausgewählt. Die resultierenden Designs n1-n6, wurden zwar aminoacyliert, mit Ausnahme von n2, waren jedoch nicht funktionell. Interessanterweise beinhaltete n2 das Haupterkennungselement von tRNA^{Ala}, das G3-U70 Wobble Basenpaar, wurde jedoch trotzdem nicht mit Ala beladen. Substituierung des 6-67 und/oder 7-68 Basenpaares stellte die Beladung durch AlaRS wieder her.

Eine Untersuchung von nativen Elongator tRNAs aus verschiedenen Organismen hat gezeigt, dass die Nukleotide innerhalb der Anticodonschleife, mit Ausnahme des Anticodon-Triplets, eher konserviert sind. Subsequenter Austausch der Nukleotide in der Anticodonschleife von n1 und n3 durch Nukleotide, die mit den höchsten Häufigkeiten an den entsprechenden Positionen vorkommen, führte zu den Designs n1A1-n1A3 und n3A1-n3A3. Die erhaltenen Designs waren jedoch inaktiv als Nonsense Suppressoren. Im Gegensatz dazu führte tRNA^{Ala}(UCA(U)), erhalten durch Transplantation des Opal Anticodon-Triplets in native tRNA^{Ala}(UGC), zu GFP Expression. Dies ließ vermuten, dass der Anticodon Kontext von tRNA^{Ala}(UCA(U)) geeigneter ist für die Nonsense Suppression. Somit wurden durch Aus-

tausch der Anticodonschleife von n1A3 entsprechend zu tRNA^{Ala}(UCA(U)) die Designs n1A3_A37-n1A5 generiert. Jedoch waren die Nonsense Suppression Level dieser Designs nicht höher als der Hintergrund, gemessen in Abwesenheit von Nonsense Suppressor tRNAs. Alle Versuche, die Nonsense Suppression durch Änderungen innerhalb der Anticodonschleife der tRNA herzustellen, waren nicht erfolgreich. Dies zeigte, dass andere tRNA Regionen für die mangelnde Funktionalität verantwortlich sind.

Während der Elongation der Translation werden tRNAs in Form eines ternären Komplexes mit EF-Tu und GTP zur ribosomalen A-Stelle transportiert. Die Bindungsaffinität einer tRNA mit seiner esterifizierten Aminosäure zu EF-Tu ist ausbalanciert, um eine uniforme Bindung von Elongator Aminoacyl-tRNAs während der Translation zu ermöglichen. Die Bindung von aa-tRNAs zu EF-Tu wird hauptsächlich durch die Sequenz der drei TΨC-Stamm Basenpaare 49-65, 50-64, 51-63 determiniert. Da alle Designs die Erkennungselemente für die Beladung durch Alanyl-tRNA Synthetase beinhalteten und daher mit Ala beladen werden sollten, wurden die drei TΨC-Stamm Basenpaare von nativer tRNA^{Ala}(UGC) in n1A3 transplantiert. Interessanterweise führte das resultierende Design TS1 nicht zur Suppression von Stop Codons. Eine weitere Erhöhung der Bindungsaffinität zu EF-Tu wurde durch Substituierung der TΨC-Stamm Basenpaare von n1A3 durch solche präsent in tRNA^{GluE2} erreicht. Das Design TS2 fungierte als aktive Nonsense Suppressor tRNA mit Suppressionslevels von $8.7 \pm 0.9\%$ im Vergleich zu Wildtyp GFP. Gemeinsame Insertion der D-Region von tRNA^{Pro1} und der TΨC-Stamm Basenpaare von tRNA^{GluE2}, wie in DTS2, erhöhte das Nonsense Suppression Level auf $15.2 \pm 2.4\%$, welches höher war als das von tRNA^{Ala}(UCA(U)) mit $12.3 \pm 3.4\%$. Inkorporierung der D-Region alleine, Design D1, zeigte Nonsense Suppression ähnlich zum Hintergrund Level. Eine Verlängerung der variablen Region von TS2 und DTS2, z.B. ähnlich wie präsent in *E. coli* tRNA^{Sec}, hob die Nonsense Suppression wieder auf. Substituierung von G37 durch A37 innerhalb von TS2 und DTS2 war letal für die *E. coli* Zellen.

Zusammengefasst zeigen die Ergebnisse, dass die Inkorporierung der TΨC-Stamm Basenpaare von tRNA^{GluE2} und daher eine starke Bindungsaffinität zu EF-Tu sich positiv auf die Funktionalität der in dieser Studie verwendeten semi *de novo* designten Nonsense Suppressor tRNAs auswirkte. Im Gegensatz zu vorherigen Studien erhöhten Veränderungen innerhalb der Anticodonregion oder eine Verlängerung der variablen Region die Nonsense Suppressionslevel nicht. Somit bestimmte der TΨC-Stamm die Nonsense Suppressionseffizienz maßgeblich, während andere tRNA Regionen, wie z.B. die D-Region, eher zum Fine Tuning der Nonsense Suppressionslevel beigetragen haben.

3 INTRODUCTION

3.1 Translation in prokaryotes

The final and most energy consuming step in the flow of information from DNA to proteins is translation. During translation, amino acids specified by mRNA codons are covalently linked to each other to generate proteins. Protein synthesis is catalyzed by a macromolecular ribonucleoprotein complex, the ribosome, which is assisted by multiple translation factors in each step of this process. The ribosome is composed of >50 ribosomal proteins and three ribosomal RNAs. While ribosomal proteins mainly serve as scaffold and are essential for structure and stability [1], the RNA entity exerts the catalytic activity [2]. The prokaryotic ribosome is composed of two subunits, the small 30S subunit, involved in decoding the triplet code of mRNA, and the large 50S subunit responsible for peptidyl transfer. 16S rRNA is part of the 30S subunit, whereas 5S and 23S rRNA belong to the 50S subunit (reviewed in [3–6]). Both subunits together build the translation competent 70S ribosome with three tRNA binding sites: the A- (aminoacyl), P- (peptidyl) and E- (exit) site [7–9]. The process of translation can be divided into four subsequent phases: initiation, elongation, termination and ribosome recycling (Figure 1) [10].

Translation begins with the formation of 30S initiation complex (30S IC) composed of the initiation factors IF1, IF2, IF3, the initiator tRNA fMet-tRNA^{fMet} and the mRNA (reviewed in [11]). Hybridization of the Shine-Dalgarno sequence to a complementary sequence located at the 3'-end of 16S rRNA aids to position the start codon, most commonly AUG, in the ribosomal P-site [12–14]. IF1 accommodates the ribosomal A-site and is suggested to guide fMet-tRNA^{fMet} to the P-site and thus, in contrast to elongator aa-tRNAs, hinders its association with the A-site [15–17]. fMet-tRNA^{fMet} binding to the ribosome is promoted by IF2·GTP [18]. The presence of the N-Formyl-methionine moiety promotes IF2·GTP binding [19] and reduces the tRNA affinity to elongation factor EF-Tu [20]. With its proofreading activity, IF3 samples mismatched codon-anticodon interactions and consequently destabilizes 30S ICs [21–23]. Upon cognate codon-anticodon in the ribosomal P-site and promoted by IF2, the 50S subunit

joins the 30S IC [24]. IF2-bound GTP is hydrolyzed to GDP and Pi, and all three initiation factors IF1, IF2, IF3 dissociate from the ribosome [25]. The precise order of events is still under debate. A recent cryo-EM study has suggested that after subunit joining, GTP on IF2 is hydrolyzed, followed by dissociation of IF1 from the ribosome. Consequently, IF2 repositions on the ribosome and after the release of Pi dissociates from the ribosomes in complex with GDP. While IF3 was not included in the ribosome assembly reaction, previous studies have shown that IF3 dissociates either prior to or shortly after subunit joining [26].

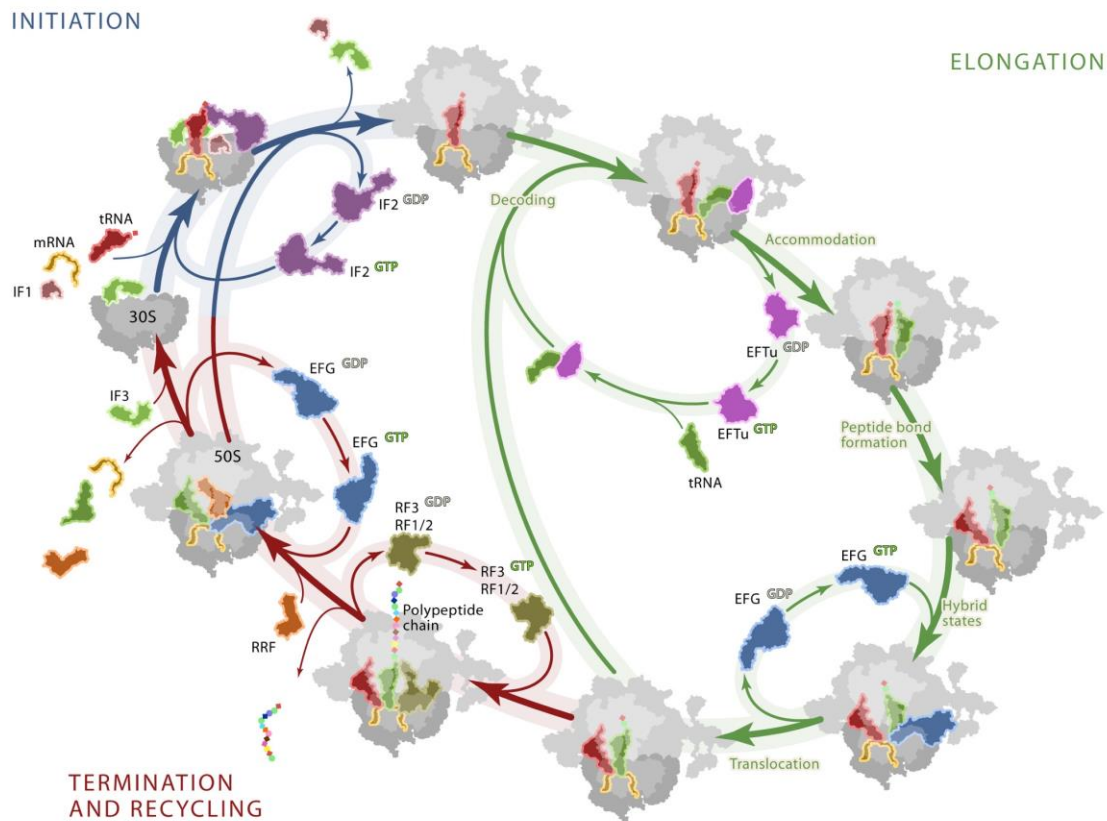


Figure 1: Schematic presentation of the prokaryotic translation cycle. Translation can be divided into initiation, elongation, termination/release and recycling and involves multiple factors (adopted from [10]).

Elongation competent 70S ribosomes possess fMet-tRNA^{fMet} in ribosomal P-site and an empty A-site. Aa-tRNAs are delivered to the ribosomal A-site as ternary complex with EF-Tu-GTP by diffusion [27–31]. Correct codon-anticodon base pairing triggers the dissociation of EF-Tu-GDP following GTP hydrolysis. The guanine nucleotide exchange factor EF-Ts recycles EF-Tu-GTP [32]. The 3'-acceptor arm of aa-tRNA enters the peptidyl transferase center of the 50S subunit. Peptide bond formation, catalyzed by 23S rRNA, results in a deacylated tRNA in the P-site and peptidyl-tRNA, extended by one amino acid, in the A-site [33–35]. GTP hydrolysis by EF-G promotes translocation of the P- and A-site tRNA to the E- and P-site,

respectively, in conjunction with advance of mRNA by one codon [29,36,37]. The A-site can be accommodated by the next aminoacyl-tRNA and deacylated tRNA dissociates from ribosomal E-site [7,8,38], allowing a new cycle of elongation with each cycle leading to extension of nascent polypeptide by one amino acid. Occurrence of one of the three stop codons (UAA, UAG, UGA) in the ribosomal A-site leads to termination of translation and the release of the synthesized polypeptide from the ribosome. In general, no aa-tRNA with an anticodon complementary to the stop codon on the mRNA is available. Instead, termination codons are recognized by release factors (RFs). Depending on the nature of the stop codon recognition occurs by either RF1 or RF2. While RF1 recognizes UAA and UAG codons, RF2 binds to UAA and UGA codons [39,40]. Upon release factor binding, the nascent polypeptide chain is transferred from the P-site tRNA to a water molecule and thus, the newly synthesized polypeptide is released from the ribosome [41–46]. The universally conserved GGQ motif of RFs is essential for promoting the hydrolysis reaction which leads to peptide dissociation [47]. RF3 promotes dissociation of RF1 or RF2 from the ribosome [48–51] and after GTP hydrolysis leaves itself [52]. In this post termination complex, deacylated tRNA in the P-site and likely E-site and the mRNA are still associated with ribosome. Ribosome recycling is mediated by the three factors RRF, EF-G and IF3, which dissociate the deacylated tRNA and mRNA and disassemble 70S ribosomes into its subunits and thus, enables a new round of translation (reviewed in [53]).

3.2 Transfer RNAs and their structure

tRNAs play a central role in translation by recognizing mRNA codons and delivering the specified amino acids to the ribosome in order to be incorporated into the growing polypeptide chain. Cytoplasmic tRNAs adopt a secondary cloverleaf structure (Figure 2), which is composed of four helical stems and three hairpin loops plus an additional variable arm, depending on the tRNA identity sometimes viewed as the 4th loop (reviewed in [54,55]). The four tRNA helices are designated as acceptor stem, D-stem, anticodon stem and TΨC-stem, with the latter three being associated with their corresponding loops. tRNA length lies between ~72 nt to 95 nt, due to the varying number of nucleotides found within the dihydrouridine loop (D-loop) and variable arm (v-arm) [56]. With respect to the length of the variable arm, tRNAs are classified as class I or II. While class I tRNAs are characterized by a small variable arm consisting of 4-5 nt, as present in the majority of tRNAs, those displaying an increased length of the v-arm are viewed as class II tRNAs. The latter includes tRNA^{Leu},

tRNA^{Ser} and tRNA^{Tyr} (tRNA database, <http://trna.bioinf.uni-leipzig.de/>). During decoding, the three nucleotides found at positions 34-36 within the anticodon loop base pair with the mRNA codon. Thus, codon-anticodon interactions specify which amino acid is inserted into the growing polypeptide chain. Position 34 is referred to as the wobble position because base pairing in this position is not restricted to Watson-Crick base pairs, enabling one and the same tRNA to read multiple mRNA codons (reviewed in [57]). At the 3'-terminus tRNAs possess a single stranded 3'-NCCA sequence, which is required for aminoacylation. N73 displays the so-called discriminator base, which can be composed of any of the four nucleotides and often serves as an important determinant for aminoacylation [58–61]. The esterified amino acid is covalently attached to the ribose of the 3'-terminal adenosine of the tRNA [62]. The 3'-CCA end also aids in positioning the ternary complex in the ribosomal A-site and in the release of the newly synthesized polypeptide from the ribosome (reviewed in [63]). Deviations from the cloverleaf structure have been found in many mitochondrial tRNAs, which in some cases completely lack the D- or TΨC-arm (reviewed in [64–66]).

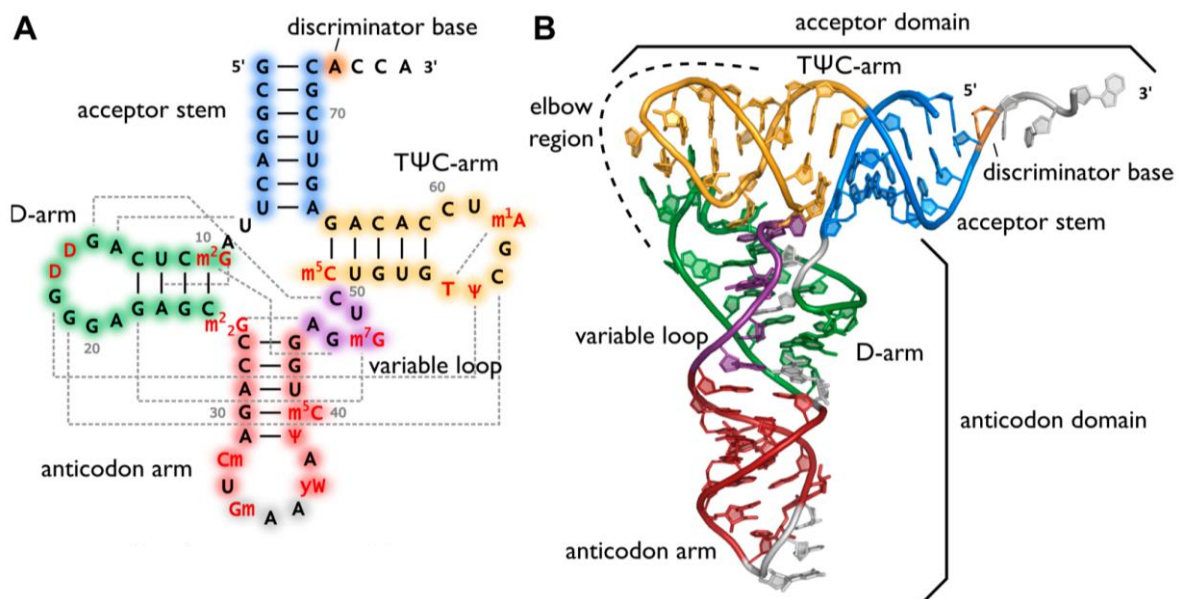


Figure 2: tRNA secondary (A) and tertiary structure (B). The cloverleaf secondary structure (A) and L-shaped tertiary structure (PDB ID: 1EHZ) (B) of cytosolic *S. cerevisiae* tRNA^{Phe} with the acceptor stem (blue), the discriminator base (orange), the single-stranded 3'-CCA terminus, the TΨC-arm (yellow), the variable arm (purple), the anticodon arm (red) with the anticodon triplet (grey) and the D-arm (green). Tertiary interactions are indicated by grey dashed lines (adopted from [63]).

To date, many crystal structures of “free” cytosolic tRNAs are available, identifying a network of nine conserved tertiary interactions involving conserved and semi-conserved nucleotides that mediate the formation of the L-shaped tRNA tertiary structure [56,67–75]. Within the L-shape, base stacking of two helical domains leaves them in a perpendicular ar-

rangement. The D- and anticodon stem as well as the acceptor and T Ψ C-stem regions together each form one of arm of the “L”. Interactions between the T Ψ C- and D-loop mediate the formation of the tRNA “elbow” and thus, stabilize joining of the two helical arms. This arrangement positions two functional important centers of tRNAs, the 3'-CCA terminus with attached peptidyl- or aminoacyl moiety as well as the anticodon, at opposing sites enabling simultaneous contact to the peptidyl transferase center of the 50S ribosomal subunit and the mRNA within the 30S decoding site, respectively. Formation of tertiary structure is stabilized by coaxial stacking and base pairing. Besides canonical Watson-Crick base pairing, tRNA architecture is achieved by a number of non-standard base pairs and base triples. The most prominent base combinations mediating tertiary interactions within class I cytoplasmic tRNAs can be found in Table 1 [76].

Table 1: Most frequent base combinations involved in tertiary interactions in class I cytosolic tRNAs.

tRNA positions	Involved Nucleotides	Occurrence	PDB	Base pairing	Type of Interaction
8-14-21	U-A-A	82%	1ehz	U8-A14 A14-A21	Reverse Hoogsteen
9-12-23	A-U-A	46%	1ehz	U12-A23 A9-A23	Watson Crick N7-amino, symmetric
10-25-45	G-C-G	35%	1ffy	G10-C25 G10-G45	Watson Crick
	m ² G-C-G	25%	1ehz	m ² G10-C25 m ² G10-G25	Watson Crick
13-22-46	C-G-m ⁷ G	49%	1ehz	C13-G22 G22-m ⁷ G46	Watson Crick N7-imino
	C-G-G	9%	1j1u	C13-G22 G22-G46	Watson Crick N7-imino
15-48	G-C	50%	1ehz	G15-C48	Reverse Watson Crick
18-55	G- Ψ	94%	1ehz	G18- Ψ 55	bifurcated
	G-U	19%	1j1u	G18-U55	bifurcated
19-56	G-C	99%	1ehz	G19-C56	Watson Crick
26-44	m ² G-A	25%	1ehz	m ² G26-A44	Imino
	G-A	12%	1j1u	G26-A44	Imino
54-58	T-A	31%	1c0a	T54-A58	Reverse Hoogsteen
	T-m ¹ A	23%	1ehz	T54-m ¹ A58	Reverse Hoogsteen
	U-A	9%	1j1u	U54-A58	Reverse Hoogsteen
	U-m ¹ A	6%		U54-m ¹ A58	Reverse Hoogsteen

As evident from Table 1, some nucleotides involved in tertiary interactions are highly conserved, while other positions are more flexible with regard to nucleotide identity. Highly conserved nucleotides include U8, A14, G18, G19, A21, T54, Ψ55, C56 and A58 [76]. In the following, tertiary interactions will be viewed in more detail using the well-studied yeast tRNA^{Phe} (PDB: 1EHZ) as example [70]. The majority of tertiary interactions can be mapped to the core region of the tRNA, consisting of the D- and v-arm. Base triples are formed at positions A9-U12-A23, C13-G22-m⁷G46 and m²G10-C25-G45 in which a nucleotide located within the D- or v-arm interacts with a canonical Watson-Crick base pair of the D-stem. Another base triple is formed at positions U8-A14-A21, where A21 interacts with the *trans* Hoogsteen base pair U8-A14, linking the acceptor helix and D-arm. An unusual m²G-A imino base pair at position 26 and 44 located at the junction between D- and anticodon-stem is present.

Interactions that mediate the formation of the tRNA elbow, also referred to as the DT-region, have been shown to be major force in joining both L-arm helices. The highly conserved *trans* Watson-Crick base pair G15-C48, known as the Levitt pair, connects the D- and variable loop and stacks with the U8-A14 reverse Hoogsteen base pair. Mutation of the Levitt base pair in yeast tRNA^{Phe} has been shown to abolish joining of the D- and TΨC-arm [77]. Thus, the Levitt base pair seems to be essential for tRNA folding. The formation of the DT-region at the corner of the L-shape is further stabilized by the bifurcated pair G18-Ψ55 and a canonical *cis* Watson-Crick base pair G19-C56. A continuous stack is formed by nucleotides A58, G18, G57, G19 and C56 [78]. Another interaction found at the tRNA elbow is the T54-A58 *trans* Hoogsteen base pair within the TΨC-loop. Formation of the TΨC-loop *trans* Hoogsteen base pair has been shown to be important for juxtaposition of the two helical arms and thus, for maintaining the tRNA L-shape [79]. The DT-region with its surface exposed G19-C56 base pair has been shown to serve as an important platform for interaction with RNAs and proteins [78]. An interaction of the tRNA elbow with the ribosome has been observed in all three tRNA binding sites [78]. Mutation of the 18-55 and 19-56 base pair in *E. coli* tRNA^{Phe} has shown that presence of either or both base pairs is important for several steps during translation elongation [80]. A summary of nucleotides that mediate the formation of the L-shaped tertiary structure is shown in Figure 3.

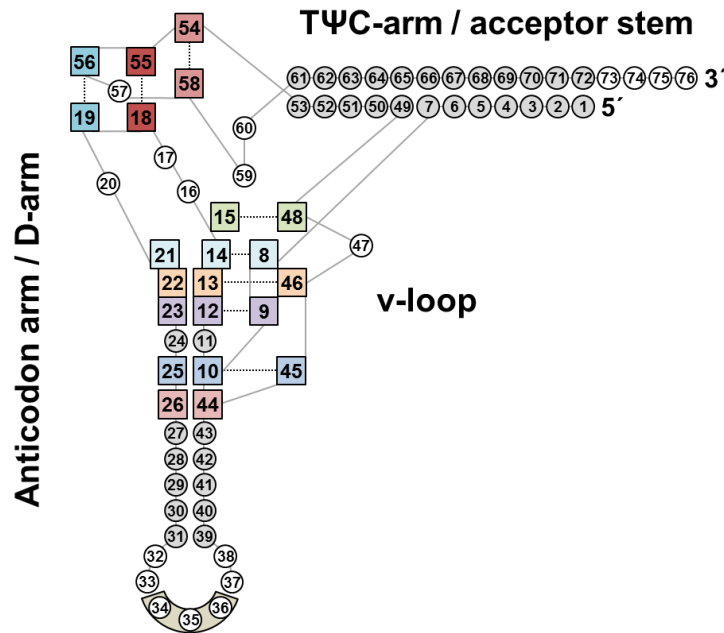


Figure 3: Scheme of tRNA L-shaped tertiary structure and interactions that mediate its formation. Nucleotides involved in tertiary interactions are shown in colored. Tertiary interactions are presented as dashed lines (adopted and modified from [76]).

During multiple processes within the life of tRNA conformational changes of the L-shape have been observed. tRNA distortions have been identified in interactions with processing enzymes, modification enzymes and aaRS. Thus, structural heterogeneity ensures specific recognition by the latter enzymes, whereas structural homogeneity is required for interaction with the ribosome (reviewed in [55,81]). Comparison of ribosome-bound and free tRNA has revealed tRNA deformations during the process of translation. This flexibility of tRNA is achieved by the rather weak connection of the D- and TΨC-loop that allows bending at the tRNA elbow. tRNA bending during translation has been shown to be essential for translocation, interaction with the ribosome and other translation factors (reviewed in [55,82]).

Westhof and Auffinger identified invariant and semi-invariant tRNA nucleotide positions by aligning 932 cytoplasmic tRNA genes (Figure 4) [54]. The alignment highlights the huge sequence heterogeneity observed among tRNAs. The most variable tRNA regions can be mapped to the stem regions. A nearly equal distribution of the four canonical bases is observed for the central base pairs of the acceptor and anticodon helix. The loop regions, with exception of the anticodon triplet, are generally more conserved. Many invariant residues can be mapped to bases involved in formation of the tertiary interaction network responsible for the uniform L-shape formation. Thus, on one hand tRNAs require the presence of certain con-

served nucleotides for tertiary structure formation. On the other hand, sequence variability ensures specific recognition by aaRS [54].

Within the anticodon loop a clear preference for specific nucleotides can be observed. Position 32 is predominantly occupied by C and to less extent by U. Almost all known tRNA sequences contain a uridine at position 33, which is important for the conformation of the anticodon loop and correct positioning of the anticodon triplet for interaction with the mRNA codon [54]. U33 is an essential element of the “U-turn” formed by residues 33-35 [83]. As evident from the crystal structure of yeast tRNA^{Phe}, the U-turn is stabilized by two hydrogens formed by N3-H of U33 with the phosphate of A36 and the 2'-hydroxyl group of U33 with N7 of A35. Furthermore, stacking of U33 between C32 and the phosphate group of A35 has been observed. The uridine conformation and its ability to stack between C32 and the phosphate of A35 have been shown to influence tRNA binding to the ribosome [84]. Nucleotides A or G, often carrying hypermodifications, are located at position 37. Position 38 is predominantly occupied by A, followed in frequency by C and U [54].

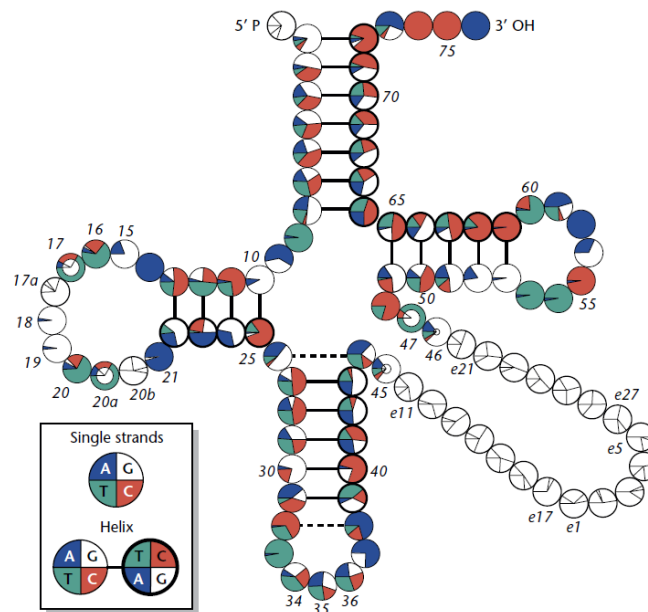


Figure 4: Distribution of nucleotides in elongator tRNAs identified by alignment of 932 tRNA genes across different organisms (adopted from [54]).

3.3 Aminoacylation of tRNAs by aminoacyl-tRNA synthetases and their recognition elements

The formation of aminoacyl-tRNAs (aa-tRNAs) that provide the amino acid which is incorporated into the growing polypeptide chain during protein synthesis is mediated by aminoacyl-

tRNA synthetases (aaRSs). aaRSs catalyze the covalent attachment of an amino acid to the 2'-OH or 3'-OH group of the terminal adenosine of tRNA (reviewed in [85,86]). Identity elements embedded within tRNAs enable aaRSs to distinguish between cognate and non-cognate tRNAs. In general, tRNA identity elements accumulate in the anticodon and acceptor stem region. Exceptions are Alanyl-, Leucyl- and Seryl-tRNA synthetase which obviate to sample the anticodon region for aminoacylation [87]. Thus, tRNA^{Ala}, tRNA^{Ser} and tRNA^{Leu} serve as good scaffolds for the design of nonsense suppressor tRNAs. SerRS mainly recognizes the variable arm of tRNA^{Ser}, whereas the length rather than sequence is of importance [88]. Identity elements of tRNA^{Leu} include the discriminator base A73 and the U8-A14 base pair [87]. The major recognition element of tRNA^{Ala} is a conserved G3-U70 wobble base pair [87,89,90]. tRNA^{Ala} mutants with altered 3-70 base pair show reduced or no aminoacylation at all [89,91]. Transplantation of the wobble pair into tRNA^{Cys} or tRNA^{Phe} amber suppressors resulted in complete or mixed incorporation of Ala instead of Cys or Phe at the nonsense site, respectively [89,90]. A73, G2-C71, G4-C69 and G20 are suggested to contribute to AlaRS specificity [87], too, albeit to lesser extent. However, substitution of G20 or C60 in tRNA^{Ala} showed no influence on aminoacylation by AlaRS and insertion of either nucleotide into tRNA^{Phe} did not transform it into a substrate for AlaRS [92]. Due to the accumulation of identity elements within the acceptor stem, aminoacylation by AlaRS is not only restricted to full-length tRNA^{Ala}. Short RNA minihelices composed of the acceptor-TΨC helix or just the acceptor stem sufficed to enable charging with Ala by AlaRS, albeit with decreased efficiency [93–95]. Lack of nucleoside modifications, as present in *in vitro* transcripts, result in a minor reduction of aminoacylation by aaRS [96–99].

High fidelity of aminoacylation reactions is pivotal for the cell. Mischarging of tRNAs by aaRSs results in incorporation of incorrect amino acids into proteins which can be detrimental to cell homeostasis. To limit misaminoacylation, some aaRS evolved an editing mechanism (reviewed in [86]). tRNA^{Ala} for example is prone to be mischarged with Gly and Ser. However, mediated by its editing domain, AlaRS can hydrolyze misacylated Gly-tRNA^{Ala} and Ser-tRNA^{Ala} and thereby limit aminoacylation of tRNA^{Ala} with amino acids other than Ala [100].

3.4 EF-Tu binding affinity is mediated by the tRNA sequence and its esterified amino acid

During polypeptide chain elongation, elongation factor thermo unstable (EF-Tu) delivers aa-tRNAs as a ternary complex with GTP to the ribosomal A-site [27–31,101]. As evident from

crystal structures, EF-Tu recognizes the 3'-CCA, the acceptor helix and the TΨC-stem of tRNAs. Interaction is mainly established by contact of EF-Tu with the tRNA phosphodiester backbone [102,103]. Mutagenesis studies have shown that the base pairs 49-65, 50-64, 51-63, located in the TΨC-stem of tRNAs, are the main determinants of EF-Tu binding affinity [104]. Of the five identified amino acids that contribute to tRNA specificity of EF-Tu, three have been shown to interact with one of the latter base pairs. EF-Tu Glu390 forms a hydrogen bond with the amino group when a guanine is present in the 51-63 base pair. Gln341 and Thr350 interact with the 2'-hydroxyl group of the ribose at position 64 and 65, respectively [102,104]. A Glu390Ala mutation of *Thermus thermophilus* EF-Tu has been shown to destabilize binding of tRNAs possessing a guanine at position 51 or 63 [105].

Substitution of these three TΨC-stem base pairs can be used to modulate the binding affinity of tRNAs to EF-Tu for a given amino acid. Since the thermodynamic contribution of each of the three base pairs is independent from each other, $\Delta\Delta G^\circ$ values for a given TΨC-stem sequence can be calculated from $\Delta\Delta G^\circ$ values obtained by substitution of the 49-65, 50-64 and 51-63 base pair of Phe-tRNA^{Phe} as shown in Table 2 [106].

Table 2: $\Delta\Delta G^\circ$ values obtained by substitution of the 49-65, 50-64 and 51-63 TΨC-stem base pairs of Phe-tRNA^{Phe}. Base pairs naturally present in Phe-tRNA^{Phe} are highlighted in bold.

49-65	$\Delta\Delta G^\circ$	50-64	$\Delta\Delta G^\circ$	51-63	$\Delta\Delta G^\circ$
C-G	0.0	G-U	1.4	A-U	0.1
U-A	-0.2	U-G	0.4	U-A	0.0
G-C	-0.4	G-C	0.0	U-G	0.0
A-U	-0.5	A-U	0.0	G-U	-0.2
G-U	-0.9	U-A	0.0	C-G	-0.5
		C-G	-0.2	A-C	-0.8
				G-C	-1.0

Despite the tRNA body, EF-Tu also shows specificity for the esterified amino acid [107]. The thermodynamic contributions of the tRNA body and its esterified amino acid to EF-Tu binding can be viewed independently and compensate each other in order to achieve nearly uniform binding of correctly aminoacylated elongator aa-tRNAs to EF-Tu (Table 3) [106,108,109]. Amino acids with intrinsically poorer EF-Tu binding capacity, e.g. Glu, are esterified to tRNA bodies that show high affinities for EF-Tu, e.g. tRNA^{Glu}, and vice versa. Imbalanced aa-tRNA binding to EF-Tu can disturb translation. If aa-tRNA binding to EF-Tu

is too weak, formation of the ternary complex EF-Tu·GTP·aa-tRNA is limited and thus, also delivery of aa-tRNAs to the ribosomal A-site during peptide chain elongation. On the other side, too tightly binding aa-tRNAs show reduced dissociation rates from EF-Tu·GDP after cognate codon-anticodon interaction, resulting in lower rates of polypeptide bond formation [63,64]. The uniformity in EF-Tu binding affinity is, however, not observed for misacylated tRNAs, for which EF-Tu interaction is either strengthened or weakened [107,110]. Thus, it has been suggested that imbalanced EF-Tu binding of misacylated tRNAs limits the misincorporation of non-cognate amino acids and thus, thermodynamic compensation has evolved to contribute to the accuracy of translation [107]. On the other hand, Asahara and coworkers suggested that by achieving comparable EF-Tu binding affinities a uniform rate of ribosomal decoding for different aa-tRNAs is ensured [110].

Table 3: Contribution of the amino acid and tRNA body to EF-Tu binding affinity. $\Delta\Delta G^\circ$ values were obtained from substitution of the amino acid, $\Delta\Delta G^\circ(\text{aa})$, or the tRNA body, $\Delta\Delta G^\circ(\text{tRNA})$, of Phe-tRNA^{Phe}. $\Delta\Delta G^\circ$ values are ranked from most stabilizing (blue) to most destabilizing (red).

$\Delta\Delta G^\circ(\text{aa})$	Amino acid	tRNA	$\Delta\Delta G^\circ(\text{tRNA})$
2.8	Glu	tRNA ^{Glu}	-2.5
1.9	Asp	tRNA ^{Thr}	-2.0
1.4	Ala	tRNA ^{Asp}	-1.8
0.7	Gly	tRNA ^{Gly}	-1.5
0.7	Leu	tRNA ^{Ala}	-1.3
0.4	Lys	tRNA ^{Cys}	-0.4
0.4	Met	tRNA ^{Leu}	-0.3
0.4	Val	tRNA ^{Met}	-0.2
0.1	Arg	tRNA ^{Pro}	-0.1
0.0	Phe	tRNA ^{Phe}	0.0
-0.1	Pro	tRNA ^{Arg}	0.1
-0.1	Thr	tRNA ^{Lys}	0.1
-0.2	Ile	tRNA ^{Ser}	0.2
-0.5	Ser	tRNA ^{Asn}	0.3
-0.7	Asn	tRNA ^{Val}	0.4
-0.9	Tyr	tRNA ^{Ile}	0.5
-1.1	Cys	tRNA ^{Trp}	0.7
-1.1	Trp	tRNA ^{Gln}	0.9
-1.4	Gln	tRNA ^{Tyr}	1.1

3.5 The role of EF-P in translation

Translation of a stretch of Pro residues leads to a slowdown of elongating ribosomes due to the intrinsically poor property of Pro as peptidyl donor and acceptor [111–116]. However, ribosome stalling caused by at least two consecutive Pro residues can be abrogated in the presence of elongation factor EF-P, which accelerates peptide bond formation between Pro-Pro residues [111,117,118]. EF-P specifically recognizes the D-arm motif of tRNA^{Pro} isoacceptors with a 9 nt loop and a stable 4 bp stem closed by two consecutive G-C base pairs. This characteristic D-arm is only shared among tRNA^{Pro} and tRNA^{Met} in *E. coli* [119]. Katoh and coworkers have shown that the length rather than the sequence of the tRNA^{Pro} D-arm is essential for EF-P recognition, as nucleotide exchanges only marginally affected EF-P binding [119]. A recent cryo EM study has shown that the all-*trans* conformation of polyproline-containing polypeptides causes a steric clash within the ribosomal exit tunnel, which in turn destabilizes the P-site tRNA. Thus, Peptidyl-tRNA drop-off or its unfavorable positioning for peptide bond formation result in ribosomal stalling. However, EF-P has been shown to stabilize the P-site tRNA, predominantly mediated by the interaction of a post-translational modification of Lys 34 of EF-P with the 3'-CCA end within the peptidyl transferase center. This in turn enables the polyproline-containing nascent chain to adopt an alternative conformation, enabling it to extend to the lumen of the ribosomal tunnel and thus, allows the tRNA substrates to position accurately for peptide bond formation [120].

In vitro translation systems, such as the PURE system, were shown to be able to synthesize a variety of proteins in the absence of EF-P [119]. In addition, *E. coli* cells lacking the *efp* gene were shown to be viable [121,122], albeit with reduced fitness [121]. This suggests a non-essential role of EF-P in protein synthesis. Rather, EF-P can be viewed as a specialized factor necessary for translation of mRNAs coding for polyproline-containing proteins [119].

3.6 Nonsense suppressor tRNAs

Mutations in tRNA genes, most commonly in the anticodon, lead to the formation of suppressor tRNAs. Depending on the nature of the suppressed codon, a distinction is made between missense, nonsense and frameshift suppressor tRNAs (reviewed in [123]). Nonsense suppressor tRNAs, the main focus of this study, recognize mRNA stop codons and upon successful competition with peptide chain release factors, lead to the incorporation of amino acids in place of termination codons (reviewed in [124]). Thus, nonsense suppressor tRNAs targeting

native stop codons result in the synthesis of C-terminally extended proteins [125]. On the other hand, read-through of PTCs by nonsense suppressor tRNAs mediates elongation of translation until the next in-frame termination codon is reached. Hence, instead of a truncated and generally dysfunctional protein, the full-length protein is synthesized (Figure 5) [126]. Depending on the identity of the inserted amino acids the functionality of the protein is either restored or not.

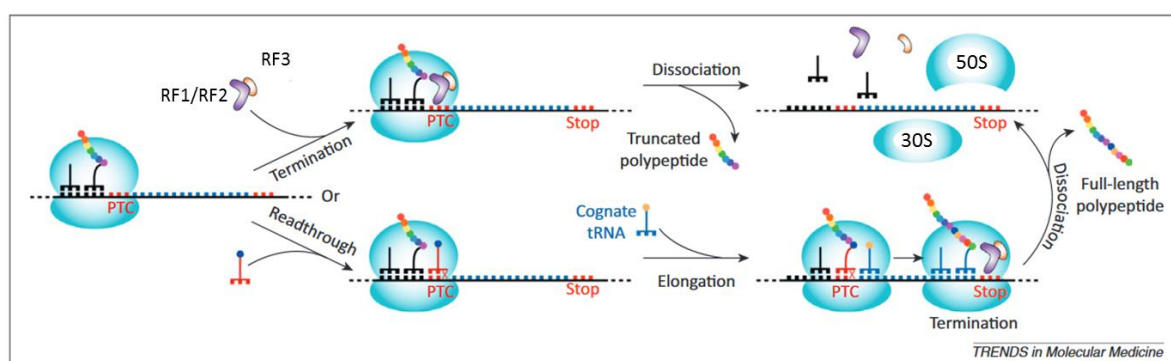


Figure 5: Scheme of translation termination and read-through of mRNAs containing PTCs. When a stop codon enters the ribosomal A-site it can be recognized by release factors, which mediate termination of translation and in the presence of mRNAs containing PTCs the release of the truncated and generally non-functional protein. However, nonsense suppressor tRNAs can base pair with the PTC on the mRNA and thus, mediate read-through of the PTC. Instead of translation termination, elongation will occur, leading to the formation of the full-length polypeptide (adopted and modified from [127]).

Stop codon read-through by suppressor tRNAs is a common strategy used by positive strand RNA viruses to expand the genetic information encoded in their genomes (reviewed in [128]). A wide variety of natural nonsense tRNA suppressors have previously been identified in *E. coli*. A summary of natural nonsense suppressor tRNAs from *E. coli* can be found in an excellent review by Eggertsson and Söll [124]. Isolation of natural nonsense suppressor tRNAs has shown that the mutations are mainly, but not exclusively, present in the anticodon triplet, enabling the tRNA to base pair to complementary stop codons on the mRNA (reviewed in [129]). One exception is the Hirsh suppressor tRNA isolated from the *E. coli* strain CAJ94, which possesses a G24A mutation in the D-arm and no changes in the anticodon triplet in comparison to wildtype tRNA^{Trp}(CCA). Even though the Hirsh mutation is located far away from the anticodon region, it enables read-through of UGA stop codons [130]. Nonsense suppression by the Hirsh suppressor tRNA is suggested to arise through additional hydrogen bonding of N6 of A24 with O6 of G44, which stabilizes the distorted A/T-conformation and thus, promotes misreading of mRNA stop codons [131].

Depending on the nature of the suppressed stop codon, tRNAs are classified as amber (UAG), ochre (UAA) or opal (UGA) suppressors. In *E. coli*, amber codons used less frequently (9%) as compared to opal (32%) and ochre (59%) termination codons (<https://www.kazusa.or.jp/codon/>, Codon Usage Database). Johnson and coworkers have shown that only a minor fraction of essential genes (7 of 302) terminate with UAG and these generally possess a second in-frame downstream stop codon [132]. Thus, design of amber suppressor tRNAs is especially appealing.

3.6.1 Nonsense suppressor tRNA designs

To date, several approaches have been used to select for functional nonsense suppressor tRNAs. Natural nonsense suppressor tRNAs mainly arose by mutations within the anticodon triplet, while the remaining tRNA body remained unchanged [129]. Thus, using nature as an example, nonsense suppressor tRNAs were designed using native tRNAs with the anticodon replaced by a base triplet that is complementary to a stop codon. Thereby, tRNA^{Ala}, tRNA^{Ser} and tRNA^{Leu} served as preferred templates, because their aminoacylation identity elements are located outside of the anticodon loop [87]. Changing the anticodon of human tRNA^{Ala}, tRNA^{Ser} and tRNA^{Leu} isodecoders to 5'-CUA-3' indicated a wide variety of suppression efficiency, which could be modulated by the length of the variable loop [133]. Hybrid nonsense suppressor tRNAs were created by transplanting the anticodon stem-loop (ASL) from one native tRNA species into another. Incorporation of the *E. coli* tRNA^{Phe} ASL into read-through inactive tRNA^{Pro}(CUA) generated an efficient amber suppressor tRNA [134]. Transplanting the anticodon region of amber suppressor tRNA Su⁺² into tRNA^{Trp} generated a glutamine-inserting hybrid suppressor tRNA, which was, however, less efficient than Su⁺⁷, derived from anticodon replacement of tRNA^{Trp} [135]. Exchange of the anticodon arm between the efficient Su⁺⁷ and weak Su⁺² suppressor tRNA enabled modulation of nonsense suppressor strength [136]. In another approach, functional nonsense suppressor tRNAs containing mitochondrial-like structures with 7-10 base pairs in the anticodon stem instead of the canonical six were created. Partially randomized tRNA libraries were used to screen and select for the optimized suppressor tRNAs [137]. Guo and coworkers created tRNA libraries in which nucleotides located within the TΨC-stem of *Methanocaldococcus jannaschii* (*Mj*) tRNA^{Tyr}(CUA) were randomized. tRNAs were selected for their ability to be aminoacylated by orthogonal aaRS and suppress an amber GFP construct. Selected suppressor tRNAs improved incorporation of non-natural amino acids by 200-2200% in comparison to wildtype *Mj*tRNA^{Tyr}(CUA) [138]. In

wheat germ extract, suppression of *in vitro* transcribed suppressor tRNA could be increased by more than two-fold by four consecutive cycles of sequence optimization. In the first generation, the anticodon of tRNA^{Ala}, tRNA^{Leu} and tRNA^{Ser} was altered to be complementary to the amber stop codon. Highest suppression efficiencies were observed for tRNA^{Ser} variants, of which effective parts were combined, leading to the second generation. Chimeras of the third generation, produced by sequence optimization of the anticodon stem and discriminator base, led to the fourth generation [139]. Another study used read-through ribosome display to select for amber suppressor tRNAs. In this approach, suppression of a UAG stop codon led to the production of the full-length polypeptide that remains attached to the mRNA, which is fused to the tRNA sequence. This way, identification of the sequence of the active suppressor tRNAs was facilitated. The suppressor tRNA was selected from anticodon- and anticodon loop-randomized genes of tRNA^{SerU} and showed protein expression levels comparable to translation reactions performed with amber-free mRNA in the absence of suppressor tRNA [140].

3.6.2 Applications of nonsense suppressor tRNAs

A wide range of different applications are attributed to nonsense suppressor tRNAs. Extensive research has focused on the usage of nonsense suppressor tRNAs for the incorporation of non-natural amino acids, thereby expanding the genetic code. The successful incorporation of non-canonical amino acids (ncAA) at a defined codon requires the use of an orthogonal aminoacyl-tRNA synthetase-tRNA pair. Often stop codons are designated as recoding sites. Orthogonality ensures the exclusive incorporation of ncAA at recoding sites due to lack of interaction with endogenous aaRS, tRNAs or amino acids (reviewed in [141,142]). One example of an orthogonal pair extensively used to incorporate ncAAs is the *Methanocaldococcus jannaschii* TyrRS and *MjtRNA*^{Tyr} [143,144]. To enable ncAA insertion, the anticodon of *MjtRNA*^{Tyr} was altered to 5'-CUA-3' enabling recognition of UAG stop codons. Underrepresentation of amber codons in the *E. coli* genome (<https://www.kazusa.or.jp/codon/>, Codon Usage Database) ensured little read-through at natural termination sites and thus, limited the fitness loss. Introducing amber stop codons into the protein coding sequence enabled the site-specific incorporation of ncAAs. Multiple rounds of positive and negative selection of active site *MjTyrRS* mutants from libraries permitted specific recognition of non-natural amino acids, which were aminoacylated to *MjtRNA*^{Tyr}(CUA) [144,145]. Orthogonal aaRS-tRNA pairs enabled the incorporation of >200 non-canonical

amino acids into proteins in a variety of organisms [146]. This way, study of protein function, stability and structure, but also the engineering of proteins with novel functions was enabled. The diverse set of incorporated ncAAs included fluorescent, crosslinkable, photocaged and post-translationally modified amino acids (reviewed in [145,147–149]). Additionally, attempts to insert D- or β -amino acids instead of canonical L- α -amino acids have been performed, which aimed at producing new biopolymers. The latter approach used a flexible *in vitro* translation system and chimeric tRNAs, which were precharged with flexizymes instead of an orthogonal aaRS-tRNA pair [150–152].

Nonsense suppressor tRNAs also served as tools to study tRNA recognition elements by aaRSs. Identity elements were assessed by mutagenesis of nonsense suppressor tRNAs and identification of the amino acid inserted at the PTC [153].

In mammalian systems, research focused on the use of nonsense suppressor tRNAs as therapeutic tools in order to treat diseases caused by premature termination codons (reviewed in [126,154]). Around 10% of human genetic diseases are caused by mutations in the protein coding sequence, which result in an in-frame PTC [155]. Translation of PTC-containing mRNA results in the production of truncated and thus, generally dysfunctional proteins. The presence of PTCs also triggers the nonsense-mediated mRNA decay which results in the degradation of the transcript and thus, reduced mRNA steady-state levels. Both events in combination result in a near complete loss of protein expression, which can ultimately result in nonsense mutation-based diseases [156]. However, supplementation with nonsense suppressor tRNAs has been shown to enable read-through of PTCs, resulting in the production of full-length proteins [157–159]. Thus, nonsense suppressor tRNAs are promising therapeutics to rescue the observed phenotypes caused by PTCs. In order to prevent missense mutations, a tight control of the amino acid inserted at the PTC is important. In addition, recognition of natural stop codons needs to be circumvented to avoid the production of C-terminally extended proteins with potential deleterious effects. Ribosome profiling experiments of mammalian cells transfected with nonsense suppressor tRNAs showed reduced levels of read-through at native stop codons as compared to PTCs. However, the presence of certain tRNA species increased the ribosome density in the 3'-UTR of transcripts, showing an unwanted suppression of native stop codons [157].

The successful production and utilization of nonsense suppressor tRNAs has been reported previously. However, studies so far are limited to cell or animal models. Temple and cowork-

ers used an anticodon-edited tRNA^{Lys} which enabled read-through of an amber PTC associated with β -thalassemia. Co-injection of the nonsense suppressor tRNA^{Lys} and the PTC-containing β -globin mRNA into *Xenopus oocytes* resulted in the production of full-length protein [158]. In line with this, co-injection of a UGA codon-recognizing tRNA^{Gly} and a CFTR_G542X mutant resulted in wildtype-like levels of chloride conductance [157]. In another study, a plasmid encoding a tRNA reading UAA nonsense codons was injected into mice modeling Duchenne muscular dystrophy (DMD). As a result, ~2.5% of muscle fibers expressed the full-length dystrophin [159]. These studies show the great potential of nonsense suppressor tRNAs for the treatment of nonsense mutation-caused diseases. In many cases, already a slight increase in full-length protein is enough to rescue the observed phenotype. However, off-target effects due to recognition of natural stop codons and the targeted delivery of therapeutic nonsense suppressor tRNAs are still challenging [126].

3.7 Factors modulating nonsense suppression efficiency

Nonsense suppression frequency is determined by the competition between release factor and nonsense suppressor tRNA for the binding of termination codons [160]. Stop codon read-through is influenced by a series of factors and inversely correlates with the efficiency of translation termination [125]. High termination efficiency results in low nonsense suppression and vice versa. One important feature accounting for the differences observed in termination efficiencies is the nucleotide context of the stop codon. The highest impact has been observed for the base directly following the stop codon, often referred to as +4 base [161–165]. In *E. coli*, hierarchy of the +4 flanking base in termination efficiency at UAA and UGA codons follows the order U>G>A~C, whereas the ranking for UAG codons differs, being G>U~A>C [164]. Termination efficiencies of tetra-nucleotide stop signals often correlate with their frequency in *E. coli* [164]. The most efficient termination signal in bacteria is UAAU, which is strongly overrepresented, especially in highly-expressed genes [161,162,164]. In contrast, UGAC, the weakest termination signal, is present to low extent in the *E. coli* genome [164] and is often found at recoding sites [166] used for frameshifting [167,168] or the incorporation of Sec [169,170]. The strong influence of the base immediately following the termination codon led to the view that the stop signal is not a triplet-, but rather a tetra-nucleotide sequence [171]. Nonsense suppression efficiencies are also influenced by the stop codon context. The influence of the codon context on suppression efficiencies at termination sites has been shown to be strongly dependent on the identity of the nonsense suppressor tRNA

[134,172]. Suppression efficiencies of the Hirsh suppressor tRNA^{Tyr} at UGA sites have been shown to follow the order A>G>C>U for the +4 base [173]. This discrepancy in reciprocity of termination and nonsense suppression efficiency is likely influenced by other codon context effects. As suggested by zero-length crosslinking studies, besides bases +1 and +4, positions +5 and +6 also mediate interaction with RF2. Substitutions in both positions have been shown to modulate RF-selection and thus, affect termination efficiencies [163]. Another study suggested an influence of the P-site tRNA on the termination efficiency of RF1. Termination efficiency of a mutant form of RF1 varied depending on the codon immediately upstream of the termination signal. The observed differences could not be attributed to the inserted amino acid or a specific position within the triplet codon, suggesting an influence of the peptidyl-tRNA in the P-site on termination. The effect of P-site tRNA was dependent on the +4 base [174].

In addition to the stop codon context, the two C-terminal amino acids adjacent to the stop codon have been shown to modulate read-through efficiencies [175,176]. For the -1 amino acid, the van der Waals volume and its propensity to form secondary structures influenced nonsense suppression. Amino acids with a small vdW-volume, such as Gly, were accompanied by high read-through levels [176]. Basic amino acids at the penultimate position resulted in efficient termination but inefficient read-through, whereas the opposite has been observed for acidic amino acids [175,176]. The effect of the -1 and -2 amino acid was cooperative [176]. However assumptions were made for a specific codon context site and thus, other stop codon reading contexts could result in different amino acid preferences.

Nonsense suppressor tRNA features have also been shown to modulate the efficiency of nonsense suppression. A well-established hypothesis by Yarus and coworkers, the “extended anticodon”, has proposed that nucleotides found within the anticodon loop and stem are optimized according to the identity of the “cardinal” nucleotide found at position 36 [136,177]. This coevolution is believed to maximize the translational efficiency of native tRNAs. Nonsense suppressor tRNAs generally possess a cardinal A and thus, those constructed from native tRNAs reading codons beginning with U were shown to be more efficient (Table 4) [177]. Nonsense suppression efficiencies of tRNAs derived from native sequences containing other nucleotides at position 36 were enhanced by replacing nucleotides within the ASL according to those present in tRNAs reading UXX codons (X: A, C, G, U) [136,177–179].

Table 4: Nucleotides found within native tRNAs containing A as cardinal nucleotide.

Nucleotide position	Nucleotide found in tRNAs with A as cardinal nucleotide
28-42	(G-C or C-G)
29-41	Pu-Py
30-40	G-C
31-39	A-Ψ or U-A
32	C, U
33	U
37	ms ² i ⁶ A
38	A

The “extended” anticodon loop maximized nonsense suppressor tRNA efficiency, despite an observed decrease in tRNA levels. In contrast, the identified anticodon stem base pairs maximized read-through levels by increasing tRNA levels. For the anticodon stem, the influence of nucleotide changes on suppression efficiency became more pivotal with further distance from the anticodon loop (Figure 6). Substitutions of nucleotides within the anticodon loop showed a generally higher impact on nonsense suppression efficiencies as compared to the anticodon stem [178].

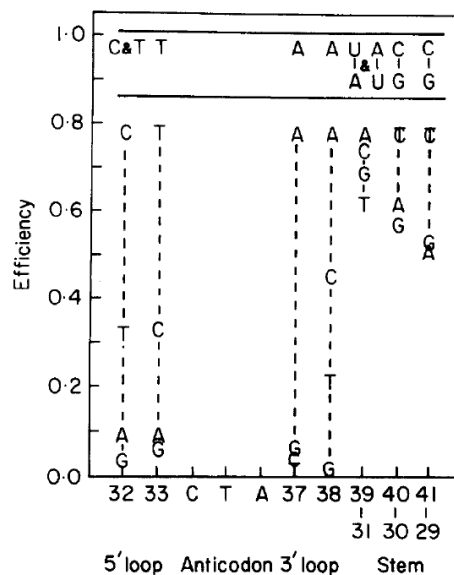


Figure 6: The influence on nonsense suppressor tRNA efficiencies varies for different positions within the ASL. Nucleotides favored at position 32-41 for native tRNAs translating codons beginning with U (top panel). Suppression efficiencies of tRNAs with nucleotide exchanges within the “extended” ASL (lower panel). (adopted from [178]).

Insertion of the ASL of UXX-translating tRNAs according to Table 4 turned the weak amber suppressor Su⁺² tRNA^{Gln} into an efficient one [136]. In line with this, base substitutions within the ASL of Su⁺⁷ tRNA^{Trp}, naturally complying with the extended anticodon rules, decreased nonsense suppression efficiency [178]. Transplantation of the “extended” ASL into tRNA^{Asp}(CUA) resulted in a 10-fold increase in nonsense suppression. Incorporation of the residues A36 and A37 into tRNA^{His}(CUA), tRNA^{Glu}(CUA) and Su2 improved stop codon read-through at all investigated codon contexts [134]. In accordance with the “extended” anticodon rules, selection of amber nonsense suppressor with randomized bases adjacent to the 5'-CUA-3' anticodon by read-through ribosome display showed highest suppression efficiencies for tRNA^{Ser} containing a CU-CUA-AA anticodon loop sequence [140].

In line with the hypothesis of Yarus, suppression efficiencies of amber nonsense suppressors have been shown to be modulated by the identity of the 32-38 pair (Table 5) [180].

Table 5: Relative efficiencies of amber nonsense suppressor tRNAs derived from native tRNA species with different 32-38 pair combinations. The 32-38 pair present in native tRNAs is highlighted in italic.

tRNA species	Relative suppression efficiency mediated by different 32-38 pairs
tRNA ₁ ^{Ala}	U-U<U-C<C-C<C-A
tRNA ₂ ^{Ala}	<i>A-U</i> <A-A
tRNA ^{Glu}	<i>C-C</i> <C-A
tRNA ₂ ^{Glu}	<i>Um-Ψ</i> <Um-C<Um-A<Cm-A
tRNA ^{His}	<i>U-U</i> <U-A
tRNA ^{Trp}	<i>Um-Ψ</i> <Um-C<Um-A<Cm-A
tRNA ^{Trp}	C-G<G-A<U-G<A-A<C-U<U-A<C-C<C-A

The 32-38 pair is an important determinant for the binding strength of aa-tRNAs to ribosomes. Studies have suggested that the 32-38 pair coevolved with the anticodon triplet in order to ensure uniform binding affinities of elongator tRNAs to the ribosomal A-site [180,181]. Substitution of the 32-38 pair within native tRNA sequences either weakened or strengthened ribosomal A-site binding. tRNA^{Ala}(GGC), which forms a tight codon-anticodon interaction, contains a A32-U38 pair. This 32-38 pair is suggested to weaken the affinity to the ribosomal A-site and thus, adjust binding of Ala-tRNA^{Ala}(GGC) to the ribosome [181]. Substitution of the anticodon in tRNA^{Ala}(GGC) resulted in weakened ribosomal A-site binding, which could be restored when the 32-38 pair was changed to U32-A38 or C32-A38

[181]. The uniform ribosomal A-site binding affinity of elongator tRNAs, which is mediated by the identity of the 32-38 pair, is suggested to prevent misreading of non-cognate codons. A U32C mutant tRNA^{Gly} was shown to decode not only cognate codons but also those containing a mismatch at the third position, likely due to tighter ribosome binding [180]. Thus, the 32-38 pair is an important determinant for tuning the efficiencies of nonsense suppressor tRNAs through adjustment of ribosomal A-site binding. Nonsense suppressors derived by anticodon substitution of native elongator tRNAs might show a preference for a different 32-38 pair than that observed for the parental tRNA. In general, amber suppressor tRNAs show highest read-through in the presence of a C32-A38 pair (Table 5) [180].

tRNAs possessing an A at position 36, reading codons beginning with U, generally carry a *N*⁶-isopentenyladenosine (*i*⁶A) or more frequent 2-methyl-thio-*N*⁶-isopentenyladenosine (*ms*²*i*⁶A) modification at position 37 (Table 4) [182–184]. The presence of the hypermodified A37 is required to stabilize the adjacent A36-U1 codon-anticodon base pair by stacking [185]. In addition, bulky modifications at base 37 prevent intra-loop base pairing with U33 at the 5'-side of the anticodon. U33 is critical for the formation of the canonical U-turn and thus, modifications at A37 retain the anticodon loop in an “open” conformation required for efficient codon-anticodon interaction during decoding [63,186–190]. Reports have shown that mutations in the *miaA* gene, leading to the absence of the *i*⁶A37 modification, which is subsequently converted into *ms*²*i*⁶A by *miaB* in *E. coli* [191], reduced nonsense suppressor efficiencies [58,192,193]. *In vitro* studies have shown reduced ribosomal binding of a suppressor tRNA^{Trp} due to lack of *i*⁶A or *ms*²*i*⁶A modification [193]. Petruccio and coworkers observed a 75% and 60-fold reduction in nonsense suppressor tRNA efficiencies at UAG- and UGA-sites, respectively, whereas UAA-sites were not affected by the *miaA* mutation [192]. A study in *Saccharomyces cerevisiae* deleted tRNA modifications at positions U34, U35, A37, U47 and C48 by gene knockouts and showed that lack of the modification *mcm*⁵U or *i*⁶A at positions 34 and 37, respectively, showed the strongest reduction of nonsense suppression. The combined absence of both modifications dropped nonsense suppression levels even further, nearly resembling those observed in absence of suppressor tRNA [194]. Lack of the hypermodification at position 37 has also been shown to result in increased codon context sensitivity of nonsense suppressor tRNAs [195–198].

Despite the mRNA and tRNA entity, other factors involved in translation have been shown to modulate nonsense suppressor tRNA efficiencies, too. Mutations in the ribosomal protein genes coding for S4, S5 and L7/L12 increased PTC read-through, while mutations in the

genes for L6, S12 and S17 showed the opposite effect (reviewed in [124,199]). Higher nonsense suppression levels have been examined for cells containing a mutation at position 1054 within the sequence of 16S ribosomal RNA and for EF-Tu mutants (reviewed in [199]). As expected, due to competition of nonsense suppressors tRNAs with RFs for binding to stop codons, mutations within the genes coding for RF1 or RF2 increased read-through levels (reviewed in [199]). A dependency of nonsense suppression on the growth phase of *E. coli* has been observed. In the active growth phase, read-through of UGA stop codons by near-cognate tRNAs was higher compared to the late exponential phase [200].

4 AIM OF THE THESIS

Cytoplasmic tRNAs show large sequence heterogeneity. This variability is necessary for the specific recognition by interaction partners, such as aminoacyl-tRNA synthetases. However, certain positions within tRNA sequences are evolutionary conserved to ensure the formation of the uniform L-shaped tertiary structure important for ribosome binding and the correct positioning of the anticodon to enable codon-anticodon interactions. By combining these preserved bases and randomized bases chosen according to the probability to fold into the cloverleaf secondary structure, functional nonsense suppressor tRNAs should be designed. Consequent substitutions aimed at elucidating which tRNA bases or regions are crucial for designing functional tRNAs by evaluating their activity as nonsense suppressors and at shedding light on the tolerance of tRNAs towards multiple sequence exchanges. *In vitro* aminoacylation and 3'-end ligation reactions were used to determine the propensity of the tRNA designs to adopt the L-shaped tertiary structure. *In vitro* and *in vivo* GFP read-through assay were applied to assess the functionality of tRNAs in translation.

5 RESULTS

5.1 Nonsense suppressor tRNA designs

Three main types of constraints were chosen in the design of nonsense suppressor tRNAs. These include recognition elements of Alanyl-tRNA synthetase (orange) [87], bases involved in tertiary interactions defined from the crystal structure of unmodified *E. coli* tRNA^{Phe} (PDB ID: 3L0U) (blue) [96] and the 5'-CUA-3' anticodon (green) (Figure 7). The remaining bases were chosen according to their probability to form the cloverleaf secondary structure characteristic for tRNAs (design I). In the second set of design (design II) (Figure 7), additional tertiary interactions were considered. Therefore, design II is considered to reflect higher resemblance to native tRNAs, which is also evident from the nomenclature of the tRNAs, which was set according to their “nativeness”. tRNAs n1, n2 were derived from design II, whereas design I resulted in the tRNAs n3, n4 and n5. The more constraints used and the higher probability to form the cloverleaf structure, the higher ranked is the tRNA (Table 7).

Most tertiary interactions present in unmodified *E. coli* tRNA^{Phe} resemble that of the modified tRNAs (Figure 7, Table 6). However, in comparison to modified yeast tRNA^{Phe} (PDB ID: 1EHZ) [70] the absence of the G10-C25-G45 triplet and G26-A44 imino base pair can be observed. Instead, a G10-C25-G44 triplet base pair is formed, which renders A26 unpaired [96]. A comparison of the tertiary interactions shows that design II included the G15-C48 Levitt, G18-U55 bifurcated and the U54-A57 *trans* Hoogsteen base pair, all of which were absent in design I. In addition, incorporation of nucleotides U54, G57, U59 and U60, representing the most frequent nucleotides in these positions (except U59), rendered the sequence of the TΨC-loop fixed.

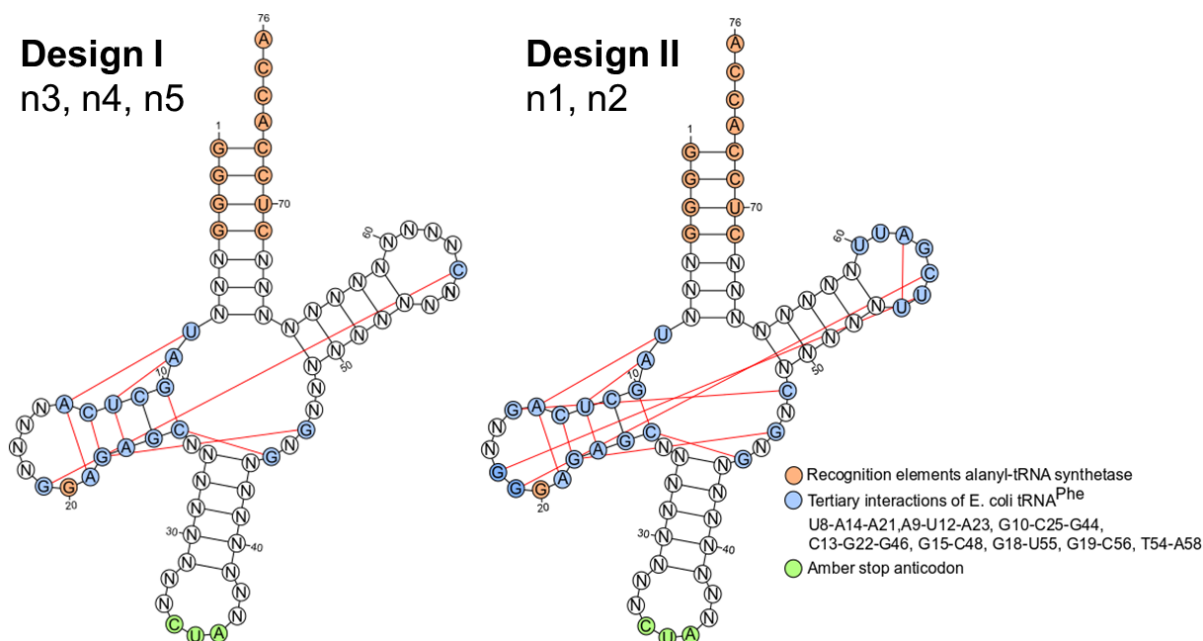


Figure 7: Sequence constraints used in the design of nonsense suppressor *E. coli* tRNAs. Constraints included recognition elements of tRNA^{Ala} (orange) [87], bases involved in tertiary interactions defined from the crystal structure of unmodified *E. coli* tRNA^{Phe} (PDB ID: 3L0U) (blue) [96] and the 5'-CUA-3' amber anticodon (green). The remaining bases (N) were chosen according to their probability to form the target secondary structure. Tertiary interactions are represented by red lines. The second design (II), resulting in n1 and n2, included additional tertiary interactions in comparison to the first design (I), used to generate n3, n4 and n5.

Table 6: Constraints used in the design of nonsense suppressor *E. coli* tRNA^{Ala} variants.

Recognition elements of AlaRS	Tertiary interactions design I	Tertiary interactions design II
A73	U8-A14-A21	U8-A14-A21
G2-C71	A9-U12-A23	A9-U12-A23
G3-U70	G10-C25-G44	G10-C25-G44
G4-C69	C13-G22-G46	C13-G22-G46
G20		G15-C48
		G18-U55
	G19-C56	G19-C56
		U54-A58

The design n6 was set up using the same constraints. However, tertiary interactions were completely compromised. Therefore, n6 unlikely adopts the L-shaped tertiary structure of native tRNAs. Other negative controls, incapable of promoting nonsense suppression, included native tRNA^{Ala} isoacceptors with a GGC- or UGC-anticodon. As positive controls, referring to tRNAs that should be functional in nonsense suppression, the anticodons of the

native tRNA^{Ala} isoacceptors were substituted by the corresponding stop anticodon. The amber anticodon was mainly used for *in vitro* experiments, whereas opal variants were chosen for *in vivo* experiments. Nonsense suppressors containing the body sequence of tRNA^{Ala}(GGC) with amber, tRNA^{Ala}(CUA), or opal anticodon, tRNA^{Ala}(UCA(G)), or tRNA^{Ala}(UGC) with opal anticodon, tRNA^{Ala}(UCA(U)), were used.

Table 7: Sequences of the designed nonsense suppressor tRNAs n1-n6 and the controls tRNA^{Ala}(GGC), tRNA^{Ala}(CUA) and tRNA^{Ala}(UGC). Sequence changes in comparison to n1 are highlighted in red. P refers to the probability of the tRNA to form the cloverleaf secondary structure.

Name	Acc-s	D-s	D-l	D-s	Ac-s	Ac-l	Ac-s	V-r	T-s	T-l	T-s	Acc-s	CCA	P			
	1	8	10	14	22	26	27	32	39	44	49	53	61	66	73	74	
n1	GGGGCGG	UA	GCUC	AGAAGGGA	GAGC	A	GCGGA	GACUAAA	UCCGC	GAGAC	GGUCC	UUUGAUU	GGACC	CCGCUCC	A	CCA	0.93
n2	GGGGCUC	UA	GCUC	AGAAGGGA	GAGC	A	GGGAC	GACUAAA	GUCC	GAGAC	GGCGC	UUUGAUU	GCGCC	GAGCUCC	A	CCA	0.88
n3	GGGGCCC	UA	GCUC	AGAAAGGA	GAGC	A	GGCAG	GACUAAA	CUGCC	GAGAA	GCAGC	GACAUAA	GCUGC	GGGCUCC	A	CCA	0.97
n4	GGGGCCC	UA	GCUC	AGAAAGGA	GAGC	A	GGCAG	GACUAAA	CUGCC	GAGAA	GCCGG	GACAUAA	CCGGC	GGGCUCC	A	CCA	0.94
n5	GGGGCGC	UA	GCUC	AAUAAGGA	GAGC	A	GGAGC	GACUAAA	GCUC	GAGAA	GUCC	GACAUAA	GCGAC	GCGCUCC	A	CCA	0.94
n6	GGGGCGG	AA	CAGG	GAAACAGA	CCUG	A	GCGGA	GACUAAA	UCCGC	AAUAA	GGUCC	GAACUAA	GGACC	CCGCUCC	A	CCA	0.95
Ala(GGC)	GGGGCUA	UA	GCUC	AGCUGGGA	GAGC	G	CUUGC	AUGGCAU	GCAAG	AGGUC	AGCGG	UUUGAUC	CCGCU	UAGCUCC	A	CCA	0.09
Ala(CUA)	GGGGCUA	UA	GCUC	AGCUGGGA	GAGC	G	CUUGC	AUCUAAU	GCAAG	AGGUC	AGCGG	UUUGAUC	CCGCU	UAGCUCC	A	CCA	0.09
Ala(UGC)	GGGGCUA	UA	GCUC	AGCUGGGA	GAGC	G	CUUGC	UUUGCAC	GCAGG	AGGUC	UGCGG	UUUGAUC	CCGCA	UAGCUCC	A	CCA	0.005

5.2 *In vitro* aminoacylation levels vary between the designed tRNAs

A prerequisite for the functionality of nonsense suppressor tRNA is the aminoacylation by the cognate aminoacyl-tRNA synthetase. aaRSs recognize specific sequence elements of tRNAs, often located the anticodon region. However, recognition elements of tRNA^{Ala}, tRNA^{Leu} and tRNA^{Ser} are entirely independent of the anticodon region [87]. The identity elements of tRNA^{Ala} are embedded almost exclusively in the acceptor stem, with the G3-U70 wobble base pair serving as main identity element [87,89,90]. This enables changing the anticodon of the designed nonsense suppressor tRNAs to be complementary to mRNA stop codons without perturbing the aminoacylation. Thus, the tRNA^{Ala} body should serve as a good scaffold for nonsense suppressor tRNA design.

The aminoacylation of tRNAs serves as a measure of overall tRNA topology. Successfully folded tRNAs show faster aminoacylation kinetics in comparison to un- or misfolded tRNAs [201]. Thus, in general aminoacylation levels appear to be influenced by the tRNA structure, suggesting that they can be used as an indication for the fraction of correctly folded tRNA. In the case of Alanyl-tRNA synthetase (AlaRS) aminoacylation levels may not be completely

representing folded structure, since the synthetase aminoacylates even microhelices composed of the acceptor-stem of tRNA^{Ala} [93]. However, microhelices in comparison to full-length tRNA^{Ala} showed reduced rates of aminoacylation and reached plateau aminoacylation levels after ~25 min [93]. In the present study, the aminoacylation duration was set to 15 minutes and thus, the difference in aminoacylation levels observed for folded in comparison to un- or misfolded tRNAs might be reduced.

Prior to aminoacylation, the presence of the single-stranded 3'-NCCA terminus, serving as the site for amino acid attachment, was assessed by ligating a fluorescently labeled oligonucleotide containing a complementary 5'-TGGN overhang. Ligation products and thus, the presence of single-stranded 3'-NCCA termini were observed for all tested *in vitro* transcribed tRNAs (Figure 8). However, only a minor fraction of tRNAs could be ligated, suggesting that the majority adopts alternative tRNA conformations in which the 3'-terminus is unexposed and thus, inaccessible for aminoacylation by AlaRS.

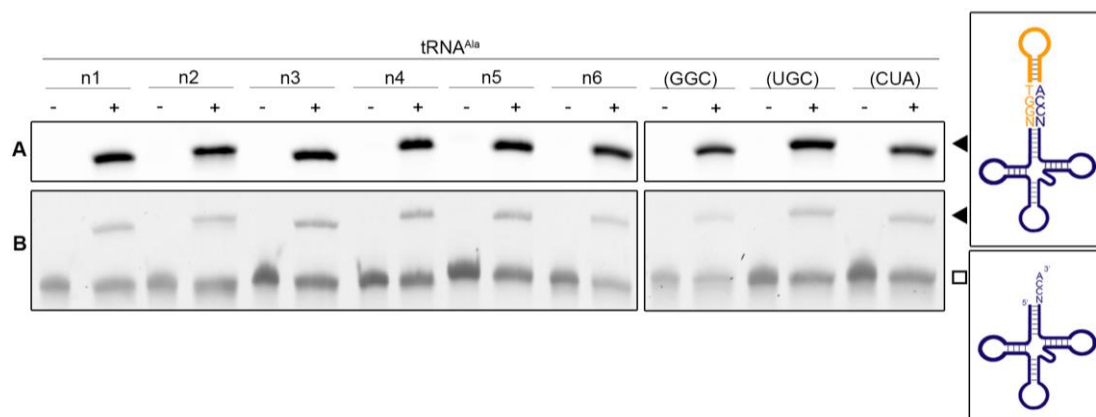


Figure 8: Designed tRNAs possess single-stranded 3'-NCCA termini. tRNAs were ligated to a Cy3-labeled hairpin oligonucleotide with a complementary 5'-TGGN-3' overhang (+). The migration behavior was compared to *in vitro* transcribed tRNAs (-). Ligation products (◄) can be detected by their slower migration in 10% denaturing PAGE compared to unligated tRNAs (◻). tRNAs were detected by fluorescence (A) or staining with SYBR gold (B) (right panel adopted from [202]).

Aminoacylation of *in vitro* transcribed tRNAs was performed with semi-purified *E. coli* Alanyl-tRNA synthetase enriched through His-tag pull-down (Figure S1). All tRNA^{Ala} variants, except for n2, were charged with Ala (Figure 9). Aminoacylated and non-aminoacylated tRNA fraction exhibited a clear difference in their migration behavior on acidic gel electrophoresis, with aminoacyl-tRNA migrating slower and this difference in migration behavior was used to determine the fraction of aminoacyl-tRNA^{Ala} from the total tRNA^{Ala}.

Charging levels ranged from $\sim 20\%$ for tRNA^{Ala}(n1), comparable to that of *in vitro* transcribed native tRNA^{Ala} (tRNA^{Ala}(UGC) or tRNA^{Ala}(GGC)), to $\sim 10\%$ for tRNA^{Ala}(n3). Aminoacylation levels were influenced by sequence changes in the tRNA body, likely influencing tertiary structure, as aaRS identity elements of tRNA^{Ala} were maintained for all designs. Aminoacylation levels of tRNAs derived from design II (n1, n2) were generally higher in comparison to design I (n3, n4, n5). The results suggest that the additional tertiary interactions considered in design II lead to a higher fraction of correctly folded tRNAs and thus, to higher aminoacylation levels. In accordance with literature, these additional base pairs appear to be essential for formation of the L-shaped tertiary structure [77,79,80]. tRNA^{Ala}(n6), thought to serve as a negative control due to depleted tertiary interactions, was aminoacylated as well. This suggested that the presence of identity elements of tRNA^{Ala} is enough to stimulate aminoacylation. However, the fraction of misfolded tRNAs appears to influence aminoacylation levels, as designs I and n6 in comparison to designs II were charged to lesser extent. Reported aminoacylation efficiencies of *in vitro* transcribed tRNAs vary. Bashkaran and coworkers observed aminoacylation levels of 60-65% for a *M. thermautotrophicus* tRNA^{Gln} transcript [201]. In contrast, applying the same experimental set up, the Kothe group did not observe aminoacylation levels higher than 40-50% for a *E. coli* tRNA^{Phe} transcript [203]. Note that, in this study, aminoacylation levels did not exceed $\sim 30\%$, even for *in vitro* transcribed native tRNA^{Ala}.

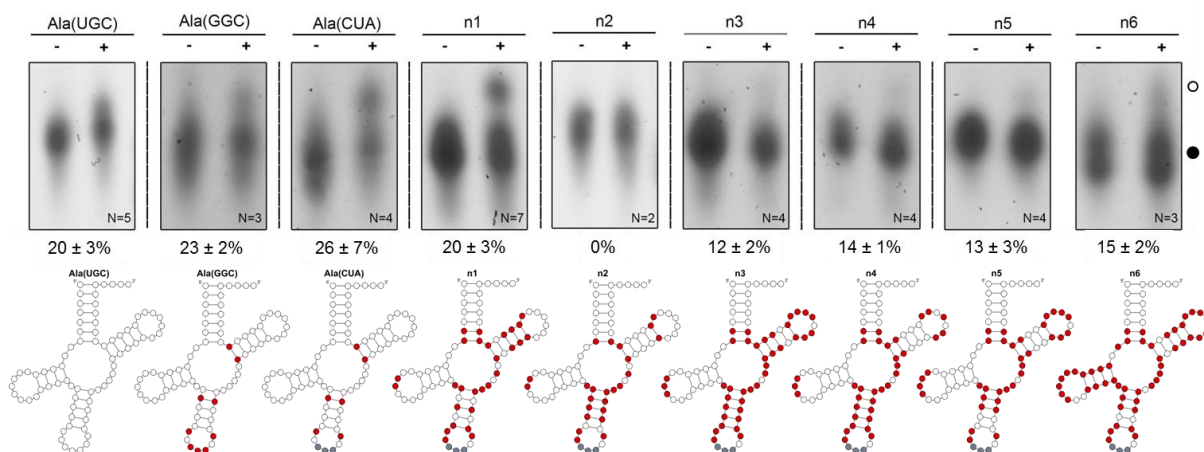


Figure 9: *In vitro* aminoacylation levels vary between designed nonsense suppressor *E. coli* tRNA^{Ala} species. Analysis of tRNAs subjected to aminoacylation with Ala by semi-purified *E. coli* Alanyl-tRNA synthetase (+) or *in vitro* transcribed tRNAs (-). Charged tRNAs (○) were detected by their slower migration compared to uncharged tRNA (●) in 6.5% acidic denaturing PAGE. tRNAs were visualized by SYBR gold staining. Aminoacylation levels are represented as mean \pm s.d. of biological replicates. The number of biological replicates (N) is given in the right lower corner. Base substitutions in comparison to native tRNA^{Ala}(UGC) are marked with red circles.

No aminoacylation of tRNA^{Ala}(n2) could be detected, even though the G3-U70 wobble base pair, serving as main identity element for aminoacylation by AlaRS, was present. Introduction of the G3-U70 base pair in the acceptor stem of tRNA^{Cys} or tRNA^{Phe} has been shown to enable aminoacylation with Ala [89,90]. In light of these results, the lack of aminoacylation of n2 was surprising. Substitution of the 7-66 base pair alone (n2 AS2) or in combination with the 6-67 base pair (n2 AS3) according to those found in n1 increased aminoacylation (Figure 10). However, exchange of only the 6-67 base pair (n2 AS1) did not show the same trend. Interestingly, n2 AS1 contained the same combination of the 6-67 and 7-66 base pair as compared to n5 (Table 8), which could be aminoacylated, although to lower extent than n1. Thus, the combination of the U6-A67 and C7-G66 or G6-C67 and C7-G66 base pairs within the sequence context of n2 seems to be incompatible with aminoacylation. The reason for the absence of recognition by AlaRS remains elusive.

Table 8: Combinations of 6-67 and 7-66 base pairs found within different tRNA designs and native tRNA^{Ala}.

tRNA species	6-67 base pair	7-66 base pair
n1	G-C	G-C
n2	U-A	C-G
n2 AS1	G-C	C-G
n2 AS2	U-A	G-C
n2 AS3	G-C	G-C
n3	C-G	C-G
n4	C-G	C-G
n5	G-C	C-G
n6	G-C	G-C
tRNA ^{Ala} (GGC)	U-A	A-U
tRNA ^{Ala} (UGC)	U-A	A-U

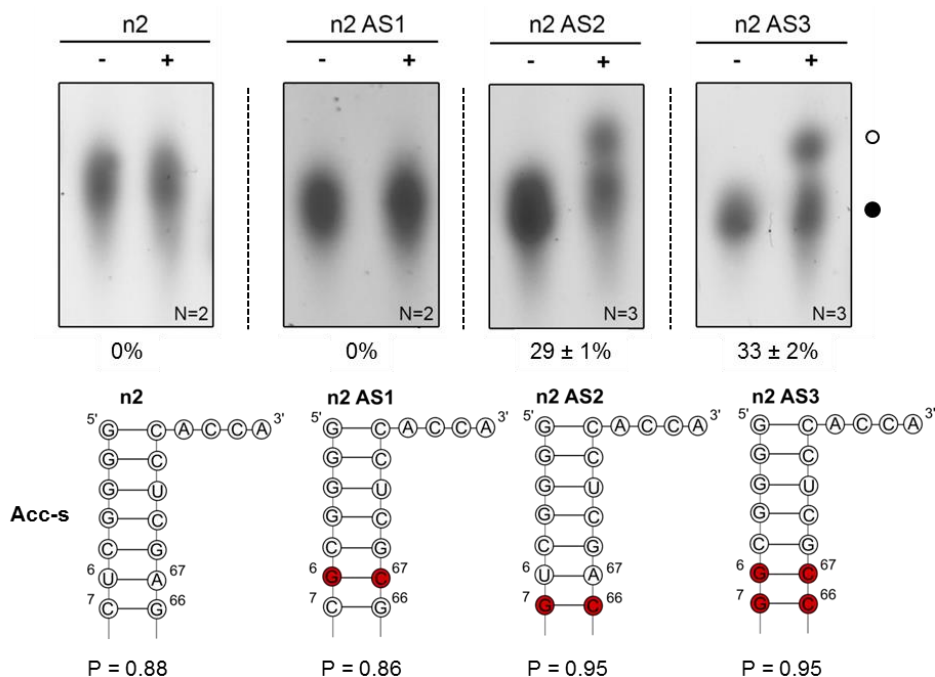


Figure 10: Aminoacylation of tRNA^{Ala} requires a specific combination of the base pairs in position 6-67 and 7-66. Base pairs 6-67 and 7-66 within the acceptor stem (Acc-s) of n2 were subsequently substituted according to those found in n1. tRNAs subjected to aminoacylation with Ala by semi-purified *E. coli* Alanyl-tRNA synthetase (+) or *in vitro* transcribed tRNAs (-) were analyzed. Charged tRNAs (○) were detected by their slower migration compared to uncharged tRNA (●) in 6.5% acidic denaturing PAGE. tRNAs were visualized by SYBR gold staining. Aminoacylation levels are represented as mean \pm s.d. of biological replicates. The number of biological replicates (N) is given in the right lower corner. Base substitutions in the acceptor stem in comparison to n2 are marked with red circles. P represents the probability of the tRNA sequences to form the cloverleaf secondary structure.

5.3 Editing of the tRNA anticodon region barely influences aminoacylation levels

As evident from the analysis of 932 elongator tRNA genes by Westhof and Auffinger [54], the bases within the seven nucleotide tRNA anticodon loop are rather conserved. With exception of the triplet anticodon, the flanking four bases exhibit a strong bias for certain nucleotides (Table 9) [54]. Especially noteworthy is the presence of the invariant uridine at position 33. This bias was not considered in the composition of the anticodon loop of the tRNA designs (Figure 7). Thus, new tRNA sequences were generated in which bases found within the anticodon loop of n1 and n3 were subsequently exchanged by the ones most frequently found at these positions, leading to the design n1A1, n1A2 and n3A1, n3A2 (Figure 11). One exception was the selected G37, which is found less frequent in comparison to A37.

Table 9: Bias for nucleotides found at position 32, 33, 37 and 38 within the anticodon loop of 932 elongator tRNA genes.

Nucleotide position	Nucleotide frequency within tRNA genes
32	C>T>A
33	T>>A
37	A>G
38	A>C>T

Substitution of the A31-U39 or G31-C39 base pair with C31-G39 generated the designs n1A3 and n3A3, respectively (Figure 11). As expected, anticodon substitutions did not drastically influence aminoacylation levels of the tRNA^{Ala} variants (Figure 11). A slight increase in aminoacylation was observed for n1A1, n1A2 and n1A3 in comparison to the original n1.

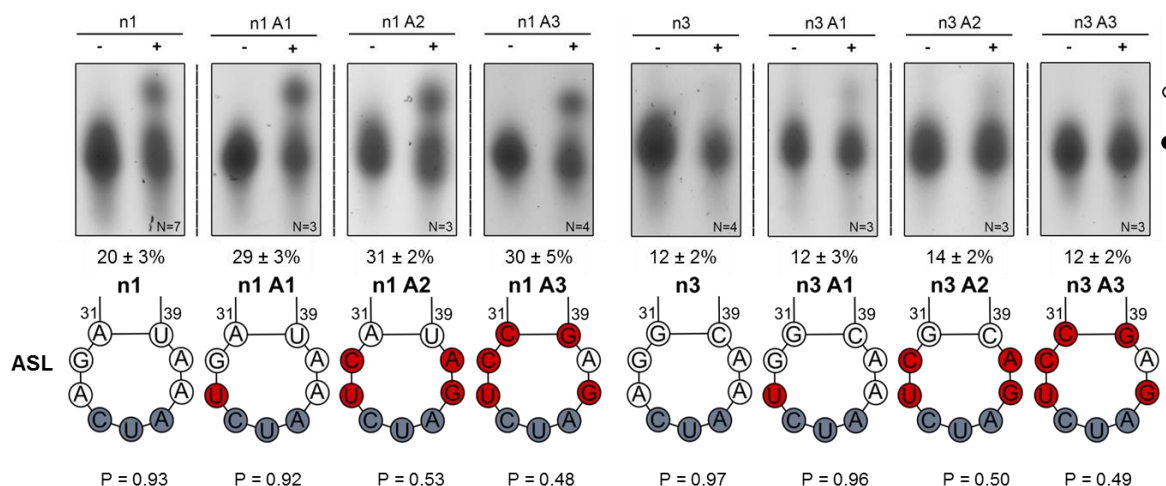


Figure 11: Anticodon substitutions barely influence aminoacylation levels of designed nonsense suppressor *E. coli* tRNA^{Ala} species. tRNAs subjected to aminoacylation with Ala by semi-purified *E. coli* Alanyl-tRNA synthetase (+) or *in vitro* transcribed tRNAs (-) were analyzed. Charged tRNAs (○) are detected by their slower migration compared to uncharged tRNA (●) in 6.5% acidic denaturing PAGE. tRNAs were visualised by SYBR gold staining. Aminoacylation levels are represented as mean ± s.d. of biological replicates. The number of biological replicates (N) is given in the right lower corner. Base substitutions in the anticodon stem-loop region (ASL) in comparison to original n1 or n3 are marked with red circles. P refers to the probability to form the cloverleaf secondary structure.

5.4 Assessing tRNA functionality by GFP read-through assay

Previous results presented evidence that the designed tRNAs fulfill one prerequisite for non-sense suppression, the successful aminoacylation by AlaRS. However, the question remains whether the tRNAs are functional in translation. tRNA functionality was assessed by their

ability to promote nonsense suppression. Therefore, a GFP read-through assay previously established by Geslain and coworkers was utilized (Figure 12) [133]. In this assay, *in vitro* or *in vivo* translation of GFP variants containing a premature termination codon (PTC) was performed in the presence of nonsense suppressor tRNAs. Functional nonsense suppressor tRNAs will incorporate Ala in place of the PTC, leading to the expression of fluorescent active GFP. On the other hand, lack of full-length GFP expression, upon recognition of the PTC by release factors and consequent termination of translation, indicates the presence of inactive nonsense suppressor tRNAs. GFP readout, thus, serves as a measure for nonsense suppression efficiency and can be determined with immunoblotting, FACS or fluorescence intensity measurements. Due to inconsistencies in the GAPDH-signal, immunoblots were not quantified. Construction of the GFP PTC variants occurred by substituting a Ser codon at position 28 or 29 for *in vitro* translation or *in vivo* translations by either of the three stop codons (TAA, TAG or TGA), respectively. Geslain and coworkers have previously shown that any amino acid can be accommodated in this position without perturbing GFP fluorescence [133]. A GFP construct with Ala instead of Ser at position 28 or 29, as expected in the case of functional nonsense suppressor tRNAs, should therefore show the same fluorescence emission as wildtype.

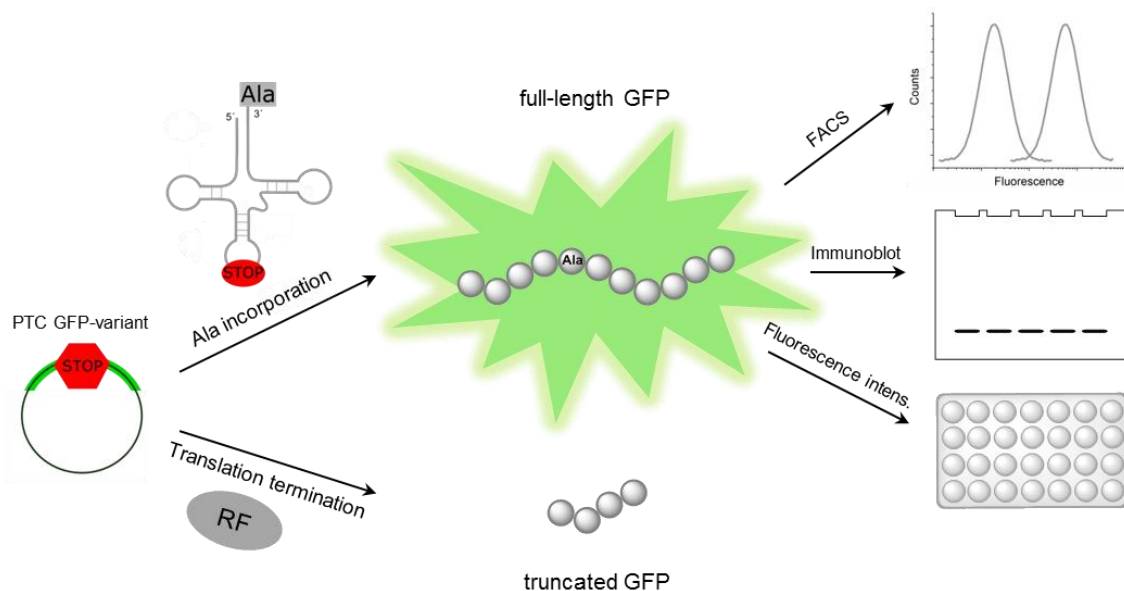


Figure 12: Scheme of the GFP read-through assay used to determine nonsense suppression efficiencies of tRNAs. *In vitro* or *in vivo* translation of a PTC-containing GFP variant can be used to assess nonsense suppressor tRNA efficiencies. Functional nonsense suppressor tRNA incorporate Ala in place of the PTC, leading to full-length GFP expression detectable by FACS, immunoblot or fluorescence intensity measurements. Lack of tRNA functionality in nonsense suppression results in recognition of PTC by RF. In turn, translation will be terminated, leading to truncated GFP and lack of fluorescence (adopted from Geslain et al. [133]).

The following experiments focused on the designs n1-n1A3, derived from design II with comparatively high aminoacylation levels, and n3-n3A3, obtained from design I with lower aminoacylation levels (Figure 7).

5.5 *In vitro* translation reactions show the importance of tRNA modifications

In vitro translation reactions were performed using *E. coli* S30 lysate supplemented with a codon optimized GFP amber or opal variant and increasing concentrations of nonsense suppressor tRNAs. Even in the absence of nonsense suppressor tRNAs, the *in vitro* translation reactions showed high background suppression (Figure 13).

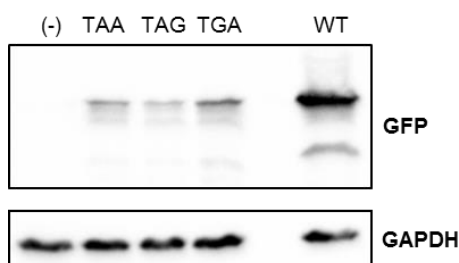


Figure 13: *In vitro* translation reactions show high background suppression in the absence of nonsense suppressor tRNAs. Representative immunoblot of *in vitro* translation reactions of TAA-, TAG-, TGA-containing GFP (N=7).

In vitro translation of the amber GFP variant supplemented with tRNA^{Ala}(CUA(G)) resulted in nonsense suppression near the background level (Figure 14A). A dose-dependent increase in PTC read-through was observed for *in vitro* translation of the opal GFP variant with addition of tRNA^{Ala}(UCA(U)) (Figure 14B).

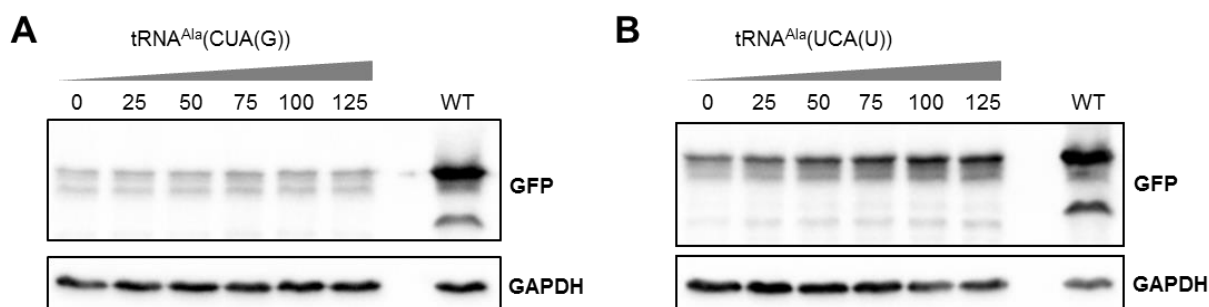


Figure 14: *In vitro* transcripts increase GFP expression levels only marginally. Representative immunoblot of *in vitro* translation reactions of the amber GFP variant supplemented with 0-125 ng tRNA^{Ala}(CUA(G)) (A) and of the opal GFP variant supplemented with 0-125 ng tRNA^{Ala}(UCA(U)) (B) (N=2).

In comparison to *in vitro* translation reactions without addition of tRNA^{Ala}(UCA(U)), the GFP expression was increased by maximal 2-fold and background suppression made it difficult to precisely assess nonsense suppression levels. Low nonsense suppression levels of *in vitro* transcripts might be caused by lack of post-transcriptional modifications of tRNAs. Thus, instead of *in vitro*, the GFP read-through assay was performed *in vivo* in order to assess whether presence of post-transcriptional modifications increases nonsense suppression levels.

5.6 0.05% (v/v) L-arabinose induces maximal GFP expression of pBAD33 vectors expressed in XL1-blue cells

For *in vivo* experiments, eGFP wildtype and its PTC variants were subcloned into the pBAD33 vector under control of the L-arabinose-inducible P_{BAD} promoter. The concentration of L-arabinose resulting in maximal eGFP wildtype expression in XL1-blue cells was assessed by immunoblot or FACS (Figure 15).

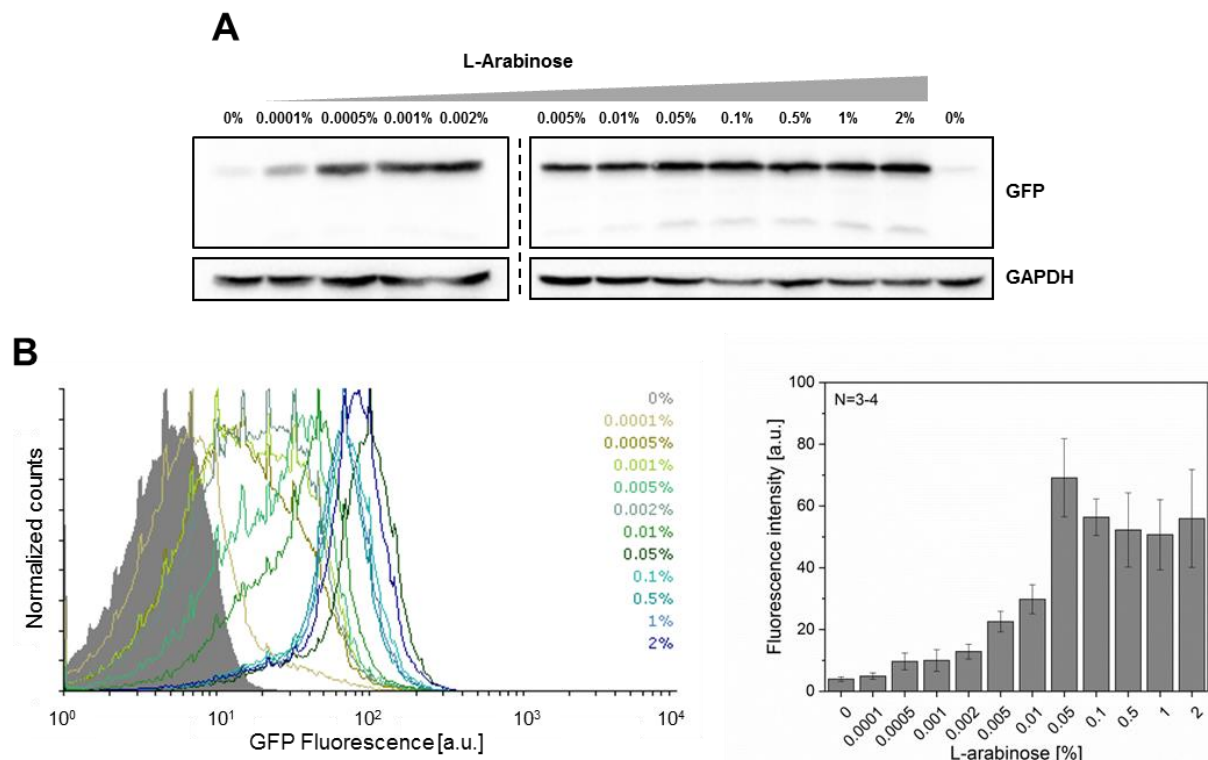


Figure 15: Concentration-dependent induction of eGFP wildtype expression in XL1-blue cells with L-arabinose. eGFP wildtype under control of L-arabinose inducible P_{BAD} promoter was expressed in XL1-blue cells and supplemented with 0%-2% L-arabinose to assess the L-arabinose concentration that induces maximal eGFP expression. Representative immunoblot (A) (N=3) with GAPDH serving as loading control and FACS results (B). FACS results are represented as the mean \pm s.d. of biological replicates. The number of biological replicates (N) is given in the left upper corner.

Presence of the P_{BAD} promoter has been shown to result in an “all-or-none” autocatalytic induction of gene expression upon supplementation with L-arabinose [204]. The same trend could be observed in this study. At intermediate concentrations of L-arabinose two populations were observed, a subpopulation of cells that was fully induced, whereas other cells were uninduced (Figure 15B, left panel). With increasing L-arabinose concentration the population of fully induced cells increased, whereas the fraction of uninduced cells decreased. Maximal wildtype eGFP expression was observed for L-arabinose concentration of 0.05% (v/v). Higher L-arabinose concentrations resulted in no further increase, but rather a repression of eGFP expression. Thus, all *in vivo* experiments were performed at L-arabinose concentration of 0.05% (v/v).

5.7 The natural read-through of termination codons in XL1-blue cells decreases in the order TAG>TGA~TAA

The natural read-through of stop codons varies between different *E. coli* strains, depending on the presence of natural nonsense suppressor tRNAs. Therefore, the natural read-through of TAA-, TAG- and TGA-containing eGFP variants in XL1-blue cells was examined (Figure 17). Construction of the PTC variants occurred by substituting the codon AGC coding for Ser at position 29 by either of the three stop codons (TAA, TAG or TGA) (Figure 16). All stop codons were inserted at the same position within the eGFP gene in order to exclude effects from reading context.

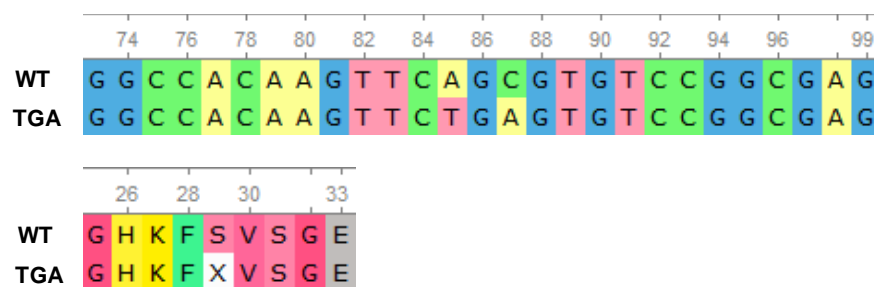


Figure 16: Nucleotide (upper panel) and amino acid (lower panel) sequence alignment of eGFP wildtype and its TGA-variant. AGC coding for Ser (S) at position 29 was replaced by the stop codon TGA (X) (alignment was performed with Unipro UGENE).

The natural stop codon read-through in XL1-blue cells decreased in the order TAG>TGA~TAA (Figure 17). This observation seemed to contradict the literature suggesting that bacteria lacking nonsense suppressor tRNA genes, read-through is most frequent at TGA, followed by TAG and TAA, respectively [205]. TGA read-through has been shown to be

more pronounced due to the misreading by tRNA^{Trp} normally decoding UGG codons [206], resulting in read-through levels of 10^{-2} - 10^{-4} [205,207]. XL1-blue cells encode a natural supE44 amber suppressor tRNA in their genomes (<https://www.chem-agilent.com/pdf/strata/200249.pdf>, Stratagene manual), explaining the high levels of read-through in the case of the TAG-containing eGFP variant. As a result, the designed amber nonsense suppressor tRNAs used in previous experiments would be in competition with supE44. PTC read-through caused by designed nonsense suppressor tRNAs or supE44 would be indistinguishable and thus, assessment of tRNA functionality altered. Thus, a eGFP opal variant (TGA) and the corresponding nonsense suppressor tRNAs containing 5'-UCA-3' anticodons were used for the *in vivo* experiments in this study.

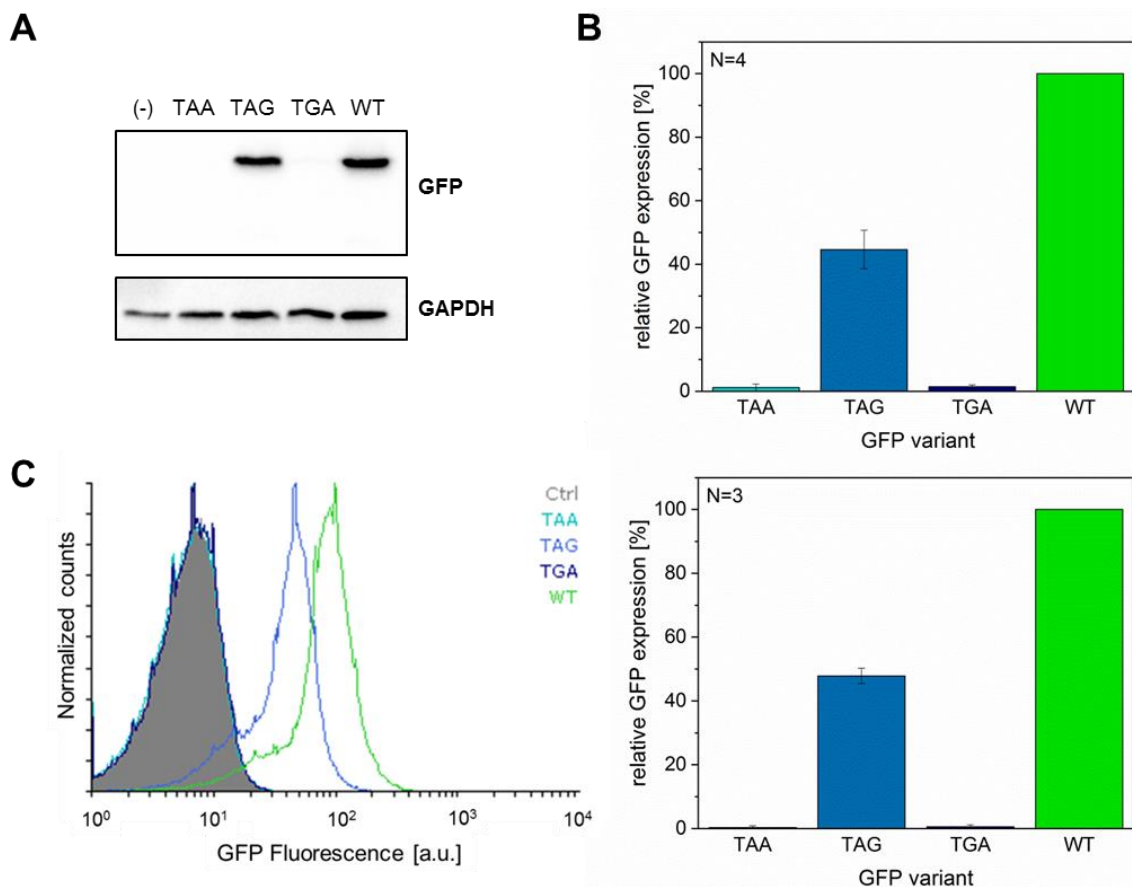


Figure 17: Natural stop codon read-through in XL1-blue cells decreases in the order TAG>TGA~TAA. GFP expression of TAA-, TAG- and TGA-containing eGFP variants in XL1-blue cells assessed by immunoblot (A), fluorescence intensity measurements (B) or FACS (C). (A) Representative immunoblot (N=9). GAPDH served as loading control. For (B) fluorescence values were normalized to OD_{600nm} of the bacterial culture. For (B) and (C) background fluorescence of a strain carrying the empty vector, designated as Ctrl, was subtracted and the fluorescence was normalized to strain-specific eGFP wildtype fluorescence. Data represent mean \pm s.d. of biological replicates. The number of biological replicates (N) is given in the left upper corner.

5.8 tRNA expression reduces cell growth

tRNAs were subcloned into the vector pBST NAV2 under control of the constitutive *lpp*-promoter and *rrnC*-terminator [208]. tRNA expression was performed in the recombination (*recA*) deficient *E. coli* strain XL1-blue. The influence of nonsense suppressor tRNA expression on XL1-blue cell growth was monitored and compared to native tRNA^{Ala} isoacceptors (Figure 18, left panel). The specific growth rate, μ , and doubling time, t_d , of each culture were determined (Table 10). Due to the fast adaptation of XL1-blue cells to the culturing conditions, duration of the lag phase could not be assessed. Monitoring cell growth by OD_{600nm} measurements is not completely accurate, because both, living and dead cells are considered. Recording the number of viable cells over time would be a more precise measurement. However, only a small fraction of dead cells is expected until reaching the stationary phase and the specific growth rate and doubling time were determined using the exponential phase. Thus, OD_{600nm} values can be a good estimate to assess differences in cell growth between cultures.

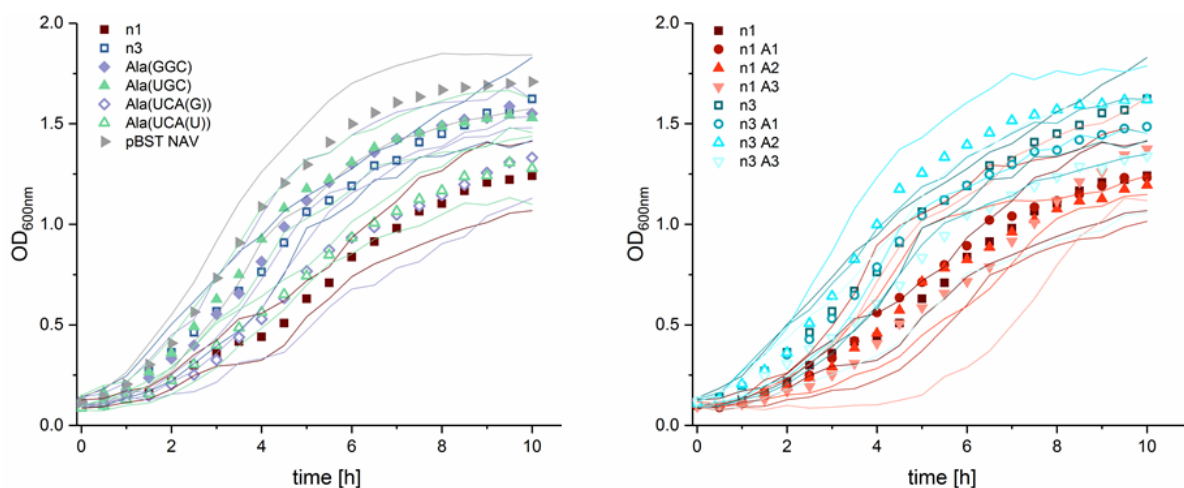


Figure 18: tRNA expression reduces XL1-blue cell growth. tRNAs were expressed under control of the constitutive *lpp* promoter and *rrnC* terminator in XL1-blue cells. Cell growth was monitored by recording OD_{600nm} every 30 min. Data represents mean \pm s.d. of at least 3 biological replicates. Standard deviations are represented as lines.

tRNA overexpression, regardless of native tRNA^{Ala} isoacceptors or nonsense suppressors, resulted in a reduction of cell growth in comparison to the empty vector pBST NAV2. According to their effect on growth, tRNAs can be divided into two groups. One group comprises tRNAs leading to a small reduction in cell growth, as observed for native tRNA^{Ala} isoacceptors and n3 variants. The other group showed a stronger impairment of cell growth, as observed for tRNA^{Ala}(UCA(G)), tRNA^{Ala}(UCA(U)) and n1 variants (Figure 18, left panel).

n1 and n3 variants edited within their anticodon region showed similar growth behavior as their parental tRNA (Figure 18, right panel).

Table 10: Specific growth rates μ and doubling times t_d of XL1-blue cells expressing different tRNA variants. Values were obtained from the exponential phase of the growth curve.

tRNA variant	Specific growth rate μ	Doubling time t_d
NAV	0.63 h ⁻¹	1.1 h
n1	0.49 h ⁻¹	1.4 h
n1A1	0.50 h ⁻¹	1.4 h
n1A2	0.44 h ⁻¹	1.6 h
n1A3	0.45 h ⁻¹	1.5 h
n3	0.54 h ⁻¹	1.3 h
n3A1	0.54 h ⁻¹	1.3 h
n3A2	0.60 h ⁻¹	1.2 h
n3A3	0.50 h ⁻¹	1.4 h
Ala(GGC)	0.58 h ⁻¹	1.2 h
Ala(UGC)	0.60 h ⁻¹	1.2 h
Ala(UCA(G))	0.51 h ⁻¹	1.4 h
Ala(UCA(U))	0.52 h ⁻¹	1.3 h

To date, only a limited number of reports on the influence of opal suppressor tRNA expression on cell growth in *E. coli* exist. Amber nonsense suppressor tRNAs, even if highly efficient, were shown to have little effect on cell growth. On the other hand, expression of ochre suppressor tRNAs inhibited cell growth [209]. This difference in the effect on growth is attributed to the abundance of the corresponding targeted termination codons [209]. The most common stop codon in *E. coli* is UAA with a frequency of ~59% (<https://www.kazusa.or.jp/codon/>, Codon Usage Database) and it is overrepresented in highly expressed genes (HEGs) [205,210]. Nonsense suppressor tRNAs targeting native stop codons will lead to generation of C-terminally extended polypeptides accompanied by loss of activity and likely degradation of the protein. Because UAA-ending genes are overrepresented in the *E. coli* genome and repeated cycles of translation are energy consuming, cell growth declined in the presence of ochre suppressor tRNAs [209]. In contrast, amber stop codons occur only with a frequency of ~9% in *E. coli* genes (<https://www.kazusa.or.jp/codon/>, Codon Usage Database) and are underrepresented in highly expressed genes [205]. Because only a minor fraction of *E. coli* genes terminates with UAG codons, the effect of amber suppression on cell

growth is less pronounced. The abundance of opal codons is 32% (<https://www.kazusa.or.jp/codon/>, Codon Usage Database) and thus, growth impact would be expected to be between that observed for amber and ochre suppressors. If opal nonsense suppressor activity, i.e. the fraction of read through stop codons, correlates with growth suppression, the growth behavior of the different tRNA designs (Figure 18) suggests a higher potential of n1 variants in promoting nonsense suppression.

5.9 Nonsense suppressor tRNAs derived from native tRNA^{Ala} promote read-through of PTCs

The eGFP opal construct as well as different tRNA designs were co-transformed into XL1-blue cells. Co-transformation was verified by double restriction digestion with XbaI and PstI, each of which restricting the eGFP and tRNA bearing vector, respectively (Supplementary Figure S2). Transformation efficiency decreased with increasing plasmid size, causing a disproportion of the ratio of both plasmids in the cell. Thus, tRNA-encoding pBST NAV2 plasmids with a size of ~3 kb showed higher transformation efficiencies compared to the eGFP opal variant containing ~6 kb.

Nonsense suppression of tRNA^{Ala} isoacceptors and their corresponding opal variants was assessed by GFP read-through assay (Figure 19). As expected, tRNA^{Ala}(GGC)- and tRNA^{Ala}(UGC)-mediated nonsense suppression was near the background levels. The strongest promotion of nonsense suppression could be observed for tRNA^{Ala}(UCA(U)), the opal suppressor of tRNA^{Ala}(UGC). In comparison, read-through levels of tRNA^{Ala}(UCA(G)), derived from anticodon substitution of tRNA^{Ala}(GGC), were reduced. Poor suppression of tRNA^{Ala}(UCA(G)) did not result from decreased tRNA levels, as evident from Northern blotting (Figure 19). tRNA levels of both nonsense suppressors were comparable, however, much less than tRNA^{Ala}(GGC) and tRNA^{Ala}(UGC).

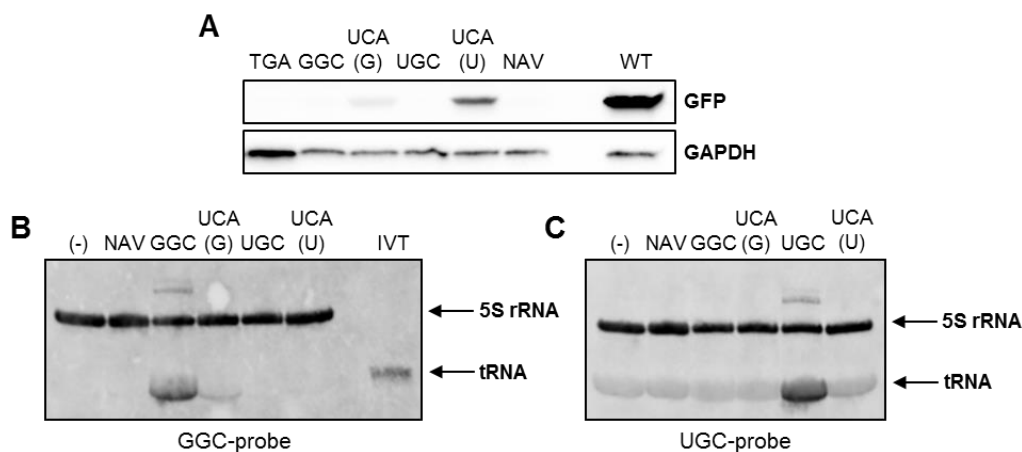


Figure 19: tRNA^{Ala}(UCA(U)) serves as a good scaffold for promoting read-through of opal PTCs. Representative immunoblot (N=3-4) of XL1-blue cells co-expressing the eGFP opal construct and native tRNA^{Ala}(GGC), tRNA^{Ala}(UGC) and their corresponding opal variants tRNA^{Ala}(UCA(G)) and tRNA^{Ala}(UCA(U)), respectively (A). XL1-blue cells expressing wildtype eGFP (WT), the eGFP opal construct solely (TGA) and in combination with the empty tRNA vector pBST NAV2 (NAV) were used as control. GAPDH served as loading control. Representative Northern blot probed against 5S rRNA and tRNA^{Ala}(GGC) (B) or tRNA^{Ala}(UGC) (C) (N=3). tRNA expression was compared to untransformed XL1-blue cells (-) and XL1-blue cells expressing the empty vector pBST NAV2 (NAV). *In vitro* transcribed tRNA^{Ala}(GGC) (IVT) was used as tRNA length standard.

Comparison of both tRNA sequences showed differences in the 28-42, 32-38 pair in the anticodon stem-loop region (ASL) and 49-65 base pair in the TΨC-stem (Table 11). This suggests that reduced nonsense suppression of tRNA^{Ala}(UCA(G)) in comparison to tRNA^{Ala}(UCA(U)) might be a result of impaired EF-Tu binding or suboptimal anticodon context.

Table 11: Sequence deviations between tRNA^{Ala}(GGC) and tRNA^{Ala}(UGC). Alignment of both native tRNA^{Ala} sequences shows difference in the base pairs at positions 28-42, 32-38 and 49-65.

Nucleotide position	tRNA ^{Ala} (GGC)	tRNA ^{Ala} (UGC)
28-42	U-A	C-G
32-38	A-U	U-C
49-65	A-U	U-A

5.10 Anticodon-edited tRNAs do not promote nonsense suppression

The positive controls tRNA^{Ala}(UCA(G)) and tRNA^{Ala}(UCA(U)) were expressed in XL1-blue cells and successfully promoted nonsense suppression of a PTC-containing GFP variant (Figure 19). Thus, nonsense suppression of the designs n1 and n3, derived from the original semi *de novo* design, as well as of their anticodon-edited variants n1A1, n1A2, n1A3 and n3A1, n3A2 and n3A3 (Figure 11), respectively, was assessed by immunoblot (Figure 20).

Anticodon-editing of n1 and n3 was performed, because a strong bias for nucleotides within the anticodon loop has been observed. (Figure 4) [54]. Thus, these evolutionary preserved nucleotides might be advantageous for tRNA functionality. Hence, nucleotides located within the anticodon loop and the 31-39 base pair of n1 and n3 were exchanged by those found most frequently among elongator tRNAs (Table 9).

GFP read-through of the nonsense suppressor tRNA designs n1 and n3 were near the background levels. The same trend was observed for the anticodon-edited designs n1A1-n1A3 and n3A1-n3A3 (Figure 20). Fluorescence intensity and FACS measurements resulted in nonsense suppression levels below the detection limit. tRNA levels of all designs based on n1 and n3 were close to the detection limit, as for some biological replicates tRNA expression was observed, for others not.

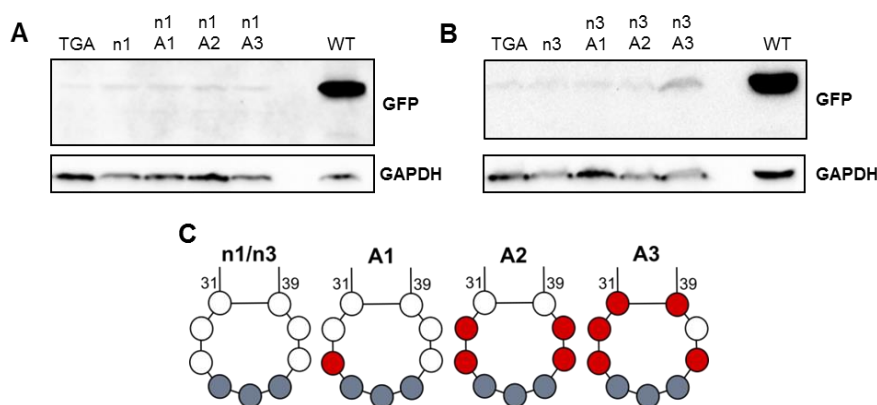


Figure 20: Nonsense suppressor tRNA^{Ala} designs n1, n3 and their anticodon-edited variants n1A1-n1A3 and n3A1-n3A3 do not promote nonsense suppression. Representative immunoblot (N=2-3) of XL1-blue cells co-expressing the eGFP opal construct and nonsense suppressor tRNA design n1 (A) and n3 (B) as well as their anticodon-edited versions n1A1-n1A3 (A) and n3A1-n3A3 (B), respectively. XL1-blue cells expressing the wildtype eGFP (WT) and the eGFP opal construct (TGA) were used as controls. GAPDH served as loading control. Scheme of the anticodon substitutions of n1 and n3 (C). Base substitutions in comparison to original n1 or n3 are marked in red. Immunoblots were overexposed to detect lowly expressed eGFP.

Because tRNA^{Ala}(UCA(U)) served as a good scaffold for nonsense suppression, the anticodon loop of n1A3 was subsequently substituted by that found in tRNA^{Ala}(UCA(U)), leading to the designs n1A3_A37, n1A4 and n1A5. Read-through of the opal eGFP-variant in XL1-blue cells was assessed by immunoblot (Figure 21). Again, low nonsense suppression levels were observed for the designs n1A3_A37, n1A4 and n1A5. As evident from Northern blot, levels of tRNA transcripts were close to the limit of detection.

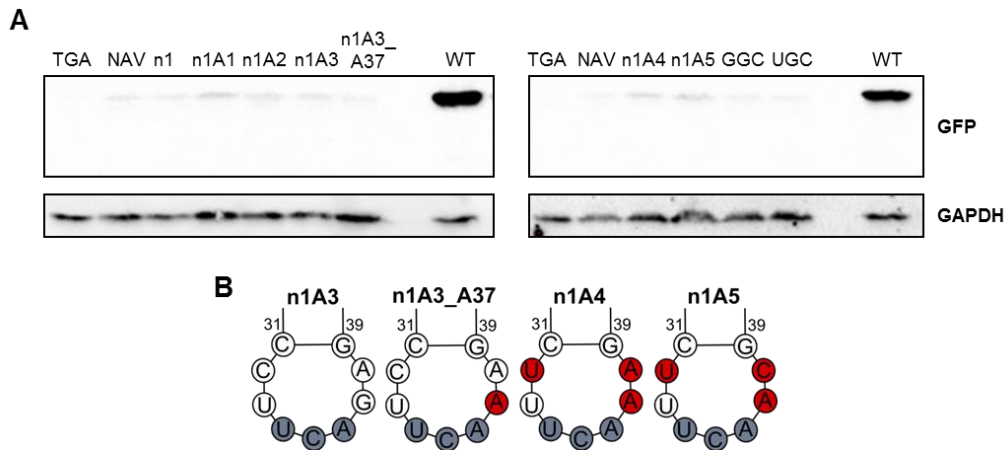


Figure 21: Transplantation of tRNA^{Ala}(UCA(U)) anticodon loop into n1A3 does not increase PTC read-through. Representative immunoblot (N=2) of XL1-blue cells co-expressing the eGFP opal construct and nonsense suppressor tRNA designs n1, n1A1, n1A2, n1A3, n1A3_A37, n1A4, n1A5, tRNA^{Ala}(GGC) and tRNA^{Ala}(UGC) (A). XL1-blue cells expressing the wildtype eGFP (WT), the eGFP opal construct (TGA) solely and in combination with the empty tRNA vector pBST NAV2 (NAV) were used as control. GAPDH served as loading control. Scheme of the anticodon substitutions of n1A3 (B). Base substitutions in comparison to original n1A3 are marked in red. Immunoblots were overexposed to detect lowly expressed eGFP.

5.11 The TΨC-stem is the main determinant of nonsense suppression

Substitutions within the anticodon region did not improve nonsense suppression, thus, suboptimal EF-Tu binding might explain the lack of tRNA activity. Elongation factor EF-Tu binds aa-tRNAs to form the ternary complex aa-tRNA·EF-Tu·GTP, which reach the ribosomal A-site by diffusion to enable decoding of the positioned mRNA codon (reviewed in [27–31,101]). Cognate codon-anticodon interaction triggers GTP hydrolysis, followed by dissociation of the aa-tRNA and its accommodation within the ribosomal A-site. Thus, EF-Tu has a crucial role in tRNA selection during decoding and binding affinities of aa-tRNAs to EF-Tu need to be finely tuned. Too weak EF-Tu binding causes reduced ternary complex formation and thus, inefficient delivery of aa-tRNAs to the ribosomal A-site [106,109]. This in turn could increase the probability of recognition of the PTC by competing release factors, which will induce termination of translation and reduce the amount of full-length polypeptide. Too strong EF-Tu binding on the other hand inhibits the release of aa-tRNAs from EF-Tu·GDP during decoding, resulting in reduced rates of peptide bond formation and thus, decreased amounts of full-length polypeptide [106,109]. EF-Tu binding affinities of aa-tRNAs are finely tuned by compensatory thermodynamic contributions of the tRNA TΨC-stem sequence and the attached amino acid [106,108,109]. Nonsense suppressor tRNAs used in this study con-

tained recognition elements of AlaRS (Figure 7) and thus, should be aminoacylated with Ala. Ala has a destabilizing effect on EF-Tu binding, which is compensated by high EF-Tu binding affinity of the tRNA^{Ala} TΨC-stem sequence (Table 3) [106,108]. Thus, the 49-65, 50-64 and 51-63 base pairs located within the TΨC-stem of n1A3 were exchanged by those found in tRNA^{Ala}(UCA(U)), leading to design TS1 (Figure 22). This replacement anticipated optimized EF-Tu binding, as these base pairs were shown to contribute maximally to EF-Tu binding affinity of aa-tRNAs [104,108]. In another attempt, the TΨC-stem base pairs of n1A3 were replaced with those found in tRNA^{GluE2}, showing one of the highest EF-Tu binding affinities among the canonical tRNA species [106,108]. This way design TS2 was generated. As the thermodynamic contributions of the 49-65, 50-64 and 51-63 TΨC-stem base pairs can be viewed as independent from each other, $\Delta G^\circ(\text{tRNA})$ values can be predicted using the sum of $\Delta\Delta G^\circ$ of single base-pair substitutions as determined for *E. coli* tRNA^{Phe} [106]. According to predicted $\Delta G^\circ(\text{tRNA})$ values, EF-Tu binding affinities should follow the order TS2>TS1>n1A3.

Katoh and coworkers have previously shown that chimeric tRNAs composed of the TΨC-stem of tRNA^{GluE2} and the D-arm of tRNA^{Pro1}, named tRNA^{Pro1E2}(CGG), enabled consecutive β - and D-amino acid incorporation into polypeptides in response to different sense codons. Incorporation of unnatural amino acids was performed using a flexible *in vitro* translation system with optimized translation factor concentrations [152]. Nonetheless, this suggested that tRNA^{Pro1E2}(CGG) is a highly efficient tRNA entity. Thus, the D-region of tRNA^{Pro1} was transplanted into design n1A3, generating the tRNA variant D1. The D-arm of tRNA^{Pro} was chosen because during translation of a stretch of L-proline residues, this motif is specifically recognized by bacterial translation factor EF-P [119]. Due to the intrinsic poor nature of Pro as peptidyl donor and acceptor [111–116], translation elongation of mRNAs containing consecutive L-Pro residues is slowed down, causing ribosome stalling. However, acceleration of peptide bond formation upon recognition by EF-P alleviates ribosomal stalling [111,117,118]. Thus, due to the presence of the tRNA^{Pro} D-arm motif, EF-P could identify the nonsense suppressor tRNA designs D1 and DTS2 used in this study as interaction partners. EF-P binding might stabilize tRNA structures in the peptidyl transferase center as observed for tRNA^{Pro} [120] and facilitate translation elongation.

Furthermore, both, the TΨC-stem of tRNA^{GluE2} and D-region of tRNA^{Pro1}, as present in tRNA^{Pro1E2}(CGG), were incorporated into n1A3, leading to the design DTS2. Design DTS1 arose from swapping the TΨC-stem base pairs and D-region of n1A3 with that found in TS1

and D1, respectively. Utilizing these multiple designs, the contribution of the TΨC-stem and D-region on nonsense suppression efficiency was examined both in isolation and in combination.

As evident from the GFP PTC read-through assay, editing of the TΨC-stem showed highest contribution to nonsense suppression (Figure 22). Incorporation of the TΨC-stem of tRNA^{GluE2} into n1A3, designs TS2 and DTS2, resulted in GFP PTC read-through. Unexpectedly, transplantation of the TΨC-stem present in a native tRNA^{Ala} species, designs TS1 and DTS1, did not promote nonsense suppression. The same trend was also observed for n1A3 variants with substitution of the D-region only, as present in design D1. TS2 exhibited higher tRNA steady-state levels in comparison to all other investigated designs (Figure 22).

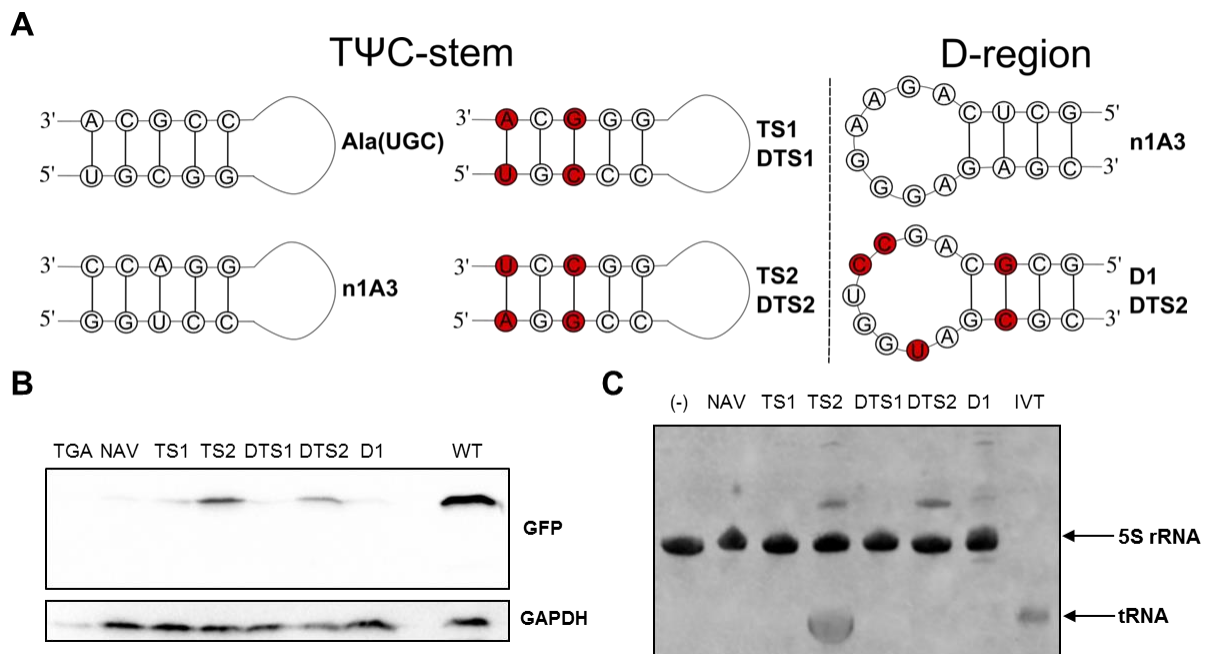


Figure 22: The TΨC-stem is the main determinant of nonsense suppression. Scheme of substitutions performed within the TΨC-stem and D-region of n1A3 (A). Substituted bases compared to original n1A3 are marked in red. Representative immunoblot (N=2-7) of XL1-blue cells co-expressing the eGFP opal construct and TΨC-stem- and/or D-arm-edited nonsense suppressor tRNAs of n1A3 (B). XL1-blue cells expressing the wildtype eGFP (WT), the eGFP opal construct (TGA) solely and in combination with the empty tRNA vector pBST NAV2 (NAV) were used as control. GAPDH served as loading control. Representative Northern blot probed against 5S rRNA; the anticodon region of n1A3 (n1A3 probe) and the acceptor stem of n1A3 (AS probe) (C) (N=1-4). tRNA expression was compared to untransformed XL1-blue cells (-) and XL1-blue cells expressing the empty vector pBST NAV2 (NAV). *In vitro* transcribed tRNA n1A3 (IVT) was used as RNA length standard.

Together, these results suggest that increased EF-Tu binding might protect tRNAs from cleavage by nucleases and thus, reduce tRNA turnover. Along that line, Kimura and Waldor

have shown that EF-Tu competes with the RNA degradosome and thus, protects hypomodified aminoacyl-tRNAs from degradation [211]. However, for design DTS2, which contains the same TΨC-stem sequence and also promoted GFP PTC read-through, no expression of RNAs with a size correlating to that of tRNAs was observed. As nonsense suppression could be observed for DTS2, tRNA levels supposedly lied below the detection limit. Instead, DTS2 showed the presence of RNA species with a size larger than 5S rRNA, as also be observed for TS2. This extended RNA species could be a result of inefficient termination of transcription despite the presence of the *rrnC* terminator following the tRNA gene. Formation of extended RNA species can also be observed by denaturing polyacrylamide gel electrophoresis (Figure S4).

5.12 Incorporation of A37 and variable loop extensions reduce nonsense suppression levels

Through editing of the TΨC-stem of n1A3 alone or in combination with the D-region, two designs, TS2 and DTS2, were identified as active nonsense suppression tRNAs. However, further base substitutions in the anticodon loop could potentially improve PTC read-through efficiencies even further. The majority of native tRNAs contain a highly modified purine at position 37 [191,212], which stabilizes the adjacent codon-anticodon interaction [185,191]. The presence of a hypermodified 2-methylthio-N⁶-isopentenyladenosine, ms²i⁶A, at position 37, 3'-adjacent to the anticodon triplet, has been observed for native tRNAs decoding codons beginning with U [184,213,214]. A variety of studies have shown that, depending on the tRNA species, a lack of the ms²i⁶A modification at A37 results in a reduction of nonsense suppression [58,192,193] and increased sensitivity to the context of the mRNA stop codon [195–198]. Thus, replacement of G37 by A37 in the designs TS2 and DTS2 might enable modification to ms²i⁶A and in turn increase the nonsense suppression levels. Importantly, the expression of the designs TS2_A37 and DTS2_A37 appeared to be lethal to XL1-blue cells. Transformation efficiencies of the pBST NAV2 vector coding for TS2_A37 and DTS2_A37 were low. Repetitive co-transformations resulted in only a few viable XL1-blue colonies. Assessment of the co-transformation of pBST NAV2 coding for A37-containing TS2 or DTS2 together with pBAD33 coding for the eGFP opal variant showed that either none or only small amounts of tRNA-encoding vector were present (Figure S3). A possible reason for the deleterious effect of TS2_A37 and DTS2_A37 on cell growth might be their high nonsense suppression activity. Highly efficient nonsense suppressor tRNAs would target native stop

codons, leading to generation of C-terminally extended proteins which might alter their folding and in turn result in a loss-of-function. Read-through of termination codons located at the end of essential genes could cause severe growth defects, explaining the reduced transformation efficiencies of TS2_A37- and DTS2_A37-encoding pBST NAV2. Due to the low transformation efficiency of tRNA-encoding vector in XL1-blue cells, nonsense suppression levels of TS2_A37- and DTS2-A37 were near the background levels (Figure 25).

Besides the acceptor stem, whose sequence is indispensable for the recognition by AlaRS, the influence of the variable region on nonsense suppression has not been evaluated yet. Geslain and coworkers have pointed out the importance of the variable loop length on the functionality of human nonsense suppressor tRNAs. They postulated that human tRNA^{Ala} confers weak suppressor activities due to the short length of the v-loop. In contrast, the enlarged variable loops of tRNA^{Leu}- and tRNA^{Ser}-derived suppressors are supposed to correlate with higher nonsense suppression efficiencies. Increasing the length of the variable loop of S07, a nonsense suppressor variant of tRNA^{Ser}, by two or three nucleotides, promoted read-through even further. This design was inspired by the 20-nt variable loop of human tRNA^{Sec}, a natural tRNA, inserting Sec at distinct UGA sequences. Thus, we next substituted the variable loop of TS2 and DTS2 with that found within the extended S07 variants and generated the designs TS2_V2, TS2_V3 and DTS2_V2 and DTS2_V3. In addition, an *E. coli* tRNA^{Sec}-like variable loop (tRNA database, <http://trna.bioinf.uni-leipzig.de/>) was incorporated, leading to TS2 V1.1 or DTS2 V1.1 (Figure 23). Extension of TS2/DTS2 V1.1 by one additional adenine at the 3'-end of the variable region, resulted in the designs TS2 V1 and DTS2 V1, respectively.

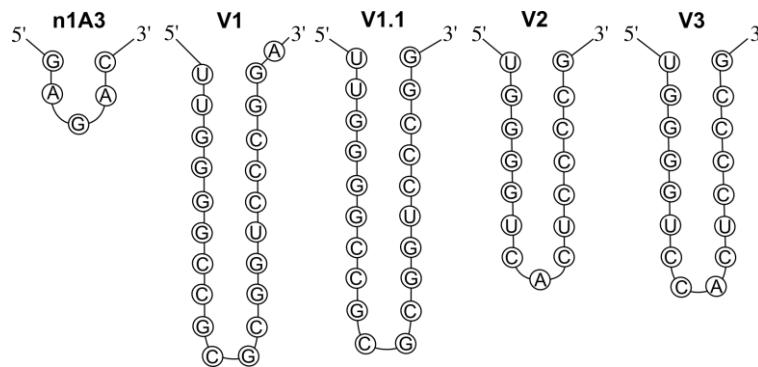


Figure 23: Scheme of the variable region extension of n1A3. Transplantation of an *E. coli* tRNA^{Sec}-like variable region into n1A3 generated the design V1.1. An additional incorporation of adenine at the 3'-terminal position of the v-region led to design V1. Transplantation of the v-region of active nonsense suppressor tRNAs derived from human tRNA^{Ser} led to designs V2 and V3, depending on the length of the v-loop.

The capacity to promote nonsense suppression by v-region extended tRNAs based on designs TS2 and DTS2 was assessed by GFP read-through assay (Figure 24).

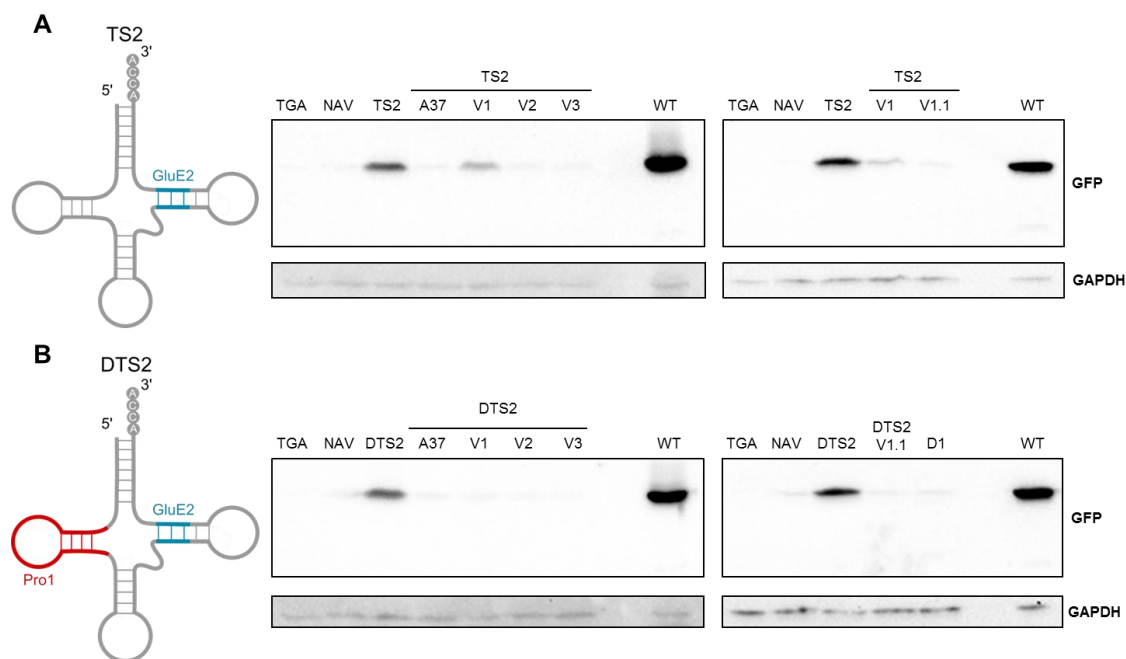


Figure 24: Extension of the variable region of TS2 and DTS2 causes a reduction of nonsense suppression. Representative immunoblot (N=1-7) of XL1-blue cells co-expressing the eGFP opal construct and variable region-extended nonsense suppressor tRNAs based on design TS2 (A) or DTS2 (B). XL1-blue cells expressing the wildtype eGFP (WT), the eGFP opal construct (TGA) alone and in combination with the empty tRNA vector pBST NAV2 (NAV) were used as controls. GAPDH served as loading control.

Enlargement of the variable loop of TS2 and DTS2 decreased the nonsense suppression levels near the background values (Figure 24). Only, TS2_V1, containing an *E. coli* tRNA^{Sec}-like variable region extended by an additional nucleotide, showed nonsense suppressor activity, albeit to much lower extent than TS2.

Reduced PTC read-through of v-region-extended tRNAs were not a result of decreased tRNA levels, as evident from Northern blot and denaturing polyacrylamide gel electrophoresis (Figure 25). On the contrary, extension of the variable region stabilized the tRNAs, leading to high steady-state levels. Due to the increased length of TS2/DTS2 V1, V1.1, V2 and V3 (★) and reduced fraction of native tRNAs migrating at the same height, denaturing polyacrylamide gel electrophoresis was sufficient to identify expression of these tRNAs. All variants analyzed showed a large fraction of extended RNA products, which were absent in the control RNAs obtained from untransformed XL1-blue cells and XL1-blue cells expressing the empty pBST NAV2 vector.

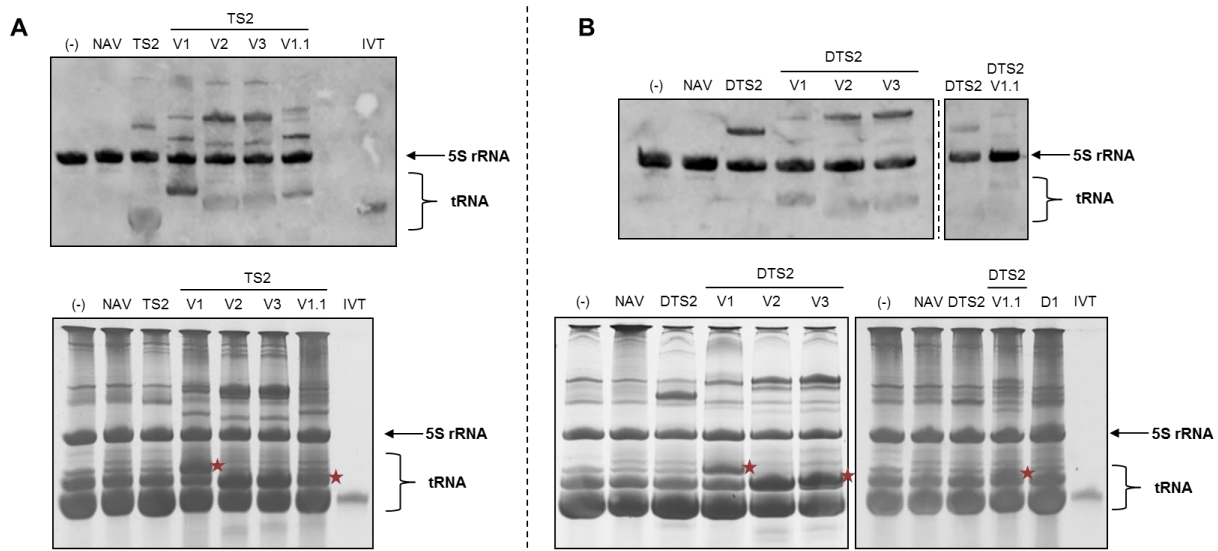


Figure 25: V-region extended TS2 and DTS2 are expressed in XL1-blue cells. Representative Northern blot (upper panel) probed against 5S rRNA and the anticodon region of n1A3 (n1A3 probe) (A, upper panel) or the acceptor stem (AS probe) (B, upper panel) (N=1-4). Representative SYBR gold-stained denaturing polyacrylamide gel electrophoresis (lower panel) of the total RNA isolated from XL1-blue cells transformed with tRNA-encoding pBST NAV2 vectors (N=1-4). tRNA expression was compared to untransformed XL1-blue cells (-) and XL1-blue cells expressing the empty vector pBST NAV2 (NAV). *In vitro* transcribed tRNA n1A3 (IVT) was used as RNA length standard.

5.13 Design DTS2 is the most active nonsense suppressor tRNA

The L-arabinose concentration to induce maximal eGFP wildtype expression in XL1-blue cells was determined as 0.05% (v/v) (Figure 27). In this experiment, protein expression was induced at $OD_{600nm}=0.4$ and cells were harvested after 2 h of induction; the cultures reached an OD_{600nm} of ~ 1.3 . In contrast, XL1-blue cells co-expressing the opal eGFP construct and nonsense suppressor tRNAs were induced at the same OD_{600nm} , but harvested at $OD_{600nm} \sim 1.0$. In addition, due to the simultaneous transformation of two vectors, transformation efficiencies of the GFP PTC variant were reduced (Figure S3). Thus, higher concentrations of L-arabinose might be required in order to induce optimal expression of the eGFP opal variant of co-transformed XL1-blue cells. Hence, the *in vivo* GFP read-through assay of actively promoting nonsense suppressor tRNAs was repeated using 0.25% (v/v) L-arabinose instead of 0.05% (v/v) (Figure 26, Figure 27). The increased L-arabinose concentration enabled the assessment of nonsense suppression levels with FACS and fluorescence intensity, raising these above the detection limit for most of the investigated designs (Figure 27).

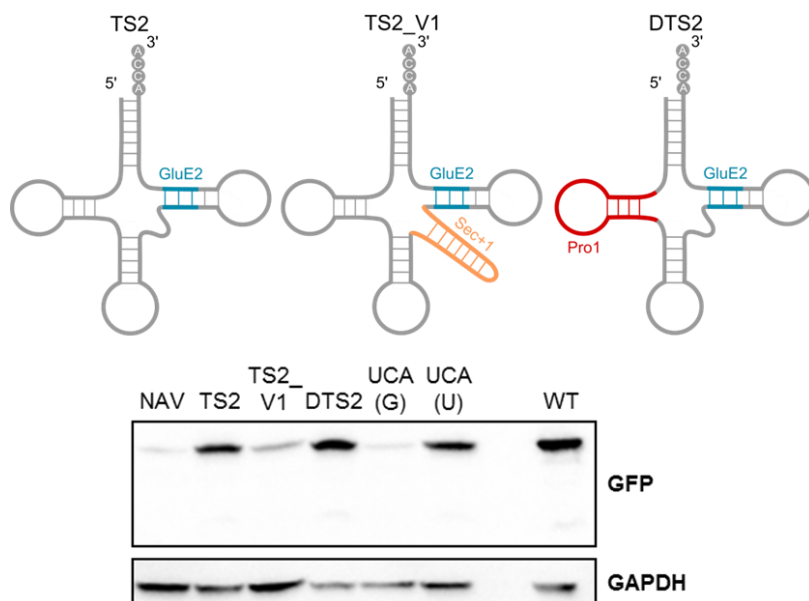


Figure 26: TS2, DTS2 and tRNA^{Ala}(UCA(U)) are the most active nonsense suppressor tRNAs. Representative immunoblot (N=3) of XL1-blue cells co-expressing the eGFP opal construct and nonsense suppressor tRNAs. XL1-blue cells expressing the wildtype eGFP (WT) and the eGFP opal construct (TGA) together with the empty tRNA vector pBST NAV2 (NAV) were used as controls. GAPDH served as loading control.

Design DTS2 exhibited the highest opal nonsense suppressor tRNA activity, followed by tRNA^{Ala}(UCA(U)) and TS2, respectively (Figure 27). According to FACS, relative GFP expression levels of DTS2, tRNA^{Ala}(UCA(U)) and TS2 in comparison to wildtype were $15.2 \pm 2.4\%$, $12.3 \pm 3.4\%$ and $8.7 \pm 0.9\%$, respectively. GFP PTC read-through caused by DTS2 increased in comparison to tRNA^{Ala}(UCA(U)), the most active opal suppressor variant derived from native tRNA^{Ala} isoacceptors used in this study. Thus, a chimeric tRNA based on tRNA design n1A3 with transplanted tRNA^{GluE2} T Ψ C-stem base pairs and tRNA^{Pro1} D-region was most efficient.

Results obtained by FACS and fluorescence reporter measurements for TS2, DTS2 and tRNA^{Ala}(UCA(U)) showed the same trend, however the nonsense suppression levels determined by fluorescence reporter assays were generally lower. According to the FACS results, design TS2_V1 served as weak opal nonsense suppressor tRNA with relative GFP expression levels in comparison to wildtype of $1.6 \pm 0.2\%$. tRNA^{Ala}(UCA(G)) did not promote GFP PTC read-through. Fluorescence intensities of both tRNAs, as determined by fluorescence reporter assay, were even below that observed for the empty pBST NAV2 vector.

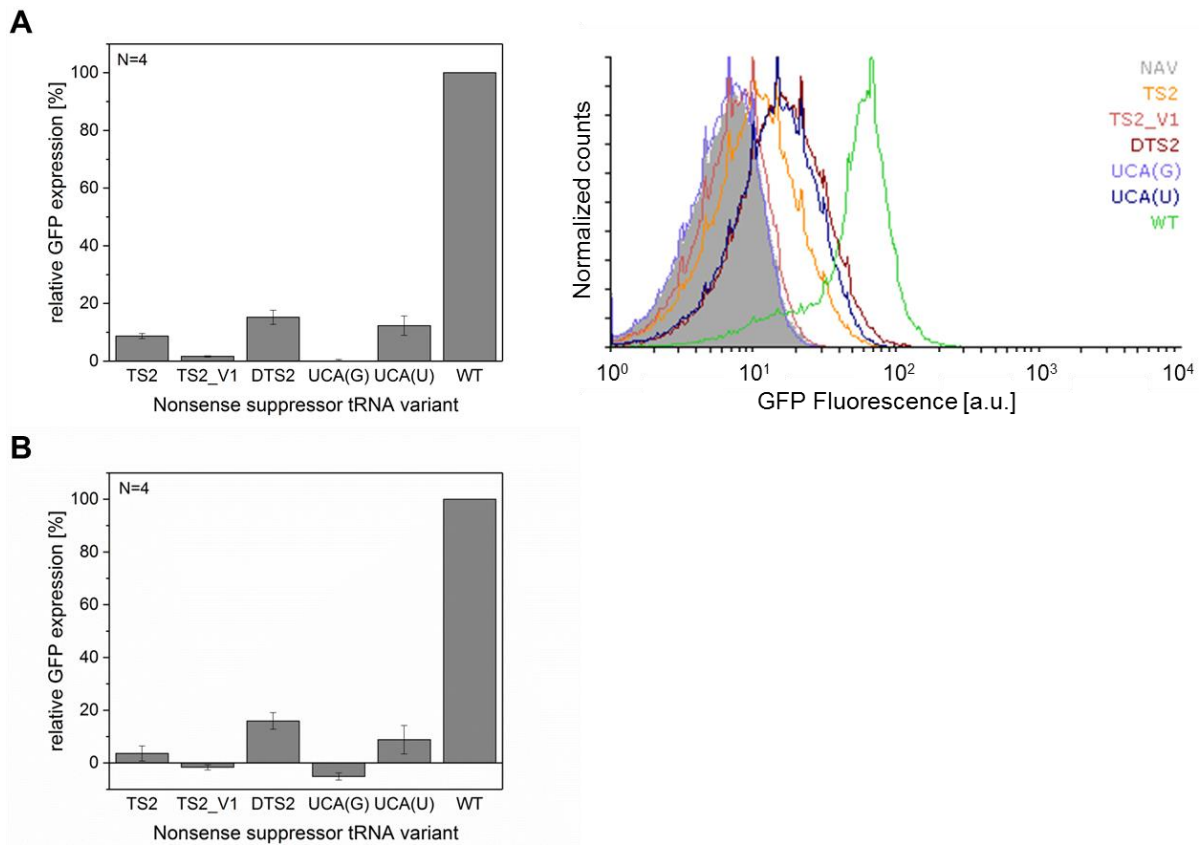


Figure 27: Design DTS2 showed highest nonsense suppression efficiency. GFP read-through promoted by nonsense suppressor tRNAs in XL1-blue cells was assessed by FACS (A) and fluorescence intensity measurements (B). XL1-blue cells expressing the wildtype eGFP (WT) and the eGFP opal construct (TGA) together with the empty tRNA vector pBST NAV2 (NAV) were used as controls. For (A) fluorescence values were normalized to OD_{600nm} of the bacterial culture. For (A) and (B) background fluorescence of NAV was subtracted and the fluorescence was normalized to strain-specific eGFP wildtype fluorescence. Data represent mean \pm s.d. of biological replicates. The number of biological replicates (N) is given in the left upper corner.

The influence of nonsense suppressor tRNA expression on the growth of XL1-blue cells was examined (Figure 28, Table 12). Expression of DTS2, the most efficient nonsense suppressor, resulted in a reduction of cell growth which was comparable to that observed in the presence of native $tRNA^{Ala}$ isoacceptors ($tRNA^{Ala}(GGC)$ and $tRNA^{Ala}(UGC)$) (Figure 28, Table 12). Thus, translationally active opal nonsense suppressor tRNAs did not severely impact growth of XL1-blue cells. This suggests no correlation between the expression of nonsense suppression efficiency and impact on cell growth. In turn, the expression of the designs TS2 and TS2_V1 slowed down cell growth and shifted the growth rates more closely to that observed for $tRNA^{Ala}(UCA(U))$ or $tRNA^{Ala}(UCA(G))$.

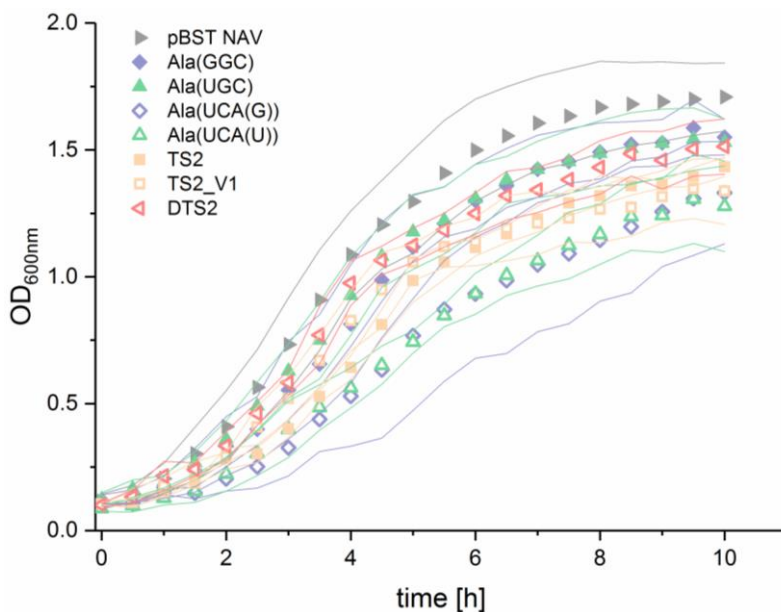


Figure 28: Expression of active opal nonsense suppressor tRNAs does not severely reduce XL1-blue cell growth. tRNAs were expressed under control of the constitutive *lpp* promoter and *rrnC* terminator in XL1-blue cells. Cell growth was monitored by recording OD_{600nm} every 30 min. Data represents mean \pm s.d. of at least 3 biological replicates. Standard deviations are represented as lines.

Table 12: Specific growth rates μ and doubling times t_d of XL1-blue cells expressing different tRNA variants. Values were obtained from the exponential phase of the growth curve.

tRNA variant	Specific growth rate	Doubling time
	μ	t_d
NAV	0.63 h^{-1}	1.1 h
Ala(GGC)	0.58 h^{-1}	1.2 h
Ala(UGC)	0.60 h^{-1}	1.2 h
Ala(UCA(G))	0.51 h^{-1}	1.4 h
Ala(UCA(U))	0.52 h^{-1}	1.3 h
TS2	0.51 h^{-1}	1.3 h
TS2_V1	0.55 h^{-1}	1.3 h
DTS2	0.58 h^{-1}	1.2 h

6 DISCUSSION

Several approaches have been used to select for efficient nonsense suppressor tRNAs. However, many studies focused on swapping the anticodon triplet to be complementary to mRNA stop codons, while the remaining tRNA body remained unchanged and thus, centered on only one aspect of the sequence of tRNA entities. In this study, nonsense suppressor tRNAs were designed by sequential modulation of different tRNA regions. First designed by *de novo* modulating nucleotides that are not involved in crucial processes (e.g. nucleotides involved in tertiary interactions, stop codon recognition and aminoacylation by AlaRS), the designs were subsequently optimized by nucleotide exchanges within each tRNA arm. Nucleotides within the acceptor arm were not exchanged to preserve the recognition elements of AlaRS. The identity elements of tRNA^{Ala} were chosen, because, besides tRNA^{Ser} and tRNA^{Leu}, no recognition elements for aminoacylation are located within the anticodon region [87] and thus, the anticodon triplet can be readily exchanged in order to recognize mRNA termination codons. Transplantation of the G3-U70 wobble base pair, which serves as main identity element of tRNA^{Ala}, into other tRNA species has previously been shown to enable aminoacylation with Ala [89,90]. Thus, tRNA^{Ala}-derived designs should tolerate a variety of sequence changes outside of the acceptor stem without perturbation of aminoacylation. This allowed the identification of nucleotides and motifs that are important for mediating tRNA functionality as read out by nonsense suppression.

6.1 3'-Heterogeneity and dimerization reduces tRNA aminoacylation levels

In vitro aminoacylation reactions were in accordance with the earlier hypothesis, showing that all semi *de novo* designs, besides n2, were esterified with Ala, even though multiple nucleotide exchanges were performed (Figure 9). Importantly, aminoacylation levels varied between the different designs, indicating their different propensities to form the L-shaped tertiary structure. Design I (n3, n4, n5) lacked important base pairs required for tertiary structure for-

mation and showed lower aminoacylation levels in comparison to design II (n1, n2). The G15-C48 Levitt, G18-U55 bifurcated and U54-A57 *trans* Hoogsteen base pair, were absent in design I and thus, appeared to be important for formation of the tRNA L-shape. As expected for tRNA^{Ala}-derived nonsense suppressors, editing within the anticodon region (designs n1/3A1, n1/3A2, n1/3A3) did not influence markedly the aminoacylation levels.

Aminoacylation levels did not exceed ~30%, which is lower than published data [201,203]. The presence of intact single stranded 3'-NCCA termini required for aminoacylation were present in only a minor fraction of the total tRNA (Figure 8), which explains this result. Together, these results suggest that a large fraction of the *in vitro* transcribed tRNAs was un- or misfolded. *In vitro* transcribed tRNAs lack post-transcriptional modifications (PTMs), that stabilize tRNA structure (reviewed in [212,215]). Thus, absence of PTMs could also account for the observed reduced aminoacylation levels. The crystal structure of unmodified *E. coli* tRNA^{Phe} showed that *in vitro* transcripts can adopt a similar overall tertiary structure compared to native, fully modified tRNA^{Phe} [96]. The same observation was also made by imino NMR studies of a yeast tRNA^{Phe} transcript at Mg²⁺ concentrations above 5 mM, reflecting the importance of Mg²⁺ in tRNA folding [99]. Aminoacylation kinetics of the yeast tRNA^{Phe} transcript closely resembled those of its fully modified analogue [98]. These results suggest that in the presence of sufficient Mg²⁺, *in vitro* transcribed tRNAs can adopt a similar L-shaped conformation and should be aminoacylated to similar extent as compared to mature tRNAs. Schulman and coworkers have shown that the Mg²⁺ concentration optima of aminoacylation differ between unmodified and mature tRNAs. For example, maximal aminoacylation for an *E. coli* tRNA^{Phe} transcript was detected at 15 mM Mg²⁺, whereas the concentration decreased to 8 mM for its native counterpart [216]. Bhaskaran and coworkers used 10 mM Mg²⁺ to assess the aminoacylation of *E. coli* tRNA^{Gln} [201]. In this study, a concentration of 12.5 mM Mg²⁺ was used in the aminoacylation reactions, which should be sufficient to maintain tRNA in the folded state. Moreover, tRNA folding was performed at relatively high Mg²⁺ concentrations of 20 mM. Thus, lack of modifications of the *in vitro* transcripts and Mg²⁺ concentrations cannot explain the reduced aminoacylation levels observed in this study.

Instead, heterogeneity at the 3'-end and oligomerization of tRNA transcripts can result in decreased aminoacylation levels. As evident from studies by Kholod and coworkers, 10-30% of transcripts produced by run-off T7 transcription are extended at their 3'-terminus by either one or two nucleotides [217]. Extension at the 3'-NCCA terminus prevents aminoacylation by aminoacyl-tRNA synthetases. In addition, tRNA dimer formation of *in vitro* transcripts has

been observed [217,218]. The extent of dimerization was largely dependent on the tRNA sequence and folding conditions [218]. Dimerization was only prevented by performing tRNA folding in water without any additives [217]. However, as described above, the presence of Mg^{2+} ions is essential for tRNA structure formation [219,220]. Even if, as previously shown, a small fraction of dimers is aminoacylatable [221], tRNA oligomerization will decrease aminoacylation levels. The extension at the 3'-end and dimerization cannot be circumvented by purifying tRNA transcripts using preparative PAGE [217], albeit applied in here. A variety of methods exists to enable the synthesis of tRNA transcripts with precise length. An elegant approach to ensure homogeneity at the 3'-end is the use of ribozymes acting in *cis* or *trans*, allowing precise cleavage at the 3'-terminus of tRNA sequences [222,223]. Alternatively, a second non-denaturing electrophoresis step could be included after denaturing preparative PAGE, which would also allow the removal of tRNA oligomers [217]. tRNAs produced with one of the methods would presumably be aminoacylated to higher extent.

6.2 Natural nonsense suppressor tRNAs read through stop codons

Natural read-through of termination codons in *E. coli* cells decreases in the order UGA>UAG>UAA [205]. However, the presence of strain-specific natural nonsense suppressor tRNAs changes this order. XL1-blue cells contain the supE44 mutation in the glnX gene, encoding an amber suppressor tRNA [224] and thus, exhibit higher read-through levels at UAG stop codons (Figure 17). The supE gene product is tRNA^{Gln}(CUG) with the anticodon changed to CUA, enabling incorporation of Gln in place of amber stop codons [225]. To avoid competition with supE44, opal suppressors tRNAs were used to assess tRNA functionality by the *in vivo* GFP read-through assay. In this study, nonsense suppression levels of ~45% were determined for supE44 (Figure 17). Singaravelan and coworkers observed a growth-dependent suppression efficiencies of 93% and 65% in the logarithmic and stationary phase, respectively [224]. SupE suppression has been shown to be particularly sensitive to stop codon context [172,226], explaining the variations in suppression levels.

6.3 Nonsense suppression levels are strongly influenced by codon context

As evident from various studies, the base located immediately 3' to the mRNA stop codon (+4 base) has a strong influence on the efficiency of translation termination [162–165,172] and thus, also nonsense suppression [173,226,227]. In this study, the Ser codon within eGFP at

position 29 (AGC) was exchanged by the opal stop codon (UGA) in order to generate a reporter for the *in vivo* stop codon read-through assay (Figure 12). The site for PTC incorporation was chosen, because accommodation of any of the 22 canonical amino acids at this position does not perturb folding and hence fluorescence properties of eGFP [133]. The nucleotide 3'-adjacent to the inserted PTC UGA was guanosine (Figure 16), enabling potentially high nonsense suppression levels in the case of a functional suppressor tRNA, as shown for the Hirsh suppressor tRNA [173]. According to the trend observed for the tRNA^{Trp} opal nonsense suppressor, incorporation of adenosine as the +4 nucleotide would optimize the codon context of the PTC for nonsense suppression even further [173]. However, looking at the *E. coli* termination efficiencies that should inversely correlate to nonsense suppression efficiencies, UGAC serves as poorest termination signal [164], that often serves as recoding site for the incorporation of Sec [169,170] or frameshifting events [167,168]. In this regard, replacement of +4G by +4C within the eGFP reporter gene might improve nonsense suppression efficiency of opal suppressor tRNAs. However, the choice of +4 base was restricted, as its substitution would change the amino acid sequence of eGFP, which could perturb its fluorescence. Besides the +4 position, crosslinking studies suggested that the +5 and +6 base also influence termination efficiency, albeit to lesser extent [163]. However, a comprehensive experimental analysis with all possible nucleotide combinations is not available, making it difficult to predict +5 base and +6 base combinations that would promote nonsense suppression.

Besides codon context, the two C-terminal amino acids adjacent to inserted PTCs were shown to influence stop codon read-through [175,176]. In this study, Phe (F) was located at the 5'-site of the opal stop codon (-1 position) (Figure 16). For the -1 amino acid, the van der Waals volume, as well as its propensity to form secondary structures, were shown to modulate nonsense suppression. A decrease in van der Waals volume is accompanied by an increase in stop codon read-through [176]. Replacing Phe by amino acids possessing a smaller van der Waals volume, e.g. Gly, could potentially increase nonsense suppression. Lysine was found as the penultimate amino acid 5' to the UGA stop codon (-2 position) (Figure 16). Basic amino acids in the -2 position have resulted in efficient termination but inefficient read-through, whereas the opposite was observed for acidic amino acids [175,176]. Thus, substituting Lys by Asp or Glu could increase nonsense suppression. However, the effect of the -1 and -2 amino acid is cooperative and previous assumptions have been made for a specific codon context. Changing the codon context could lead to other amino acid preference for efficient nonsense suppres-

sion. In addition, amino acid substitutions would require using another reporter gene, which would tolerate these specific codon combinations.

6.4 Post-transcriptional modifications are important for tRNA's non-sense suppressor functionality

In vitro translation reactions showed a slight increase in PTC read-through for tRNA^{Ala}(UCA(U)), whereas that of tRNA^{Ala}(CUA(G)) was nearly at the background level (Figure 14). However, the *in vivo* GFP read-through assay clearly showed that tRNA^{Ala}(UCA(U)) promoted nonsense suppression (Figure 19). Thus, lack of nonsense suppression could be attributed to the absence of post-transcriptional modifications of *in vitro* transcribed tRNAs. Controversially, several studies have shown that unmodified tRNA transcripts actively promote protein synthesis *in vitro* with efficiencies comparable to their native fully-modified counterparts [228–231]. On the other hand, the importance of distinct post-transcriptional modifications for the functionality of tRNAs in translation has been uncovered, suggesting that maybe only a specific subset of tRNAs tolerates lack of modifications and maintains functionality in *in vitro* translation reactions. Modifications at the wobble position or 3'-adjacent to the anticodon triplet are important for maintaining translation fidelity by modulating the decoding ability of tRNAs. Thereby, codon recognition is either expanded to enable recognition of cognate and synonymous codons or restricted to ensure selection against near-cognate codons (reviewed in [57,232–235]). In addition, these modifications promote reading frame maintenance and thus, prevent frameshifting [59,215,236,237]. Modifications located in the core region in general stabilize tRNAs and promote structure formation (reviewed in [238,239]). Others modulate the protein synthesis rate and fidelity of translation [240]. For tRNA^{Ala}-derived nonsense suppressors, the presence of post-transcriptional modifications appeared to be important for tRNA functionality in translation, as observed from the different tendency of tRNA^{Ala}(UCA(U)) to promote nonsense suppression *in vitro* and *in vivo*.

6.5 The anticodon stem-loop is not the main determinant of nonsense suppression efficiency

Even though designs n1 and n3 were aminoacylated (Figure 9), they did not promote nonsense suppression (Figure 20). Pioneering work by Yarus and coworkers have suggested the anticodon stem loop sequence as the main determinant of nonsense suppressor tRNA efficiency [136,177,179]. Thus, substitution of nucleotides within the ASL of n1 or n3 might enable

GFP PTC read-through. However, for the tRNA^{Ala}-based designs chosen in this study, the anticodon region appeared to have little effect on PTC read-through. Neither replacing bases in the ASL of n1 by those found most frequently among elongator tRNAs (design n1A3), nor by those found in tRNA^{Ala}(UCA(U)) (design n1A5) promoted nonsense suppression (Figure 20, Figure 21).

The ASL of designs n1A2, n1A3_A37 and n1A4 showed the closest resemblance to the sequence proposed to support read-through according to the extended anticodon hypothesis (Table 13) [177]. Yarus and coworkers suggested that suppressor efficiencies increase with similarity of the ASL to that of tRNAs naturally decoding codons beginning with U [177]. Selection of amber nonsense suppressor by read-through ribosome display with randomized bases adjacent to the CUA anticodon showed maximal nonsense suppression efficiencies for tRNA^{Ser} containing CU-CUA-AA anticodon loop sequence. Single nucleotide substitutions within the ASL, e.g. U32C and A37U, resulted in loss of nonsense suppressor activity [140]. Substitution of bases according to the extended anticodon rules into the ASL of tRNA^{Asp}(CUA) resulted in a 10-fold increase in nonsense suppression. Incorporation of A36-A37 residues into tRNA^{His}(CUA), tRNA^{Glu}(CUA) and Su2 improved suppression at all investigated codon contexts [134]. Thus, an increased GFP read-through would be expected for n1A2, n1A3_A37 and n1A4. However, nonsense suppression of n1A2, n1A3_A37 and n1A4 were close to background levels.

Table 13: Comparison of the ASL sequence of n1A2, n1A3, n1A3_A37 and n1A4 to the extended anticodon proposed by Yarus. Deviations to the extended anticodon sequence are highlighted in red.

Nucleotide position	Nucleotide found in tRNAs with A as cardinal nucleotide	n1A2	n1A3	n1A3_A37	n1A4
28-42	(G-C or C-G)	C-G	C-G	C-G	C-G
29-41	Pu-Py	G-C	G-C	G-C	G-C
30-40	G-C	G-C	G-C	G-C	G-C
31-39	A-Ψ or U-A	A-U	C-G	C-G	C-G
32	C, U	C	C	C	U
33	U	U	U	U	U
37	ms ² i ⁶ A	G	G	A	A
38	A	A	A	A	A

In contrast to the optimal ASL sequence according to Yarus [177], n1A3_A37 and n1A4 pos-

sessed a C31-G39 instead of an A31-Ψ39 or U31-A39 base pair at the end of the anticodon stem, whereas n1A2 contains a G37 instead of A37. It has been shown that the influence of nucleotides located within the anticodon loop on nonsense suppression efficiencies are much stronger than those present in the anticodon stem (Figure 6) [178]. At positions 31-39 all four possible base pair combinations are tolerated with only small effects on translational efficiency [178], suggesting a higher potential for n1A3_A37 or n1A4 to function as nonsense suppressor tRNAs in comparison to n1A2. Mutagenesis of the C31-G39 base pair of a tRNA^{Glu} ochre suppressor tRNA to U31-A39 increased nonsense suppression 2- or 3-fold depending on the codon context [179]. A similar trend could be observed for a tRNA^{Ser}-derived amber suppressor tRNA in wheat germ extract for which all base pair combinations resulted in similar nonsense suppression efficiencies. Increased nonsense suppression efficiencies could only be observed in the presence of a U31-A39 base pair, which is suggested to promote optimal positioning of the anticodon for decoding [139]. Thus, substitution of the C31-G39 base pair by U31-A39 in n1A3_A37 or n1A4 might increase GFP PTC read-through, however, only to low extent. The remaining base pairs within the anticodon stem are suggested to be more sensitive to substitutions. However, for the design n1A3 and its derived variants these were in accordance with the extended anticodon sequence [177]. The anticodon stem of tRNA designs based on n1A3 was very GC-rich, which has been shown to promote nonsense suppression, presumably by increasing the rigidity of the tRNA [139]. Thus, the ASL sequence, including the C31-G39 base pair, in the designs n1A3_A37 and n1A4 cannot explain the lack of nonsense suppression activity.

Besides the extended anticodon, the identity of bases found at positions 32-38 are important determinants for the binding strength of aa-tRNAs to ribosomes. Olejniczak and coworkers suggested that the 32-38 pair evolved with the anticodon triplet in order to ensure uniform binding affinities of aa-tRNAs to the ribosomal A-site [180,181]. 32-38 pair combinations of tRNA^{Ala}(UGC)-derived amber suppressors promote nonsense suppression in the order CA>CC>UU>UC, whereas A-A>A-U mirrors the tendency observed for tRNA^{Ala}(GGC)-based variants. Among different nonsense suppressor tRNA species, there is a preference for a C32-A38 pair as being most efficient [180]. Thus, the C32-A38 pair found in n1A3 is supposed to increase binding affinity to ribosomal A-site and thus, promote read-through in comparison to n1A4 and n1A5. However, all variants were deficient in nonsense suppression. Because the identities of the 32-38 pair evolved with the anticodon triplet, the observed trends

for different 32-38 base pair combinations may hold true for amber, but not for opal suppressor tRNAs.

In the context of the tRNA^{Ala}-based semi *de novo* designs used in this study, the sequences resembling the extended anticodon did not promote nonsense suppression. tRNA levels of the anticodon-edited designs were close to the detection limit as assessed by Northern blot. Thus, it is possible that low tRNA expression or rapid turnover could account for reduced nonsense suppression efficiencies.

As editing within the anticodon region did not influence nonsense suppression efficiencies, the effect of nucleotide substitutions within other tRNA regions was examined. Therefore, design n1A3 was chosen as tRNA body in which substitutions within the TΨC-stem and/or D-region were performed. n1A3 contains the C32-A38 pair and U33, which is essential for formation of the U-turn and thus, for the anticodon loop conformation, both of which should promote nonsense suppression. n1A3 contains the C31-G38 base pairs, which should have little effect on PTC read-through efficiencies and G37, which could easily be mutated to A37 to be in accordance to the extended anticodon hypothesis.

6.6 The TΨC-stem is the main determinant of nonsense suppression

During translation elongation, EF-Tu delivers aa-tRNAs as ternary complex to the ribosomal A-site and thus, aa-tRNA binding affinity to EF-Tu is crucial for the decoding event (reviewed in [27–31,101]). Mutagenesis experiments have determined the 49-65, 50-64 and 51-63 TΨC-stem base pairs as main determinants contributing to EF-Tu binding affinity [104]. The thermodynamic contributions of native elongator tRNA bodies, mainly mediated by the TΨC-stem base pairs, and their esterified amino acids are tightly balanced in order to achieve uniform EF-Tu binding affinities [106,108,109]. In this study, TΨC-stem base pairs were randomized and chosen according to the highest probability to form the L-shaped structure. However, this combination of base pairs might not be optimal for Ala-inserting tRNAs, which could lead to imbalanced EF-Tu binding and thus, perturbation of decoding. Thus, lack of nonsense suppression of design n1 and its anticodon-edited variants might be the result of suboptimal EF-Tu binding. Interestingly, transplantation of the TΨC-stem base pairs of native tRNA^{Ala}(UGC) into n1A3, as present in the design TS1, did not enhance the nonsense suppression over the background (Figure 22). However, incorporation of tRNA^{GluE2} TΨC-stem base pairs, design TS2 and DTS2, resulted in GFP PTC read-through (Figure 22). According

to the TΨC-stem base pair combination, tRNA^{Glu} is rated among tRNAs with the highest binding affinity to EF-Tu (Table 3) [106,108]. $\Delta\Delta G^\circ$ values obtained for different TΨC-stem base pairs [106], predict EF-Tu binding affinity to follow the order n1A3<TS1<TS2. Predicted $\Delta\Delta G^\circ$ values for substituting the TΨC-stem base pairs of Phe-tRNA^{Phe} by those present in n1A3, TS1 and TS2 were -0.4 kcal/mol, -0.7 kcal/mol and -1.5 kcal/mol, respectively (Table 2). According to Uhlenbeck and coworkers $\Delta\Delta G^\circ$ values for the tRNA^{Ala} body should be -1.3 kcal/mol [106], which comes closest to values obtained for TS2. Thus, strong EF-Tu binding capacity of aa-tRNAs counteracted the alterations within other tRNAs parts and supported nonsense suppression. Theoretically, release from EF-Tu·GDP after cognate codon-anticodon interaction would be expected to be decelerated for aa-tRNAs that bind tightly to EF-Tu [109]. As a consequence, ribosomes might be stalled, which consequently results in decreased amounts of full-length polypeptide produced and therefore reduced nonsense suppression efficiencies. On the other hand, high EF-Tu binding affinity increases the amount of ternary complex, aa-tRNA·EF-Tu·GTP, formed. Consequently, the probability of delivery of nonsense suppressor tRNAs to the ribosomal A-site, where it competes with RFs for the binding of mRNA stop codons, is increased. Thus, the higher concentration of the ternary complex might shift the equilibrium in favor of stop recognition by nonsense suppressor tRNA instead of release factors. Along that line, Vijgenboom and coworkers have shown a roughly two fold reduction of read-through at UGA stop codons in *E. coli* cells in which EF-Tu levels were decreased by ~40% [241].

Here, we show that the TΨC-stem is the most crucial factor mediating nonsense suppression, as substitution of the D-region alone, design D1, did not increase GFP expression above the background level. In contrast, both designs, TS2 and DTS2, with transplanted TΨC-stem base pairs of tRNA^{GluE2} acted as active nonsense suppressor tRNAs. Nonsense suppression efficiencies of DTS2, produced by combinatorial transplantation of tRNA^{GluE2} TΨC-stem base pairs and the D-region of tRNA^{Pro1} into n1A3, were superior in comparison to TS2. The D-region of tRNA^{Pro} serves as recognition element for translation factor EF-P [119]. EF-P accelerates peptide bond formation of stalled ribosomes caused by non-optimal substrates, such as Pro [111,117,118]. Thus, nonsense suppression mediated by DTS2 could be assisted by EF-P due to recognition of the tRNA^{Pro} D-region. EF-P binding may facilitate translation elongation by stabilizing tRNA structures within the 50S peptidyl transferase center [120] and explain increased nonsense suppression efficiencies. Interestingly, TS2 showed high tRNA steady-state levels in comparison to DTS2 (Figure 22), even though the latter was identified as a

more efficient nonsense suppressor tRNA. XL1-blue cells expressing the pBST NAV2 vector coding for TS2 or DTS2 showed the presence of extended RNA transcripts, which represent the major fraction observed for DTS2. Maximized nonsense suppressor tRNA efficiency, as observed for DTS2, might be compensated by reducing tRNA levels in order to minimize effects on cell viability.

6.7 Incorporation of A37 and variable loop extensions reduce nonsense suppression

The ms^2i^6A37 modification has been identified in almost all native tRNAs that decode codons beginning with U [184,213,214], the same nucleotide is present in termination codons. Yarus and coworkers have highlighted the importance of this hypermodification on nonsense suppression efficiencies [177,178]. Their hypothesis was supported by studies from several groups showing that lack of the ms^2i^6A modification at position 37 results in reduced nonsense suppression efficiencies [58,192,193] and increased context sensitivity [195–198]. However, incorporation of A37, enabling the opportunity for modification to ms^2i^6A , into the designs TS2 or DTS2 appeared to be lethal to *E. coli* cells (Figure S2). The same trend was not observed for n1A3_A37, n1A4 and n1A5, which also possessed an adenine at position 37. This suggests that incorporation of A37 into TS2 and DTS2, that presented active nonsense suppressor tRNAs, improved nonsense suppression efficiencies even further. Besides PTCs, nonsense suppressor tRNAs can target natural stop codon sites, albeit generally to lesser extent [126]. However, recognition of these off-targets results in the formation of C-terminally extended polypeptides, which are often characterized by loss-of-function. Because UGA stop codons appear with a frequency of 32% in the *E. coli* genome (<https://www.kazusa.or.jp/codon/>, Codon Usage Database), multiple genes would be targeted by highly active opal nonsense suppressor tRNAs. The accumulation of read-through products, including such from genes encoding essential proteins (Table 14), can cause severe growth defects and explain the mortality of *E. coli* when transformed with TS2_A37 and DTS2_A37. In contrast, inefficient nonsense suppressor tRNAs such as tRNAs n1A3_A37, n1A4, n1A5, tolerated the presence of A37 or ms^2i^6A37 .

Table 14: Summary of essential genes ending with TGA stop codons in *E. coli* MG1655 (DEG database, www.essentialgene.org) [122].

Gene name	Function
ffr	ribosome recycling factor
dxr	1-deoxy-D-xylulose 5-phosphate reductoisomerase
ribD	fused diaminohydroxyphosphoribosylaminopyrimidine deaminase and 5-amino-6-(5-phosphoribosylamino) uracil reductase
dnaX	DNA polymerase III/DNA elongation factor III, tau and gamma subunits
fabG	3-oxoacyl-[acyl-carrier-protein] reductase
yejM	predicted hydrolase, inner membrane
nrdA	ribonucleoside-diphosphate reductase 1, alpha subunit
cca	fused tRNA nucleotidyl transferase/2'3'-cyclic phosphodiesterase/2'nucleotidase and phosphatase
fmt	10-formyltetrahydrofolate:L-methionyl-tRNA(fMet) N-formyltransferase
gmK	guanylate kinase
yidC	membrane protein insertase
ubiB	2-octaprenylphenol hydroxylase
ubiD	3-octaprenyl-4-hydroxybenzoate decarboxylase
murI	glutamate racemase
ubiA	p-hydroxybenzoate octaprenyltransferase
ssb	single-stranded DNA-binding protein

Extension of the variable loop of TS2 or DTS2 according to that found in human tRNA^{Ser}-derived nonsense suppressors or similar to that present in *E. coli* tRNA^{Sec}, a natural tRNA decoding UGA codons in specific contexts, did not increase nonsense suppression levels (Figure 24), even though tRNAs showed high steady-state levels in XL1-blue cells (Figure 25). Sec-tRNA^{Sec} is delivered to the ribosome in complex with SelB-GTP, which specifically recognizes the 13 base pair tRNA acceptor arm. Removal of a single base pair from the amino acceptor branch of tRNA^{Sec}, leading to canonical 12 bp, enables binding by EF-Tu-GTP and abolishes recognition by SelB [242]. Thus, binding of variable loop-extended tRNAs to EF-Tu-GTP and subsequent delivery to the ribosomal A-site should not be perturbed. Codon-anticodon interaction is unlikely affected, because Sec-tRNA^{Sec} can be accommodated in the ribosomal A-site without steric hindrances. Increased nonsense suppression levels by tRNAs possessing a long variable region have previously only been shown for human cells [133]. However, for the *E. coli* tRNA^{Ala}-derived designs used in this study the same trend could not be observed.

6.8 Additional base substitutions could further increase nonsense suppression efficiency

DTS2 was identified as the most efficient opal nonsense suppressor tRNA, followed by tRNA^{Ala}(UCA(U)) and TS2, respectively. TS2_V1 acted as weak suppressors (Figure 27). DTS2 showed higher nonsense suppression activity than tRNA^{Ala}(UCA(U)), derived from anticodon substitution of tRNA^{Ala}(UGC). However, nonsense suppression levels of supE44, a natural amber suppressor tRNA present in XL1-blue cells, were the highest (Figure 17). Comparability of nonsense suppression levels is questionable since the experimental set-up differed and supE44 is an amber instead of an opal suppressor tRNA. Nonetheless, certain nucleotide substitutions of DTS2 might increase nonsense suppression levels to values higher than ~15% of wildtype eGFP.

All of the designs used in this study were created based on tertiary interactions from the crystal structure of unmodified *E. coli* tRNA^{Phe}. Unmodified *E. coli* tRNA^{Phe} contains a G10-C25-G44 base triplet and thus, A26 is unpaired [96]. In contrast, mature yeast tRNA^{Phe} possesses a m²G10-C25-G45 base triplet and a m²G26-A44 *cis* Watson-Crick base pair. Structural differences between unmodified tRNA^{Phe} and its mature counterpart are an increased angle between the acceptor and anticodon stem [96]. Thus, due to the absence of modifications, tRNA^{Phe} cannot fold as tightly and is characterized by a less stable tertiary structure. Lack of post-transcriptional modifications of *in vitro* transcripts reduced nonsense suppression levels, as observed for tRNA^{Ala}(UCA(U)) (Figure 14). Thus, nonsense suppressor tRNAs were expressed *in vivo* from the pBST NAV2 vector. Therefore, the chosen tertiary interactions of unmodified *E. coli* tRNA^{Phe} might not be optimal. Substitution of the tertiary interactions used in the designs by that found most frequent among native tRNAs (Table 1) [76] might stabilize tRNA structure and result in higher nonsense suppression efficiencies.

Deviations in the anticodon stem-loop of TS2 and DTS2 and the sequence proposed to promote nonsense suppression according to the extended anticodon hypothesis can be observed [177]. These include the presence of G37 and the C31-G39 base pair within the ASL of TS2 and DTS2. However, tRNAs TS2_A37 and DTS2_A37, obtained through substitution of G37 by A37, were lethal to *E. coli* cells as shown by the reduced transformation efficiencies in XL1-blue cells (Figure S3). Maybe the combinatorial replacement of base 37 and the base pair C31-G39 by U31-A39 reduces mortality and leads to generation of more active nonsense suppressor tRNAs. On the other hand, the 31-39 base pair within the ASL have been shown to

have little effect on PTC read-through efficiencies [178]. In addition, a highly efficient nonsense suppressor tRNA [243], as well as native tRNA^{Ser}(GGA), reading codons beginning with U, have been shown to lack ms²¹⁶A37 [244].

Besides the tRNA sequence, other components of the translational machinery have been shown to modulate nonsense suppression efficiencies of tRNAs. Mutations in ribosomal proteins, ribosomal RNA, EF-Tu or RFs have been shown to increase PTC read-through (reviewed in [124,199]). Expression of nonsense suppressor tRNAs in *E. coli* strains containing one of the above mentioned mutations might increase nonsense suppression levels. However, the aim of this study was to focus solely on the tRNA entity.

6.9 Application of designed nonsense suppressor tRNAs

The chimeric tRNA, produced by transplanting the TΨC-stem of tRNA^{GluE2} into tRNA^{Pro1}, has previously been utilized by Katoh and coworkers for consecutive incorporation of D- and β-amino acids at multiple sense codon sites in a flexible *in vitro* translation system with optimized translation factor concentrations [152]. This study does not provide a comparison to nonsense suppression efficiencies of tRNA^{Pro1E2}(CGG). Nonetheless, analogous to tRNA^{Pro1E2}(CGG), the active nonsense suppressor tRNA designs, TS2 and DTS2, could potentially be used to incorporate unnatural amino acids in response to opal nonsense codons and by mutation of the anticodon triplet presumably to other codons.

The initial aim of the study was the utilization of *E. coli* as model system to study the contribution of different bases and sequence batches on tRNA functionality, as read out by nonsense suppression. In comparison to mammalian cells, *E. coli* enables a much faster and less expensive evaluation of nonsense suppression efficiencies. However, to what extent the information obtained in *E. coli* correlates with mammalian cells, remains to be examined, because little is known about the mechanisms of tRNA recognition by eEF-1α, the eukaryotic analog of EF-Tu. However, if the trends observed in this study could be transferred to design functional mammalian nonsense suppressor tRNAs, these could be used as therapeutics in order to treat diseases caused by PTCs. The successful rescuing of PTCs by nonsense suppressor tRNAs has previously been shown for genes associated with β-thalassemia [158], DMD [159], xeroderma pigmentosum [245] and CFTR [157]. However, these studies were limited to cell or mouse models. A challenge in the development of therapeutic nonsense suppressor tRNAs is their off-target effect and targeted delivery [126]. Nonsense suppressor

tRNAs base pair with their anticodon to the complementary mRNA stop codon. Thus, recognition is not only restricted to PTCs, but undesirably native stop codons serve as targets, too. Read-through of native stop codons leads to the C-terminal extension of proteins, which can potentially be detrimental to the cell. However, PTCs are more susceptible to read-through by nonsense suppressor tRNAs than natural termination codons [126]. In addition, ribosome profiling of HEK293 cells supplemented with nonsense suppressor tRNAs has shown no or a maximal 2-fold increase in ribosome density within 3'-UTRs [157]. However, already a minor fraction of suppressed natural termination codons could potentially be detrimental to the cell. One strategy to overcome this challenge would be the extension of the anticodon of nonsense suppressor tRNAs in order to increase specificity. Another prerequisite for successful application of therapeutic nonsense suppressor tRNAs is the incorporation of the cognate amino acid in place of the PTC to restore the wildtype protein sequence and prevent missense mutations. Thus, it would be interesting to examine if TS2 and DTS2 incorporate exclusively Ala, as expected from incorporation of AlaRS recognition elements. In addition, it would be interesting to examine if the designs TS2 or DTS2 by substitution of tRNA identity elements could serve as universal tRNA body, which could be charged with the flexizyme and thus, be used to incorporate a variety of different amino acids in response to the PTCs.

7 CONCLUSION

This study elucidates the contribution of different tRNA bases and regions on tRNA functionality as read out by nonsense suppression efficiency. Starting from different computational tRNA designs including constraints necessary for aminoacylation, tertiary structure formation and stop codon recognition, the design was sequentially optimized. *In vitro* aminoacylation reactions proved that tRNA^{Ala} served as a good scaffold and tolerated many nucleotide changes outside of the acceptor stem without perturbation of aminoacylation. For the chosen design n1A3, substitutions within the anticodon region and v-region did not influence nonsense suppression. However, the TΨC-stem appeared to be the most prominent factor supporting read-through of premature termination codons and thus, modulating tRNA functionality. It is well established that the TΨC-stem base pairs contribute to EF-Tu binding affinity and that the thermodynamic contribution of the tRNA TΨC-stem base pairs and esterified amino acid is balanced in order to ensure uniform EF-Tu binding affinity. In the case of nonsense suppressor tRNAs, strong EF-Tu binding, as evident from incorporation of the TΨC-stem of tRNA^{Glu}, promoted nonsense suppression. In combination with the D-region of tRNA^{Pro}, recognized by EF-P, which is known to alleviate ribosome stalling during translation of polypeptides containing consecutive proline residues, nonsense suppression was even further supported. The results suggest that strong EF-Tu binding is the main factor determining read-through of PTCs, while nonsense suppression levels can be further fine-tuned by changes within other tRNA regions.

8 MATERIALS AND METHODS

8.1 Materials

8.1.1 Enzymes

T4 PNK, 10,000 U/mL	NEB
T7 RNA polymerase, 20 U/ μ L	Thermo Fisher Scientific
DNase I, RNase free 1 U/ μ L	Thermo Fisher Scientific
Phusion High-Fidelity DNA polymerase, 2 U/ μ L	Thermo Fisher Scientific
Benzonase Nuclease, Purity >90%	Merck Millipore
RevertAid Reverse Transcriptase, 200 U/ μ L	Thermo Fisher Scientific
T4 DNA Ligase, 5 U/ μ L	Thermo Fisher Scientific
FastDigest PstI	Thermo Fisher Scientific
FastDigest XbaI	Thermo Fisher Scientific
DpnI, 10 U/ μ L	Thermo Fisher Scientific

8.1.2 Kits

GeneJET PCR purification Kit	Thermo Fisher Scientific
GeneJET Plasmid Miniprep Kit	Thermo Fisher Scientific
GeneJET Gel Extraction Kit	Thermo Fisher Scientific

8.1.3 Reagents

TRIzol reagent	Invitrogen
Phenol/Chloroform/Isoamylalcohol 25:24:1	Carl Roth
SYBR gold	Invitrogen
Ribolock RNase inhibitor, 40 U/ μ L	Thermo Fisher Scientific
Ni-NTA agarose	Qiagen
cOmplete TM Protease Inhibitor Cocktail	Roche
RedSafe TM Nucleic Acid Staining Solution (20,000 x)	iNtRON biotechnology
Glycogen, 20 mg/mL	Thermo Fisher Scientific

8.1.4 Antibodies

Table 15: Antibodies used in this study.

Name	Target	Source	Dilution	Application	Manufacturer
α -GFP	GFP	mouse	1:1,000	Immunoblot	Roche
α -GAPDH HRP	GAPDH	mouse	1:1,000	Immunoblot	Thermo Fisher Scientific
α -mouse HRP	mouse IgG	goat	1:10,000	Immunoblot	BioRad

8.1.5 Vectors

The following vectors were used in this study. Different inserts were subcloned into the vectors to express wildtype GFP or its nonsense variants, tRNAs or *E. coli* AlaRS (Table 16).

Table 16: Original vectors used in this study and their purpose.

Vector	Purpose
pBAD33	eGFP expression for <i>in vivo</i> GFP read-through assay
pBST NAV2	<i>In vivo</i> tRNA expression
pIVEX 2.3 (Biotechrabbit, supplemented with the RTS 100 <i>E. coli</i> HY Kit)	GFP expression for <i>in vitro</i> translation
pQE30	<i>E. coli</i> AlaRS expression

8.1.6 *E. coli* cell strains

Table 17: *E. coli* cell strains used in this study and their purpose.

<i>E. coli</i> cell strain	Purpose
DH5 α	Cloning
XL1-blue	<i>In vivo</i> GFP read-through assay tRNA expression
BL21 (DE3)	S30 <i>E. coli</i> lysate preparation Expression of <i>E. coli</i> AlaRS

8.1.7 Oligonucleotides

All oligonucleotides were purchased from Microsynth in desalted quality. Fluorescently labelled oligonucleotides were ordered in PAGE- or HPLC-purified quality. Lyophilized oligonucleotides were resuspended in water to reach a concentration of 100 μ M and stored at -20°C.

Table 18: Fluorescently labeled oligonucleotides used in this study.

Name	Sequence (5'→3')	Modification
tRNA oligo	pCGCACUGCdTdTXdTdTdGdCdAdGdTdGdCdGdTdGdGdN	X = Cy3-dT
n1A3 NB-probe	CGCGGCTCTAGAGGCCGCTGCTCTCC	5'-Cy3
AS NB-probe	TGGTGGAGCGG	5'-Cy3
Ala(GGC) NB-probe	GCTGACCTCTTGCATGCCATGCAAGC	5'-Cy3
Ala(UGC) NB-probe	GCAGACCTCCTGCGTGCAAAGCAG	5'-Cy3
5S rRNA NB-probe	CGTTTCACTTCTGAGTTCGGCATGGGGTCAGG	5'-Cy5

8 MATERIALS AND METHODS

Table 19: tRNA sequences used in this study. tRNA sequences were aligned according to following tRNA regions: acceptor-stem (Acc-s), D-stem (D-s), D-loop (D-l), anticodon-stem (Ac-s), anticodon-loop (Ac-l), v-region (V-r), TΨC-stem (T-s), TΨC-loop (T-l) and 3'-CCA end. Nucleotide substitutions in the anticodon region of n1A1-n1A3 and n3A1-n3A3 in comparison to n1 and n3 (red); of n1A3_A37, n1A4, n1A5 in comparison to n1A3 (purple), of n2 AS1-3 in comparison to n2 (orange) and of n2-n6 in comparison to n1 (dark red) are shown. Substitutions within the D-region (light green), variable-region (blue) and TΨC-region (dark green) are highlighted and the anticodon triplet is underlined.

Name	Acc-s	D-s	D-l	D-s	Ac-s	Ac-l	Ac-s	V-r	T-s	T-l	T-s	Acc-s	CCA			
	1	8	10	14	22	26	27	32	39	44	49	53	61	66	73	74
n1	GGGGCGG	UA	GCUC	AGAAGGGA	GAGC	A	GCGGA	<u>GACUAAA</u>	UCCGC	GAGAC	GGUCC	UUCGAUU	GGACC	CCGCUCC	A	CCA
	GGGGCGG	UA	GCUC	AGAAGGGA	GAGC	A	GCGGA	<u>GAUCAAA</u>	UCCGC	GAGAC	GGUCC	UUCGAUU	GGACC	CCGCUCC	A	CCA
n1A1	GGGGCGG	UA	GCUC	AGAAGGGA	GAGC	A	GCGGA	<u>GUCUAAA</u>	UCCGC	GAGAC	GGUCC	UUCGAUU	GGACC	CCGCUCC	A	CCA
	GGGGCGG	UA	GCUC	AGAAGGGA	GAGC	A	GCGGA	<u>GUUCAAA</u>	UCCGC	GAGAC	GGUCC	UUCGAUU	GGACC	CCGCUCC	A	CCA
n1A2	GGGGCGG	UA	GCUC	AGAAGGGA	GAGC	A	GCGGA	<u>CUUCAGA</u>	UCCGC	GAGAC	GGUCC	UUCGAUU	GGACC	CCGCUCC	A	CCA
	GGGGCGG	UA	GCUC	AGAAGGGA	GAGC	A	GCGGA	<u>CUUCAGA</u>	UCCGC	GAGAC	GGUCC	UUCGAUU	GGACC	CCGCUCC	A	CCA
n1A3	GGGGCGG	UA	GCUC	AGAAGGGA	GAGC	A	GCGGC	<u>CUUCAGA</u>	<u>GCCGC</u>	GAGAC	GGUCC	UUCGAUU	GGACC	CCGCUCC	A	CCA
	GGGGCGG	UA	GCUC	AGAAGGGA	GAGC	A	GCGGC	<u>CUUCAGA</u>	<u>GCCGC</u>	GAGAC	GGUCC	UUCGAUU	GGACC	CCGCUCC	A	CCA
n1A3_A37	GGGGCGG	UA	GCUC	AGAAGGGA	GAGC	A	GCGGC	<u>CUUCAAA</u>	GCCGC	GAGAC	GGUCC	UUCGAUU	GGACC	CCGCUCC	A	CCA
n1A4	GGGGCGG	UA	GCUC	AGAAGGGA	GAGC	A	GCGGC	<u>UUUCAAA</u>	GCCGC	GAGAC	GGUCC	UUCGAUU	GGACC	CCGCUCC	A	CCA
n1A5	GGGGCGG	UA	GCUC	AGAAGGGA	GAGC	A	GCGGC	<u>UUUCAAC</u>	GCCGC	GAGAC	GGUCC	UUCGAUU	GGACC	CCGCUCC	A	CCA
n1A3_TS1	GGGGCGG	UA	GCUC	AGAAGGGA	GAGC	A	GCGGC	<u>CUUCAGA</u>	<u>GCCGC</u>	GAGAC	<u>UGCCC</u>	UUCGAUU	<u>GGGCA</u>	CCGCUCC	A	CCA
n1A3_TS2	GGGGCGG	UA	GCUC	AGAAGGGA	GAGC	A	GCGGC	<u>CUUCAGA</u>	<u>GCCGC</u>	GAGAC	<u>AGGGG</u>	UUCGAUU	<u>CCCCU</u>	CCGCUCC	A	CCA
n1A3_D1	GGGGCGG	UA	<u>GCGC</u>	<u>AGCCUGGUA</u>	<u>GCGC</u>	A	GCGGC	<u>CUUCAGA</u>	<u>GCCGC</u>	GAGAC	GGUCC	UUCGAUU	GGACC	CCGCUCC	A	CCA
n1A3_DTS1	GGGGCGG	UA	<u>GCGC</u>	<u>AGCCUGGUA</u>	<u>GCGC</u>	A	GCGGC	<u>CUUCAGA</u>	<u>GCCGC</u>	GAGAC	<u>UGCCC</u>	UUCGAUU	<u>GGGCA</u>	CCGCUCC	A	CCA
n1A3_DTS2	GGGGCGG	UA	<u>GCGC</u>	<u>AGCCUGGUA</u>	<u>GCGC</u>	A	GCGGC	<u>CUUCAGA</u>	<u>GCCGC</u>	GAGAC	<u>AGGGG</u>	UUCGAUU	<u>CCCCU</u>	CCGCUCC	A	CCA
DTS2_A37	GGGGCGG	UA	<u>GCGC</u>	<u>AGCCUGGUA</u>	<u>GCGC</u>	A	GCGGC	<u>CUUCAAA</u>	<u>GCCGC</u>	GAGAC	<u>AGGGG</u>	UUCGAUU	<u>CCCCU</u>	CCGCUCC	A	CCA
DTS2_V1	GGGGCGG	UA	<u>GCGC</u>	<u>AGCCUGGUA</u>	<u>GCGC</u>	A	GCGGC	<u>CUUCAGA</u>	<u>GCCGC</u>	<u>UUGGGGCCGCGCGGUCCCGA</u>	<u>AGGGG</u>	UUCGAUU	<u>CCCCU</u>	CCGCUCC	A	CCA
DTS2_V1.1	GGGGCGG	UA	<u>GCGC</u>	<u>AGCCUGGUA</u>	<u>GCGC</u>	A	GCGGC	<u>CUUCAGA</u>	<u>GCCGC</u>	<u>UUGGGGCCGCGCGGUCCCGG</u>	<u>AGGGG</u>	UUCGAUU	<u>CCCCU</u>	CCGCUCC	A	CCA
DTS2_V2	GGGGCGG	UA	<u>GCGC</u>	<u>AGCCUGGUA</u>	<u>GCGC</u>	A	GCGGC	<u>CUUCAGA</u>	<u>GCCGC</u>	<u>UUGGGUACUCCCCG</u>	<u>AGGGG</u>	UUCGAUU	<u>CCCCU</u>	CCGCUCC	A	CCA

Name	Acc-s	D-s	D-l	D-s	Ac-s	Ac-l	Ac-s	V-r	T-s	T-l	T-s	Acc-s	CCA			
	1	8	10	14	22	26	27	32	39	44	49	53	61	66	73	74
DTS2_V3	GGGGCGG	UA	GCGC	AGCCUUGGUA	GCGC	A	GCGGC	CUUCAGA	GCCGC	UGGGGUCCACUCCCCG	AGGGG	UUCGAUU	CCCCU	CCGCUCC	A	CCA
TS2_A37	GGGGCGG	UA	GCUC	AGAAGGGA	GAGC	A	GCGGC	CUUCAAA	GCCGC	GAGAC	AGGGG	UUCGAUU	CCCCU	CCGCUCC	A	CCA
TS2_V1	GGGGCGG	UA	GCUC	AGAAGGGA	GAGC	A	GCGGC	CUUCAGA	GCCGC	UUGGGGCCGCGCGGUCCCCGA	AGGGG	UUCGAUU	CCCCU	CCGCUCC	A	CCA
TS2_V1.1	GGGGCGG	UA	GCUC	AGAAGGGA	GAGC	A	GCGGC	CUUCAGA	GCCGC	UUGGGGCCGCGCGGUCCCCG	AGGGG	UUCGAUU	CCCCU	CCGCUCC	A	CCA
TS2_V2	GGGGCGG	UA	GCUC	AGAAGGGA	GAGC	A	GCGGC	CUUCAGA	GCCGC	UGGGGUACUCCCCG	AGGGG	UUCGAUU	CCCCU	CCGCUCC	A	CCA
TS2_V3	GGGGCGG	UA	GCUC	AGAAGGGA	GAGC	A	GCGGC	CUUCAGA	GCCGC	UGGGGUCCACUCCCCG	AGGGG	UUCGAUU	CCCCU	CCGCUCC	A	CCA
n2	GGGGCUC	UA	GCUC	AGAAGGGA	GAGC	A	GGGAC	GACUAAA	GUCCC	GAGAC	GGCGC	UUCGAUU	GCGCC	GAGCUCC	A	CCA
	GGGGCUC	UA	GCUC	AGAAGGGA	GAGC	A	GGGAC	GAUCAAA	GUCCC	GAGAC	GGCGC	UUCGAUU	GCGCC	GAGCUCC	A	CCA
n2 AS1	GGGGCGC	UA	GCUC	AGAAGGGA	GAGC	A	GGGAC	GACUAAA	GUCCC	GAGAC	GGCGC	UUCGAUU	GCGCC	GCGCUCC	A	CCA
n2 AS2	GGGGCUG	UA	GCUC	AGAAGGGA	GAGC	A	GGGAC	GACUAAA	GUCCC	GAGAC	GGCGC	UUCGAUU	GCGCC	CAGCUCC	A	CCA
n2 AS3	GGGGCGG	UA	GCUC	AGAAGGGA	GAGC	A	GGGAC	GACUAAA	GUCCC	GAGAC	GGCGC	UUCGAUU	GCGCC	CCGCUCC	A	CCA
n3	GGGGCCC	UA	GCUC	AGAAAGGA	GAGC	A	GGCAG	GACUAAA	CUGCC	GAGAA	GCAGC	GACAUAA	GCUGC	GGGCUCC	A	CCA
	GGGGCCC	UA	GCUC	AGAAAGGA	GAGC	A	GGCAG	GAUCAAA	CUGCC	GAGAA	GCAGC	GACAUAA	GCUGC	GGGCUCC	A	CCA
n3A1	GGGGCCC	UA	GCUC	AGAAAGGA	GAGC	A	GGCAG	GUCUAAA	CUGCC	GAGAA	GCAGC	GACAUAA	GCUGC	GGGCUCC	A	CCA
	GGGGCCC	UA	GCUC	AGAAAGGA	GAGC	A	GGCAG	GUUCAAA	CUGCC	GAGAA	GCAGC	GACAUAA	GCUGC	GGGCUCC	A	CCA
n3A2	GGGGCCC	UA	GCUC	AGAAAGGA	GAGC	A	GGCAG	CUUCAGA	CUGCC	GAGAA	GCAGC	GACAUAA	GCUGC	GGGCUCC	A	CCA
	GGGGCCC	UA	GCUC	AGAAAGGA	GAGC	A	GGCAG	CUUCAGA	CUGCC	GAGAA	GCAGC	GACAUAA	GCUGC	GGGCUCC	A	CCA
n3A3	GGGGCCC	UA	GCUC	AGAAAGGA	GAGC	A	GGCAC	CUUCAGA	GUGCC	GAGAA	GCAGC	GACAUAA	GCUGC	GGGCUCC	A	CCA
	GGGGCCC	UA	GCUC	AGAAAGGA	GAGC	A	GGCAC	CUUCAGA	GUGCC	GAGAA	GCAGC	GACAUAA	GCUGC	GGGCUCC	A	CCA
n4	GGGGCCC	UA	GCUC	AGAAAGGA	GAGC	A	GGCAG	GACUAAA	CUGCC	GAGAA	GCCGG	GACUAAA	CCGGC	GGGCUCC	A	CCA
n5	GGGGCGC	UA	GCUC	AUAAGGA	GAGC	A	GGAGC	GACUAAA	GUCCC	GAGAA	GUCGC	GACAUAA	GCGAC	GCGCUCC	A	CCA
n6	GGGGCGG	AA	CAGG	GAAACAGA	CCUG	A	GCGGA	GACUAAA	UCCGC	AAUAA	GGUCC	GAACUAA	GGACC	CCGCUCC	A	CCA
Ala(GGC)	GGGGCUA	UA	GCUC	AGCUGGGA	GAGC	G	CUUGC	AUGGCAU	GCAAG	AGGUC	AGCGG	UUCGAUC	CCGCU	UAGCUCC	A	CCA
Ala(UCA(G))	GGGGCUA	UA	GCUC	AGCUGGGA	GAGC	G	CUUGC	AUUCAAU	GCAAG	AGGUC	AGCGG	UUCGAUC	CCGCU	UAGCUCC	A	CCA
Ala(CUA)	GGGGCUA	UA	GCUC	AGCUGGGA	GAGC	G	CUUGC	AUCUAAU	GCAAG	AGGUC	AGCGG	UUCGAUC	CCGCU	UAGCUCC	A	CCA

8 MATERIALS AND METHODS

Name	Acc-s	D-s	D-l	D-s	Ac-s	Ac-l	Ac-s	V-r		T-s	T-l	T-s	Acc-s	CCA			
	1	8	10	14	22	26	27	32	39	44		49	53	61	66	73	74
Ala(UGC)	GGGGCUA	UA	GCUC	AGCUGGGA	GAGC	G	CCUGC	UUUGC <u>C</u> AC	GCAGG	AGGUC		UGCGG	UUCGAUC	CCGCA	UAGCUCC	A	CCA
Ala(UCA(U))	GGGGCUA	UA	GCUC	AGCUGGGA	GAGC	G	CCUGC	UUU <u>C</u> AAC	GCAGG	AGGUC		UGCGG	UUCGAUC	CCGCA	UAGCUCC	A	CCA

8.1.8 Buffers

Buffers used in RNA work were prepared under RNase-free conditions using RNase-free water and filter-sterilized.

3.2x energy mix

1.7 mM DTT

0.8 mM CTP/GTP/UTP

1.2 mM ATP

1x EM buffer

80 mM creatine phosphate

0.175 g/L purified bulk tRNA from BL21 cells

200 mM monopotassium glutamate

2% PEG 8000

10x EM buffer

550 mM HEPES-KOH pH 7.5

350 µg/mL folinic acid

280 mM NH₄OAc

110 mM Mg(OAc)₂

0.5% NaN₃

5x RT buffer

250 mM Tris-HCl pH 8.3

250 mM KCl

20 mM MgCl₂

50 mM DTT

5x Transcription buffer

200 mM Tris-HCl pH 7.9

30 mM MgCl₂

50 mM DTT

50 mM NaCl

10 mM spermidine

2x acidic RNA Loading Dye

0.1 M NaOAc pH 4.8

8 M urea

5% glycerol

0.025% bromophenol blue

0.025% xylene cyanol FF

5x SDS loading dye

313 mM Tris-HCl pH 6.8

5% SDS

0.5% bromophenol blue

50% glycerol

5% β -mercaptoethanol

ECL solution I

0.1 M Tris-HCl pH 8.5

400 μ M cumaric acid

2.5 mM luminole

ECL solution II

0.2 M Tris-HCl pH 8.5

0.02% H₂O₂

10x PBS

80 g NaCl

2 g KCl

14.4 g Na₂HPO₄·2 H₂O

2.4 g KH₂PO₄

Volume was adjusted with water to 1 L and autoclaved

Recette Church buffer

250 mM Na₂HPO₄ pH 7.2

1 mM EDTA pH 8.0

7% SDS

0.5% BSA

4 mg herring sperm DNA (Promega)

NB wash buffer 1

2x SSC

0.2% SDS

NB wash buffer 2

1x SSC

0.1% SDS

20x SSC

3 M NaCl

0.3 M Na-citrate, pH 7.0

10x T4 DNA ligase buffer

400 mM Tris-HCl pH 7.8

100 mM MgCl₂

100 mM DTT

5 mM ATP

Stripping buffer

15 g glycine

1 g SDS

1% (v/v) Tween 20

pH was adjusted to 2.2 and volume was filled up to 1 L with water

Buffer 1

10 mM Tris-OAc pH 8.2

60 mM KOAc

14 mM Mg(OAc)₂

1 mM DTT

7 mM β-mercaptoethanol

Buffer 2

10 mM Tris-OAc pH 8.2

60 mM KOAc

14 mM Mg(OAc)₂

1 mM DTT

Buffer 3

10 mM Tris-OAc pH 8.2

60 mM KOAc

14 mM Mg(OAc)₂

Buffer A

20 mM Tris-HCl pH 8.0

500 mM NaCl

Buffer B

20 mM Tris-HCl pH 8.0

500 mM NaCl

200 mM imidazol

NPI-10 buffer

50 mM NaH₂PO₄

300 mM NaCl

10 mM imidazole

pH was adjusted to 8.0

5x Native purification buffer

250 mM NaH₂PO₄ pH 8.0

2.5 M NaCl

pH was adjusted to 8.0

Native binding buffer

1x Native purification buffer

10 mM imidazole pH 6.0

pH was adjusted to 8.0

3M imidazole pH 6.0

3 M imidazole

500 mM NaCl

20 mM sodium phosphate buffer

pH was adjusted to 6.0

Native wash buffer

50 mL 1x Native purification buffer

335 μ L 3 M imidazole pH 6.0

pH was adjusted to 8.0

Native elution buffer

13.75 mL 1x Native purification buffer

1.25 mL 3 M imidazole pH 6.0

pH was adjusted to 8.0

S30 Medium

5.6 g KH_2PO_4

28.9 g K_2HPO_4

10 g yeast extract

15 mg thiamine

40 mL 25% glucose

Volume was adjusted with water to 1 L and autoclaved, thiamine and glucose were sterile-filtered and added after autoclaving

Preincubation buffer

300 mM Tris-OAc pH 7.6

10 mM $\text{Mg}(\text{OAc})_2$

10 mM ATP

80 mM phosphoenol pyruvate

5 mM DTT

40 μ M amino acid mix

8 U/mL pyruvate kinase

1x TBST

1x TBS

0.05% (v/v) Tween-20

10x TBS

0.2 M Tris-HCl pH 7.6

1.5 M NaCl

8.2 Methods

8.2.1 Cloning and transformation

For *in vitro* experiments GFP or PTC GFP variants were subcloned into pIVEX 2.3, optimized for *in vitro* translation reactions, under control of T7 promoter. For *in vivo* experiments GFP or PTC GFP variants were subcloned into pBAD33 under control of the L-arabinose inducible promoter P_{BAD}. tRNAs were subcloned into pBST NAV2 (kindly provided by Dr. Axel Innis, Institut Européen de Chimie et Biologie) under control of the *lpp* promoter and *rrnC* terminator. Expression was performed in XL1-blue cells grown in LB medium at 37°C supplemented with ampicillin (100 mg/mL) and/or chloramphenicol (34 mg/mL).

GFP nonsense mutations were introduced by site-directed mutagenesis. Briefly, the wildtype GFP vector was amplified using suitable primers for insertion of the nonsense site with Phusion DNA polymerase. Parental plasmid was digested with DpnI. Reactions were purified with GeneJET PCR Purification Kit and transformed into competent *E. coli* DH5 α cells. Plasmids were purified using the GeneJET Plasmid Miniprep Kit and verified by Sanger sequencing (GATC Biotech). Positive constructs were transformed into XL1-blue cells for *in vivo* experiments. For generation of the tRNA-containing pBST NAV2 plasmids, the tRNA sequences were added to the terminus of the primers. Primers were phosphorylated using T4 PNK and used to amplify the pBST NAV2 plasmid with Phusion DNA polymerase. Prior to transformation into *E. coli* DH5 α cells, ligation of amplified DNA was performed using T4 DNA Ligase. The remaining protocol was performed as described above.

Co-transformation of pBAD33 and pBST NAV2 constructs into *E. coli* XL1-blue cells was verified by double restriction digestion with PstI and XbaI and consequent visualization by 2% agarose gel electrophoresis and RedSafe staining.

8.2.2 Growth curves

XL1-blue cells transformed with the tRNA-containing pBST NAV2 plasmid were grown in LB medium at 37°C 250 rpm supplemented with ampicillin (100 mg/mL). Growth was determined by recording OD_{600nm} data every 30 min over a period of 10 h. Obtained OD_{600nm} values were zeroed with LB medium.

8.2.3 tRNA design

tRNA designs were performed by Marco Matthies and Prof. Andrew Torda (University of Hamburg). Briefly, candidate sequences were generated with DSS-Opt (DSS-Opt commit c0c1e0f47f5346453a9e73f26ba08a6e826d5a9b) [246]. Constraints used in the design included recognition elements of tRNA^{Ala}, bases involved in tertiary interactions defined from the crystal structure of unmodified *E. coli* tRNA^{Phe} (PDB ID: 3LOU) [96] and the stop anticodon. The remaining sequence was calculated *de novo*. Sequences were ranked according to the probability of target secondary structure formation, which was calculated using the Vienna suite implementation (Vienna 1.8.5) of the nearest-neighbor model [247]. Target secondary and tertiary interactions were calculated from protein databank coordinates with DSSR (DSSR 1.4.0) [248].

8.2.4 *In vitro* T7 transcription

Templates for *in vitro* T7 transcription were generated by annealing and primer extension of two overlapping DNA oligonucleotides bearing the tRNA sequence and an upstream T7 promoter (5'-TAATACGACTCACTATA-3'). 24 μ M Primers were denatured for 2 min at 95°C and incubated for 3 min at room temperature in 20 mM Tris-HCl (pH 7.5). Primer extension was performed in the presence of 1x RT buffer, 0.4 mM dNTPs, 4 U/ μ L RevertAid Reverse Transcriptase for 40 min at 37°C. The dsDNA template was extracted using phenol/chloroform, ethanol precipitated, washed with 80% EtOH and resuspended in DEPC-H₂O.

In vitro T7 transcription of 1 μ g template DNA was performed in the presence of 2 mM NTPs, 1.25-5 mM GMP, 1x transcription buffer, 30 U T7 RNA polymerase or self-made T7 RNA polymerase overnight at 37°C. The reactions were ethanol precipitated and purified using 10% preparative denaturing polyacrylamide gel electrophoresis. tRNAs were eluted in 50 mM KOAc, 200 mM KCl pH 7 at 1000 rpm overnight at 4°C. The tRNA eluates were filtered to remove gel pieces. tRNAs were ethanol precipitated, washed with 80% EtOH and resuspended in DEPC-H₂O. tRNA integrity was monitored by 10% denaturing PAGE, followed by SYBR gold staining.

8.2.5 tRNA folding

tRNAs were denatured by incubation for 2 min at 85°C in 45 mM Tris-HCl (pH 7.5). Consequently, tRNAs were folded by incubation at room temperature for 3 min, addition of 20 mM MgCl₂ and further incubation for 10 min at 37°C.

8.2.6 Fluorescent labeling of tRNAs

Fluorescent labeling of 500 ng tRNA was performed in the presence of 1x T4 DNA ligase buffer, 15% (v/v) DMSO, 5 µM Cy3-labeled RNA/DNA stem-loop oligonucleotide (Table 18) and 2.5 U T4 DNA ligase. The reaction was incubated overnight at 16°C. Ligated and unligated RNA fractions were separated by 10% denaturing polyacrylamide gel electrophoresis. RNAs were visualized by fluorescence using Bio-Rad ChemiDocTM XRS+ system and by SYBR gold staining.

8.2.7 *In vitro* aminoacylation

In vitro aminoacylation of 1 µg folded tRNA was performed in the presence of 60 mM Tris-HCl (pH 7.5), 10 mM KCl, 12.5 mM MgCl₂, 1 mM spermine, 1.5 mM DTT, 1.5 mM ATP, 20 U RiboLock RNase inhibitor, 1 mM L-alanine and 1 µM of His-tag enriched *E. coli* Alanyl-tRNA synthetase for 15 min at 37°C. Aminoacylated tRNAs were ethanol precipitated and directly dissolved in 2x acidic RNA loading dye. Charged and uncharged tRNA fractions were separated by denaturing acidic polyacrylamide gel electrophoresis (6.5% (19:1) acrylamide:bisacrylamide, 8 M urea, 0.1 M NaOAc pH 5) at 4°C. tRNAs were visualized by SYBR gold staining.

8.2.8 Purification and enrichment of His-tagged *E. coli* Alanyl-tRNA synthetase

BL21 (DE3) cells transformed with pQE30 *E. coli* AlaRS (kindly provided by Dr. Ya-Ming Hou, Jefferson Univ.) were grown in LB-medium containing ampicillin (100 mg/mL) at 37°C and 250 rpm. At OD_{600nm}=0.4-0.6 cells were induced with 1 mM IPTG and further grown for 3-4 h at 180-200 rpm. Cells were harvested by centrifugation at 5000 xg for 15 min at 4°C. Cells were resuspended in buffer A or NPI-10 buffer (supplemented with 1x cComplete protease inhibitor, 1 mM PMSF and 0.5% (v/v) benzonase nuclease) and lysed by four repeti-

tive cycles of cryogenic disruption for 2 min at a frequency of 300 1/s using RetschMill MM400. *E. coli* AlaRS was enriched from cell lysate using two different approaches.

In one approach buffer A was added to the cell lysate and samples were centrifuged for 15 min at 6000 xg and 4°C to remove cell debris. Cell lysate was incubated with Ni-NTA agarose for 2 h or overnight under agitation at 4°C. The Ni-NTA resin was washed with 0 mM – 50 mM imidazole to remove non-specific bound proteins. *E. coli* AlaRS was eluted by washing with 100 mM – 200 mM imidazole and concentrated using Microcon 30 size exclusion filters (Amicon). Protein concentration was determined by Bradford and the values obtained were corrected for the fraction of *E. coli* AlaRS compared to the total amount of proteins after Ni-NTA purification as determined by Coomassie-staining of 10% SDS-PAGE. 50 % glycerol was added for long-term storage at -20°C.

In the second approach the cell lysate was centrifuged for 15 min at 5000 xg 4°C. Native binding buffer and Ni-NTA agarose were added to the cell lysate and incubated for 1 h or overnight under agitation at 4°C. The Ni-NTA resin was washed four times with native wash buffer. *E. coli* AlaRS was eluted by addition of native elution buffer. *E. coli* AlaRS was concentrated and imidazole was removed using Centricon YM-10 filter device (Merck Millipore). Protein concentration was determined as described earlier.

8.2.9 Preparation of *E. coli* S30 cell-free expression system

E. coli S30 cell-free expression system was prepared from BL21 (DE3) cells grown in S30 medium at 180 rpm 37°C. At OD_{600nm}=1.5-2 cells were harvested by centrifugation for 30 min at 6000 xg 4°C. The cell pellet was resuspended in buffer 1 and centrifuged for 20 min at 5000 xg 4°C. Resuspension of the cell pellet in buffer 2 was followed by four repetitive cycles of cryogenic disruption for 2 min at a frequency of 300 1/s using RetschMill MM400. Cell lysate was cleared by two cycles of ultracentrifugation at 30,000 xg for 30 min 4°C (Beckman Coulter SW55Ti swinging bucket rotor). Preincubation buffer was added to the supernatant and samples were incubated under agitation in the dark for 90 min at 37°C. The cell lysate was dialyzed against buffer 3 using ZelluTrans V-series (Roth) with a molecular cut off of 5000 Da.

E. coli S30 lysate expressing T7 RNA polymerase was prepared the same way. At OD_{600nm}=0.8-1 cells were induced with 0.5 mM IPTG and harvested after 3-4 h.

8.2.10 *In vitro* translation

E. coli S30 cell-free expression system was prepared as described earlier. GFP with an amber or opal stop codon at position 28 cloned in pIVEX 2.3 was *in vitro* translated along with different concentrations (0 ng – 100 ng) of *in vitro* transcribed, folded tRNAs. 10 ng/ μ L GFP template were *in vitro* translated in the presence of 40% (v/v) S30 lysate, 5% (v/v) T7 lysate, 1x energy mix, 2 mM amino acids, 80 μ g/mL creatine kinase and the corresponding amount of tRNAs. Reactions were incubated for 6 h at 30°C. The samples were precipitated using acetone, washed with 80% acetone and resuspended in 1x SDS-loading buffer. *In vitro* translations were heated for 5 min at 95°C prior to treatment with 0.5 μ L benzonase (Merck Millipore) and centrifuged for 5 min at 13000 xg 4°C to remove cell debris. Immunoblotting was performed (8.2.11).

8.2.11 Immunoblotting

Co-transformed XL1-blue cells were grown in LB-medium containing ampicillin (100 mg/mL) and chloramphenicol (34 mg/mL). At $OD_{600nm}=0.4$ GFP expression was induced with 0.05% or 0.25% L-arabinose and cells were further cultivated till $OD_{600nm}=1.0$ was reached. Cells were harvested by centrifugation 13000 xg for 5 min at 4°C. Cells were washed with 1x PBS and resuspended in 1x SDS loading dye. Cells were heated for 5 min at 95°C and placed on ice. 1 μ L benzonase nuclease was added and the samples were centrifuged 13000 xg for 5 min at 4°C to remove cell debris. Lysate was separated by 12% SDS-PAGE and transferred to a PDVF membrane (Merck Millipore). Membranes were blocked in 5% milk in TBST (1x) for 1 h at room temperature. Immunoblots were probed with α -GFP antibody (Table 15) overnight at 4°C. Detection was performed using HRP-conjugated α -mouse IgG antibody (Table 15) and ECL (Bio-Rad Gel Doc XRS+). Membranes were incubated in stripping buffer to remove bound antibodies, washed and incubated with HRP-conjugated α -GAPDH antibody (Table 15) overnight at 4°C, followed by ECL-detection. Stop codon read-through activity as determined by GFP expression were normalized to the expression level of GAPDH. The expression data was analyzed using Photoshop CS6.

8.2.12 Northern blotting

tRNA sequences were cloned into the pBST NAV2 vector under control of a consecutive *lpp* promoter and *rrnC* terminator. XL1 blue cells, transformed with corresponding pBST NAV2

plasmids, were grown in LB medium containing ampicillin (100 mg/mL) until $OD_{600nm}=0.8$. Total RNA was extracted using TRIzol reagent (Invitrogen) according to the manufacturer's protocol. Total RNA was resuspended in 1x RNA loading dye, separated on a 10% denaturing polyacrylamide gel and transferred onto a Hybond-N+ membrane (GE Healthcare) overnight at 4°C. Membranes were dried for 10 min at 60°C and crosslinked using 254 nm UV twice at 9999 $\mu J/cm^2$. Membranes were blocked with Recette Church buffer for >5 h at 28°C. 5 μL 5'-Cy3-labeled tRNA probe and 5 μL 5'-Cy5-labeled 5S rRNA probe were added (Table 18). Hybridization was performed overnight at 28°C. Northern blots were washed twice with NB wash buffer 1 for 10 min and NB wash buffer 2 for 7 min at 28°C. RNAs were visualized by fluorescence using Bio-Rad ChemiDoc™ XRS+ system.

8.2.13 Fluorescence intensity measurements

Cells were grown and harvested as described earlier (8.2.11). Cells were washed and resuspended in PBS (1x). GFP fluorescence and OD_{600nm} values were measured using black 96-well plates with transparent bottom. GFP was allowed to mature for at least 24 h prior to the measurement. GFP fluorescence was measured at 485 nm excitation and 535 nm emission. Cell density was determined by absorption at 600 nm (GENios plate reader, Tecan; Victor5, PerkinElmer; Varioskan LUX, Thermo Fisher Scientific). Fluorescence values were normalized to corresponding OD_{600nm} values.

8.2.14 FACS

Cells were grown and harvested as described earlier (8.2.11). Cells were washed and resuspended in PBS (1x). Samples were subjected to flow cytometry on FACS Calibur (Becton Dickinson). GFP fluorescence was recorded for a total of 100,000 events with the following settings: FSC=E01, log, SSC=400, log, FL1=736, log and the following threshold: FSC=52. The data was analyzed using Flowing Software version 2.5.1.

9 REFERENCES

All cited reviews include the references within.

- [1] D.J. Klein, P.B. Moore, T.A. Steitz, The roles of ribosomal proteins in the structure assembly, and evolution of the large ribosomal subunit, *J. Mol. Biol.* 340 2004, 141–177.
- [2] P. Nissen, J. Hansen, N. Ban, P.B. Moore, The Structural Basis of Ribosome Activity in Peptide Bond Synthesis, *Science.* 289 2013, 920–931.
- [3] T.M. Schmeing, V. Ramakrishnan, What recent ribosome structures have revealed about the mechanism of translation, *Nature.* 461 2009, 1234–1242.
- [4] T.A. Steitz, A structural understanding of the dynamic ribosome machine, *Nat. Rev. Mol. Cell Biol.* 9 2008, 242–253.
- [5] V. Ramakrishnan, Ribosome structure and the mechanism of translation., *Cell.* 108 2002, 557–72.
- [6] R. Brimacombe, The bacterial ribosome at atomic resolution, *Structure.* 8 2000, 195–200.
- [7] D.N. Wilson, K.H. Nierhaus, The E-site story: The importance of maintaining two tRNAs on the ribosome during protein synthesis, *Cell. Mol. Life Sci.* 63 2006, 2725–2737.
- [8] N. Burkhardt, R. Jünemann, C.M.T. Spahn, K.H. Nierhaus, Ribosomal tRNA binding sites: Three-site models of translation, *Crit. Rev. Biochem. Mol. Biol.* 33 1998, 95–149.
- [9] H.J. Rheinberger, H. Sternbach, K.H. Nierhaus, Three tRNA binding sites on *Escherichia coli* ribosomes., *Proc. Natl. Acad. Sci.* 78 1981, 5310–5314.
- [10] D. Sohmen, J.M. Harms, F. Schlünzen, D.N. Wilson, Enhanced SnapShot: Antibiotic

- Inhibition of Protein Synthesis II, *Cell*. 139 2009, 212-212.e1.
- [11] C.O. Gualerzi, C.L. Pon, Initiation of mRNA translation in bacteria: Structural and dynamic aspects, *Cell. Mol. Life Sci.* 72 2015, 4341–4367.
- [12] G.Z. Yusupova, M.M. Yusupov, J.H.D. Cate, H.F. Noller, The path of messenger RNA through the ribosome, *Cell*. 106 2001, 233–241.
- [13] J. Shine, L. Dalgarno, The 3'-terminal sequence of Escherichia coli 16S ribosomal RNA, *Proc. Natl. Acad. Sci. USA*. 71 1974, 1342.
- [14] A. Korostelev, S. Trakhanov, H. Asahara, M. Laurberg, L. Lancaster, H.F. Noller, Interactions and dynamics of the Shine Dalgarno helix in the 70S ribosome, *Proc. Natl. Acad. Sci.* 104 2007, 16840–16843.
- [15] D. Moazed, R.R. Samaha, C. Gualerzi, H.F. Noller, Specific protection of 16S rRNA by translational initiation factors, *J. Mol. Biol.* 248 1995, 207–210.
- [16] A.P. Carter, D.E. Brodersen, R.J. Morgan-warren, T. Hartsch, B.T. Wimberly, V. Ramakrishnan, Crystal Structure of an Initiation Factor Bound to the 30S Ribosomal Subunit, *Science*. 291 2001, 498–501.
- [17] K.D. Dahlquist, J.D. Puglisi, Interaction of translation initiation factor IF1 with the E. coli ribosomal A site, *J. Mol. Biol.* 299 2000, 1–15.
- [18] P. Milon, M. Carotti, A.L. Konevega, W. Wintermeyer, M. V. Rodnina, C.O. Gualerzi, The ribosome-bound initiation factor 2 recruits initiator tRNA to the 30S initiation complex, *EMBO Rep.* 11 2010, 312–316.
- [19] R.M. Sundari, E.A. Stringer, L.H. Schulman, U. Maitra, Interaction of Bacterial Initiation Factor 2 with Initiator tRNA, *J. Biol. Chem.* 251 1976, 3338–3345.
- [20] B.L. Seong, U.L. RajBhandary, Mutants of Escherichia coli formylmethionine tRNA: a single base change enables initiator tRNA to act as an elongator in vitro., *Proc. Natl. Acad. Sci. U. S. A.* 84 1987, 8859–63.
- [21] J.K. Sussman, E.L. Simons, R.W. Simons, Escherichia coli translation initiation factor 3 discriminates the initiation codon in vivo, *Mol. Microbiol.* 21 1996, 347–360.
- [22] T. Meinnel, C. Sacerdot, M. Graffe, S. Blanquet, M. Springer, Discrimination by

- Escherichia coli initiation factor IF3 against initiation on non-canonical codons relies on complementarity rules, *J. Mol. Biol.* 290 1999, 825–837.
- [23] D. Hartz, J. Binkley, T. Hollingsworth, L. Gold, Domains of initiator tRNA and initiation codon crucial for initiator tRNA selection by Escherichia coli IF3, *Genes Dev.* 4 1990, 1790–1800.
- [24] A.R. Marshall, C.E. Aitken, J.D. Puglisi, GTP hydrolysis by IF2 guides progression of the ribosome into elongation, *Mol. Cell.* 35 2009, 37–47.
- [25] A.G. Myasnikov, S. Marzi, A. Simonetti, A.M. Giuliadori, C.O. Gualerzi, G. Yusupova, M. Yusupov, B.P. Klaholz, Conformational transition of initiation factor 2 from the GTP- to GDP-bound state visualized on the ribosome, *Nat. Struct. Mol. Biol.* 12 2005, 1145–1149.
- [26] S. Kaledhonkar, Z. Fu, K. Caban, W. Li, B. Chen, M. Sun, R.L. Gonzalez, J. Frank, Late steps in bacterial translation initiation visualized using time-resolved cryo-EM, *Nature.* 2019,.
- [27] I.M. Krab, A. Parmeggiani, Mechanisms of EF-Tu, a pioneer GTPase, *Prog. Nucleic Acid Res. Mol. Biol.* 71 2002, 513–51.
- [28] R. Berisio, A. Ruggiero, L. Vitagliano, Elongation factors EF1A and EF-Tu: Their role in translation and beyond, *Isr. J. Chem.* 50 2010, 71–79.
- [29] M. V Rodnina, W. Wintermeyer, Fidelity of Aminoacyl-tRNA Selection on the Ribosome: Kinetic and Structural Mechanisms, *Annu. Rev. Biochem.* 70 2001, 415–435.
- [30] H.S. Zaher, R. Green, Fidelity at the Molecular Level: Lessons from Protein Synthesis, *Cell.* 136 2009, 746–762.
- [31] X. Agirrezabala, J. Frank, Elongation in translation as a dynamic interaction among the ribosome, tRNA, and elongation factors EF-G and EF-Tu, *Q Rev Biophys.* 42 2009, 159–200.
- [32] K.B. Gromadski, H.J. Wieden, M. V. Rodnina, Kinetic mechanism of elongation factor Ts-catalyzed nucleotide exchange in elongation factor Tu, *Biochemistry.* 41 2002, 162–169.

- [33] N. Polacek, A.S. Mankin, The ribosomal peptidyl transferase center: Structure, function, evolution, inhibition, *Crit. Rev. Biochem. Mol. Biol.* 40 2005, 285–311.
- [34] Y.S. Polikanov, T.A. Steitz, C.A. Innis, A proton wire to couple aminoacyl-tRNA accommodation and peptide bond formation on the ribosome, *Nat. Struct. Mol. Biol.* 21 2014, 787–793.
- [35] M.D. Erlacher, N. Polacek, Ribosomal catalysis: The evolution of mechanistic concepts for peptide bond formation and peptidyl-tRNA hydrolysis, *RNA Biol.* 5 2008,.
- [36] M. V. Rodnina, A. Savelsbergh, W. Wintermeyer, Dynamics of translation on the ribosome: Molecular mechanics of translocation, *FEMS Microbiol. Rev.* 23 1999, 317–333.
- [37] M. V Rodnina, W. Wintermeyer, R. Green, *Ribosomes Structure, Function, and Dynamics*, SpringerWienNewYork, 2011.
- [38] G. Dinos, D.L. Kalpaxis, D.N. Wilson, K.H. Nierhaus, Deacylated tRNA is released from the E site upon A site occupation but before GTP is hydrolyzed by EF-Tu, *Nucleic Acids Res.* 33 2005, 5291–5296.
- [39] E. Scolnick, R. Tompkins, T. Caskey, M. Nirenberg, Release factors differing in specificity for terminator codons., *Proc. Natl. Acad. Sci. U. S. A.* 61 1968, 768–74.
- [40] Y. Nakamura, K. Ito, M. Uno, A tripeptide “anticodon” deciphers stop codons in messenger RNA, *Nature.* 403 2000, 680–684.
- [41] A.A. Korostelev, Structural aspects of translation termination on the ribosome, *RNA.* 17 2011, 1409–1421.
- [42] J.J. Shaw, R. Green, Two distinct components of release factor function uncovered by nucleophile partitioning analysis, *Mol. Cell.* 28 2007, 458–467.
- [43] M. Laurberg, H. Asahara, A. Korostelev, J. Zhu, S. Trakhanov, H.F. Noller, Structural basis for translation termination on the 70S ribosome, *Nature.* 454 2008, 852–857.
- [44] A. Korostelev, H. Asahara, L. Lancaster, M. Laurberg, A. Hirschi, J. Zhu, S. Trakhanov, W.G. Scott, H.F. Noller, Crystal structure of a translation termination complex formed with release factor RF2, *Proc. Natl. Acad. Sci.* 105 2008, 19684–

- 19689.
- [45] A. Weixlbaumer, H. Jin, C. Neubauer, R.M. Voorhees, S. Petry, A.C. Kelley, V. Ramakrishnan, Insights into translational termination from the structure of RF2 bound to the ribosome, *Science*. 322 2008, 953–956.
- [46] S. Trobro, J. Åqvist, A Model for How Ribosomal Release Factors Induce Peptidyl-tRNA Cleavage in Termination of Protein Synthesis, *Mol. Cell*. 27 2007, 758–766.
- [47] L. Mora, V. Heurgué-Hamard, S. Champ, M. Ehrenberg, L.L. Kisselev, R.H. Buckingham, The essential role of the invariant GGQ motif in the function and stability in vivo of bacterial release factors RF1 and RF2, *Mol. Microbiol*. 47 2003, 267–275.
- [48] M. Graf, P. Huter, C. Maracci, M. Peterek, M. V. Rodnina, D.N. Wilson, Visualization of translation termination intermediates trapped by the Apidaecin 137 peptide during RF3-mediated recycling of RF1, *Nat. Commun*. 9 2018, 1–11.
- [49] D. V. Freistoffer, M.Y. Pavlov, J. MacDougall, R.H. Buckingham, M. Ehrenberg, Release factor RF3 in *E. coli* accelerates the dissociation of release factors RF1 and RF2 from the ribosome in a GTP-dependent manner, *EMBO J*. 16 1997, 4126–4133.
- [50] K.S. Koutmou, M.E. McDonald, J.L. Brunelle, R. Green, RF3:GTP promotes rapid dissociation of the class 1 termination factor, *RNA*. 20 2014, 609–620.
- [51] H. Gao, Z. Zhou, U. Rawat, C. Huang, L. Bouakaz, C. Wang, Z. Cheng, Y. Liu, A. Zavialov, R. Gursky, S. Sanyal, M. Ehrenberg, J. Frank, H. Song, RF3 Induces Ribosomal Conformational Changes Responsible for Dissociation of Class I Release Factors, *Cell*. 129 2007, 929–941.
- [52] A. V. Zavialov, R.H. Buckingham, M. Ehrenberg, A posttermination ribosomal complex is the guanine nucleotide exchange factor for peptide release factor RF3, *Cell*. 107 2001, 115–124.
- [53] A. Seshadri, U. Varshney, Mechanism of recycling of post-termination ribosomal complexes in eubacteria: A new role of initiation factor 3, *J. Biosci*. 31 2006, 281–289.
- [54] E. Westhof, P. Auffinger, Transfer RNA Structure, *ELS. John Wiley Sons, Ltd Chichester*. 2012,.

- [55] R. Giegé, F. Jühling, J. Pütz, P. Stadler, C. Sauter, C. Florentz, Structure of transfer RNAs: Similarity and variability, *Wiley Interdiscip. Rev. RNA*. 3 2012, 37–61.
- [56] R. Giegé, M. Frugier, *Transfer RNA Structure and Identity*, Madame Curie Bioscience Database [Internet]. Austin (TX): Landes Bioscience, 2000-2013, available from: <https://www.ncbi.nlm.nih.gov/books/NBK6236/>.
- [57] P.F. Agris, E.R. Eruysal, A. Narendran, V.Y.P. Väre, S. Vangaveti, S. V. Ranganathan, Celebrating wobble decoding: Half a century and still much is new, *RNA Biol.* 15 2018, 537–553.
- [58] J. Vacher, H. Grosjean, C. Houssier, R.H. Buckingham, The effect of point mutations affecting Escherichia coli tryptophan tRNA on anticodon-anticodon interactions and on UGA suppression, *J. Mol. Biol.* 177 1984, 329–342.
- [59] E.M. Gustilo, F.A. Vendeix, P.F. Agris, tRNA's modifications bring order to gene expression, *Curr. Opin. Microbiol.* 11 2008, 134–140.
- [60] M. Shimizu, H. Ashara, K. Tamura, T. Hasegawa, H. Himeno, The Role of Anticodon Bases and the Discriminator Nucleotide in the Recognition of some E. coli tRNAs by Their Aminoacyl-tRNA Synthetases, *J. Mol. Evol.* 35 1992, 436–443.
- [61] Y.M. Hou, Discriminating among the discriminator bases of tRNAs, *Chem. Biol.* 4 1997, 93–96.
- [62] P. Deutscher, Synthesis and Functions of the -C-C-A Terminus of Transfer RNA, *Prog. Nucleic Acid Res. Mol. Biol.* 13 1973, 51–92.
- [63] C. Lorenz, C.E. Lünse, M. Mörl, tRNA modifications: Impact on structure and thermal adaptation, *Biomolecules.* 7 2017, 1–29.
- [64] Y. Watanabe, T. Suematsu, T. Ohtsuki, Losing the stem-loop structure from metazoan mitochondrial trnas and co-evolution of interacting factors, *Front. Genet.* 5 2014, 1–8.
- [65] T. Salinas-Giegé, R. Giegé, P. Giegé, tRNA biology in mitochondria, *Int. J. Mol. Sci.* 16 2015, 4518–4559.
- [66] K. Watanabe, Unique features of animal mitochondrial translation systems, *Proc. Japan Acad. Ser. B.* 86 2010, 11–39.

- [67] S. Kim, F. Suddath, G. Quigley, A. McPherson, J. Sussman, A. Wang, N. Seeman, A. Rich, Three-Dimensional Tertiary Structure of Yeast Phenylalanine Transfer RNA, *Science*. 185 1974, 435–440.
- [68] S.H. Kim, G.J. Quigley, F.L. Suddath, A. Mcpherson, D. Sneden, J.J. Kim, J. Weinzierl, A. Rich, Three-dimensional structure of yeast phenylalanine transfer RNA: Folding of the polynucleotide chain, *Science*. 179 1973, 285–288.
- [69] L. Jovine, S. Djordjevic, D. Rhodes, The crystal structure of yeast phenylalanine tRNA at 2.0 Å resolution: Cleavage by Mg²⁺ in 15-year old crystals, *J. Mol. Biol.* 301 2000, 401–414.
- [70] H. Shi, P.B. Moore, The crystal structure of yeast phenylalanine tRNA at 1.93 Å resolution: A classic structure revisited, *RNA*. 6 2000, 1091–1105.
- [71] R. Basavappa, P.B. Sigler, The 3 Å crystal structure of yeast initiator tRNA: functional implications in initiator/elongator discrimination., *EMBO J.* 10 1991, 3105–3111.
- [72] J.D. Robertus, J.E. Ladner, J.T. Finch, D. Rhodes, R.S. Brown, B.F.C. Clark, A. Klug, Structure of yeast phenylalanine tRNA at 3 Å resolution, *Nature*. 250 1974, 546–551.
- [73] J.E. Ladner, A. Jack, J.D. Robertus, R.S. Brown, D. Rhodes, B.F. Clark, A. Klug, Structure of yeast phenylalanine transfer RNA at 2.5 Å resolution., *Proc. Natl. Acad. Sci.* 72 1975, 4414–4418.
- [74] R.S. Brown, J.C. Dewan, A. Klug, Crystallographic and Biochemical Investigation of the Lead(II)-Catalyzed Hydrolysis of Yeast Phenylalanine tRNA, *Biochemistry*. 24 1985, 4785–4801.
- [75] Y. Itoh, S. Chiba, S.I. Sekine, S. Yokoyama, Crystal structure of human selenocysteine tRNA, *Nucleic Acids Res.* 37 2009, 6259–6268.
- [76] R. Oliva, L. Cavallo, A. Tramontano, Accurate energies of hydrogen bonded nucleic acid base pairs and triplets in tRNA tertiary interactions, *Nucleic Acids Res.* 34 2006, 865–879.
- [77] K.N. Nobles, C.S. Yarian, G. Liu, R.H. Guenther, P.F. Agris, Highly conserved modified nucleosides influence Mg²⁺-dependent tRNA folding, *Nucleic Acids Res.* 30 2002, 4751–4760.

- [78] J. Zhang, A. Ferré-D'Amaré, The tRNA Elbow in Structure, Recognition and Evolution, *Life*. 6 2016, 3.
- [79] E.I. Zagryadskaya, F.R. Doyon, S. V. Steinberg, Importance of the reverse Hoogsteen base pair 54-58 for tRNA function, *Nucleic Acids Res.* 31 2003, 3946–3953.
- [80] D. Pan, C.M. Zhang, S. Kirillov, Y.M. Hou, B.S. Cooperman, Perturbation of the tRNA tertiary core differentially affects specific steps of the elongation cycle, *J. Biol. Chem.* 283 2008, 18431–18440.
- [81] C.D. Kuhn, RNA versatility governs tRNA function: Why tRNA flexibility is essential beyond the translation cycle, *BioEssays*. 38 2016, 465–473.
- [82] X. Agirrezabala, M. Valle, Structural insights into tRNA dynamics on the ribosome, *Int. J. Mol. Sci.* 16 2015, 9866–9895.
- [83] G.J. Quigley, A. Rich, Structural domains of transfer RNA molecules, *Science*. 194 1976, 796–806.
- [84] S.S. Ashraf, G. Ansari, R. Guenther, E. Sochacka, A. Malkiewicz, P.F. Agris, The uridine in “U-turn”: Contributions to tRNA-ribosomal binding, *RNA*. 5 1999, 503–511.
- [85] M. Ibba, D. Soll, M. Ibba, S. Dieter, Aminoacyl-tRNA synthesis, *Annu Rev Biochem.* 69 2000, 617–50.
- [86] S. Kim, *Aminoacyl-tRNA synthetases in biology and disease*, Springer-Verlag Berlin Heidelberg, 2014.
- [87] R. Giegé, M. Sissler, C. Florentz, Universal rules and idiosyncratic features in tRNA identity, *Nucleic Acids Res.* 26 1998, 5017–5035.
- [88] K.S. Hoffman, A. Crnković, D. Söll, Versatility of synthetic tRNAs in genetic code expansion, *Genes (Basel)*. 9 2018,.
- [89] Y.M. Hou, P. Schimmel, A simple structural feature is a major determinant of the identity of a transfer RNA, *Nature*. 333 1988, 140–145.
- [90] W.H. McClain, K. Foss, I. May, Changing the Identity of a tRNA by introducing a G-U wobble pair near the 3' acceptor end, *Science*. 240 1960, 793–796.

- [91] W.H. McClain, Y.M. Chen, K. Foss, J. Schneider, Association of transfer RNA acceptor identity with a helical irregularity, *Science*. 242 1988, 1681–1684.
- [92] J. Normanly, J. Abelson, tRNA Identity, *Annu Rev Biochem*. 58 1989, 1029–1049.
- [93] C. Francklyn, P. Schimmel, Aminoacylation of RNA minihelices with alanine, *Nature*. 337 1989, 478–481.
- [94] C. Francklyn, J.P. Shi, P. Schimmel, Overlapping nucleotide determinants for specific aminoacylation of RNA microhelices, *Science*. 255 1992, 1121–1125.
- [95] J.P. Shi, C. Francklyn, K. Hill, P. Schimmel, A Nucleotide That Enhances the Charging of RNA Minihelix Sequence Variants with Alanine, *Biochemistry*. 29 1990, 3621–3626.
- [96] R.T. Byrne, A.L. Konevega, M. V. Rodnina, A.A. Antson, The crystal structure of unmodified tRNAPhe from Escherichia coli, *Nucleic Acids Res*. 38 2010, 4154–4162.
- [97] L.H. Schulman, H. Pelka, An anticodon change switches the identity of E.coli tRNAMet from methionine to threonine, *Nucleic Acids Res*. 18 1990, 285–289.
- [98] J.R. Sampson, O.C. Uhlenbeck, Biochemical and physical characterization of an unmodified yeast phenylalanine transfer RNA transcribed in vitro, *Proc. Natl. Acad. Sci. USA*. 85 1988, 1033–1037.
- [99] K.B. Hall, J.R. Sampson, O.C. Uhlenbeck, A.G. Redfield, Structure of an Unmodified tRNA Molecule, *Biochemistry*. 28 1989, 5794–5801.
- [100] K. Beebe, L.R. De Pouplana, P. Schimmel, Elucidation of tRNA-dependent editing by a class II tRNA synthetase and significance for cell viability, *EMBO J*. 22 2003, 668–675.
- [101] R.A. Marshall, C.E. Aitken, M. Dorywalska, J.D. Puglisi, Translation at the Single-Molecule Level, *Annu. Rev. Biochem*. 77 2008, 177–203.
- [102] P. Nissen, M. Kjeldgaard, S. Thirup, G. Palekhina, L. Reshetnikava, B.F.C. Clark, J. Nyborg, Crystal structure of the Ternary Complex of Phe-tRNAPhe, EF-Tu, and a GTP Analog, *Science*. 270 1995, 1464–1472.
- [103] P. Nissen, S. Thirup, M. Kjeldgaard, J. Nyborg, The crystal structure of Cys-

- tRNA(Cys)-EF-Tu-GDPNP reveals general and specific features in the ternary complex and in tRNA, *Structure*. 7 1999, 143–156.
- [104] J.M. Schrader, S.J. Chapman, O.C. Uhlenbeck, Understanding the Sequence Specificity of tRNA Binding to Elongation Factor Tu using tRNA Mutagenesis, *J. Mol. Biol.* 386 2009, 1255–1264.
- [105] L.E. Sanderson, O.C. Uhlenbeck, Exploring the specificity of bacterial elongation factor Tu for different tRNAs, *Biochemistry*. 46 2007, 6194–6200.
- [106] O.C. Uhlenbeck, J.M. Schrader, Evolutionary tuning impacts the design of bacterial tRNAs for the incorporation of unnatural amino acids by ribosomes, *Curr. Opin. Chem. Biol.* 46 2018, 138–145.
- [107] F.J. LaRiviere, A.D. Wolfson, O.C. Uhlenbeck, Uniform binding of aminoacyl-tRNAs to elongation factor Tu by thermodynamic compensation, *Science*. 294 2001, 165–168.
- [108] T. Dale, O.C. Uhlenbeck, Amino acid specificity in translation, *Trends Biochem. Sci.* 30 2005, 659–665.
- [109] J.M. Schrader, S.J. Chapman, O.C. Uhlenbeck, Tuning the affinity of aminoacyl-tRNA to elongation factor Tu for optimal decoding, *Proc. Natl. Acad. Sci.* 108 2011, 5215–5220.
- [110] H. Asahara, O.C. Uhlenbeck, The tRNA Specificity of *Thermus thermophilus* EF-Tu, *Proc. Natl. Acad. Sci.* 99 2002, 3499–3504.
- [111] L.K. Doerfel, I. Wohlgemuth, C. Kothe, F. Peske, H. Urlaub, M. V. Rodnina, EF-P Is Essential for Rapid Synthesis of Proteins Containing Consecutive Proline Residues, *Science*. 339 2013, 85–88.
- [112] L.K. Doerfel, I. Wohlgemuth, V. Kubyshkin, A.L. Starosta, D.N. Wilson, N. Budisa, M. V. Rodnina, Entropic contribution of elongation factor P to proline positioning at the catalytic center of the ribosome, *J. Am. Chem. Soc.* 137 2015, 12997–13006.
- [113] I. Wohlgemuth, S. Brenner, M. Beringer, M. V. Rodnina, Modulation of the rate of peptidyl transfer on the ribosome by the nature of substrates, *J. Biol. Chem.* 283 2008, 32229–32235.

- [114] M. Johansson, K.-W. Jeong, S. Trobro, P. Strazewski, J. Aqvist, M.Y. Pavlov, M. Ehrenberg, pH-sensitivity of the ribosomal peptidyl transfer reaction dependent on the identity of the A-site aminoacyl-tRNA, *Proc. Natl. Acad. Sci.* 108 2010, 79–84.
- [115] M.Y. Pavlov, R.E. Watts, Z. Tan, V.W. Cornish, M. Ehrenberg, A.C. Forster, Slow peptide bond formation by proline and other N-alkylamino acids in translation, *Proc. Natl. Acad. Sci.* 106 2008, 50–54.
- [116] H. Muto, K. Ito, Peptidyl-prolyl-tRNA at the ribosomal P-site reacts poorly with puromycin, *Biochem. Biophys. Res. Commun.* 366 2008, 1043–1047.
- [117] L. Peil, A.L. Starosta, J. Lassak, G.C. Atkinson, K. Virumae, M. Spitzer, T. Tenson, K. Jung, J. Remme, D.N. Wilson, Distinct XPPX sequence motifs induce ribosome stalling, which is rescued by the translation elongation factor EF-P, *Proc. Natl. Acad. Sci.* 110 2013, 15265–15270.
- [118] S. Ude, J. Lassak, A.L. Starosta, T. Kraxenberger, D.N. Wilson, K. Jung, Translation Elongation Factor EF-P Alleviates Ribosome Stalling at Polyproline Stretches, *Science.* 339 2013, 82–85.
- [119] T. Katoh, I. Wohlgemuth, M. Nagano, M. V. Rodnina, H. Suga, Essential structural elements in tRNA^{Pro} for EF-P-mediated alleviation of translation stalling, *Nat. Commun.* 7 2016, 1–12.
- [120] P. Huter, S. Arenz, L. V. Bock, M. Graf, J.O. Frister, A. Heuer, L. Peil, A.L. Starosta, I. Wohlgemuth, F. Peske, J. Nováček, O. Berninghausen, H. Grubmüller, T. Tenson, R. Beckmann, M. V. Rodnina, A.C. Vaiana, D.N. Wilson, Structural Basis for Polyproline-Mediated Ribosome Stalling and Rescue by the Translation Elongation Factor EF-P, *Mol. Cell.* 68 2017, 515-527.e6.
- [121] C.J. Balibar, D. Iwanowicz, C.R. Dean, Elongation factor P is dispensable in *Escherichia coli* and *Pseudomonas aeruginosa*, *Curr. Microbiol.* 67 2013, 293–299.
- [122] T. Baba, T. Ara, M. Hasegawa, Y. Takai, Y. Okumura, M. Baba, K.A. Datsenko, M. Tomita, B.L. Wanner, H. Mori, Construction of *Escherichia coli* K-12 in-frame, single-gene knockout mutants: the Keio collection., *Mol. Syst. Biol.* 2 2006, 2006.0008.
- [123] D. Hatfield, B.J. Lee, D.W.E. Smith, S. Oroszlan, Role of Nonsense, Frameshift, and

- Missense Suppressor tRNAs in Mammalian Cells, 2011, 115–146.
- [124] G. Eggertsson, D. Söll, Transfer ribonucleic acid-mediated suppression of termination codons in *Escherichia coli.*, *Microbiol. Rev.* 52 1988, 354–74.
- [125] J. Karijolich, Y.T. Yu, Therapeutic suppression of premature termination codons: Mechanisms and clinical considerations, *Int. J. Mol. Med.* 34 2014, 355–362.
- [126] K.M. Keeling, X. Xiaojiao, G. Gunn, D.M. Bedwell, Therapeutics based on Stop Codon Readthrough, *Annu Rev Genomics Hum Genet.* 15 2014, 371–394.
- [127] L. Bidou, V. Allamand, J.P. Rousset, O. Namy, Sense from nonsense: Therapies for premature stop codon diseases, *Trends Mol. Med.* 18 2012, 679–688.
- [128] A.E. Firth, I. Brierley, Non-canonical translation in RNA viruses, *J. Gen. Virol.* 93 2012, 1385–1409.
- [129] E.J. Murgola, tRNA , Suppression, and the Code, *Ann Rev Genet.* 1985, 57–80.
- [130] D. Hirsh, Tryptophan transfer RNA as the UGA suppressor, *J. Mol. Biol.* 58 1971, 439–458.
- [131] T.M. Schmeing, R.M. Voorhees, A.C. Kelley, V. Ramakrishnan, How mutations in tRNA distant from the anticodon affect the fidelity of decoding, *Nat. Struct. Mol. Biol.* 18 2011, 432–437.
- [132] D.B.F. Johnson, C. Wang, J. Xu, M.D. Schultz, R.J. Schmitz, J.R. Ecker, L. Wang, Release factor one is nonessential in *Escherichia coli.*, *ACS Chem. Biol.* 7 2012, 1337–44.
- [133] R. Geslain, T. Pan, Functional Analysis of Human tRNA Isodecoders, *J. Mol. Biol.* 396 2010, 821–831.
- [134] L.G. Kleina, J.M. Masson, J. Normanly, J. Abelson, J.H. Miller, Construction of *Escherichia coli* amber suppressor tRNA genes. II. Synthesis of additional tRNA genes and improvement of suppressor efficiency, *J. Mol. Biol.* 213 1990, 705–717.
- [135] M. Yarus, C. McMillan, S. Cline, D. Bradley, M. Snyder, Construction of a composite tRNA gene by anticodon loop transplant, *Proc. Natl. Acad. Sci.* 77 2006, 5092–5096.

- [136] M. Yarus, S. Cline, L. Raftery, P. Wier, D. Bradley, The translational efficiency of tRNA is a property of the anticodon arm, *J. Biol. Chem.* 261 1986, 10496–10505.
- [137] V. Bourdeau, S. V. Steinberg, G. Ferbeyre, R. Emond, N. Cermakian, R. Cedergren, Amber suppression in *Escherichia coli* by unusual mitochondria-like transfer RNAs, *Proc. Natl. Acad. Sci.* 95 2002, 1375–1380.
- [138] J. Guo, C.E. Melancon, H.S. Lee, P.G. Schultz, Evolution of Amber Suppressor tRNAs for Efficient Bacterial Production of Unnatural Amino Acid-Containing Proteins, *Angew Chem Int Ed Engl.* 48 2009, 9148–9151.
- [139] A. Ogawa, Y. Doi, N. Matsushita, Improvement of in vitro-transcribed amber suppressor tRNAs toward higher suppression efficiency in wheat germ extract, *Org. Biomol. Chem.* 9 2011, 8495–8503.
- [140] A. Ogawa, M. Hayami, S. Sando, Y. Aoyama, A Concept for Selection of Codon-Suppressor tRNAs Based on Read-Through Ribosome Display in an In Vitro Compartmentalized Cell-Free Translation System, *J. Nucleic Acids.* 2012 2012, 1–7.
- [141] S. V. Melnikov, D. Söll, Aminoacyl-tRNA Synthetases and tRNAs for an Expanded Genetic Code: What Makes them Orthogonal?, *Int. J. Mol. Sci.* 20 2019, 1929.
- [142] T. Mukai, M.J. Lajoie, M. Englert, D. Söll, Rewriting the Genetic Code, *Annu. Rev. Microbiol.* 71 2017, 557–577.
- [143] Y. Ryu, P.G. Schultz, Efficient incorporation of unnatural amino acids into proteins in *Escherichia coli*, *Nat. Methods.* 3 2006, 263–265.
- [144] T.A. Cropp, P.G. Schultz, An expanding genetic code, *Trends Genet.* 20 2004, 625–630.
- [145] L. Wang, P.G. Schultz, Expanding the genetic code, *Annu. Rev. Biophys. Biomol. Struct.* 35 2006, 225–249.
- [146] O. Vargas-Rodriguez, A. Sevostyanova, D. Söll, A. Crnković, Upgrading aminoacyl-tRNA synthetases for genetic code expansion, *Curr. Opin. Chem. Biol.* 46 2018, 115–122.
- [147] A. Dumas, L. Lercher, C.D. Spicer, B.G. Davis, Designing logical codon reassignment

- Expanding the chemistry in biology., *Chem. Sci.* 6 2015, 50–69.
- [148] C.C. Liu, P.G. Schultz, Adding New Chemistries to the Genetic Code, *Annu. Rev. Biochem.* 79 2010, 413–444.
- [149] H. Xiao, P.G. Schultz, At the interface of chemical and biological synthesis: An expanded genetic code, *Cold Spring Harb. Perspect. Biol.* 8 2016,.
- [150] T. Katoh, K. Tajima, H. Suga, Consecutive Elongation of D-Amino Acids in Translation, *Cell Chem. Biol.* 24 2017, 46–54.
- [151] T. Fujino, Y. Goto, H. Suga, H. Murakami, Ribosomal Synthesis of Peptides with Multiple β -Amino Acids, *J. Am. Chem. Soc.* 138 2016, 1962–1969.
- [152] T. Katoh, Y. Iwane, H. Suga, Logical engineering of D-arm and T-stem of tRNA that enhances D-amino acid incorporation, *Nucleic Acids Res.* 45 2017, 12601–12610.
- [153] Z. Lu, Interaction of nonsense suppressor tRNAs and codon nonsense mutations or termination codons, *Adv. Biol. Chem.* 02 2012, 301–314.
- [154] M. Asiful Islam, F. Alam, M.A. Kamal, S.H. Gan, K.K. Wong, T.H. Sasongko, Therapeutic Suppression of Nonsense Mutation: An Emerging Target in Multiple Diseases and Thrombotic Disorders, *Curr. Pharm. Des.* 23 2017, 1598–1609.
- [155] M. Mort, D. Ivanov, D.N. Cooper, N.A. Chuzhanova, A meta-analysis of nonsense mutations causing human genetic disease, *Hum. Mutat.* 29 2008, 1037–1047.
- [156] K.M. Keeling, D. Wang, S.E. Conard, D.M. Bedwell, Suppression of Premature Termination Codons as a Therapeutic Approach, *Crit Rev Biochem Mol Biol.* 47 2012, 444–463.
- [157] J.D. Lueck, J.S. Yoon, A. Perales-Puchalt, A.L. Mackey, D.T. Infield, M.A. Behlke, M.R. Pope, D.B. Weiner, W.R. Skach, P.B. McCray, C.A. Ahern, Engineered transfer RNAs for suppression of premature termination codons, *Nat. Commun.* 10 2019, 1–11.
- [158] G.F. Temple, A.M. Dozy, K.L. Royt, Y.W. Kan, Construction of a functional human suppressor tRNA gene: an approach to gene therapy for β -thalassaemia, *Nature.* 296 1982, 537–540.
- [159] A.V. Kiselev, O.V. Ostapenko, E.V. Rogozhkina, N.S. Kholod, A.S. Seit Nebi, A.N.

- Baranov, E.A. Lesina, T.E. Ivashchenko, V.A. Sabetskiĭ, M.M. Shavlovskiĭ, V.O. Rechinskiĭ, L.L. Kiselev, V.C. Baranov, Suppression of nonsense mutations in the Dystrophin gene by a suppressor tRNA gene, *Mol. Biol.* 36 2002, 30–33.
- [160] J.P. Richardson, I. Stansfield, S. Innes, O. Minella, G. Bertram, Endless possibilities: translation termination and stop codon recognition, *Microbiology.* 147 2015, 255–269.
- [161] W.P. Tate, E.S. Poole, M.E. Dalphin, L.L. Major, D.J.G. Crawford, S.A. Mannering, The translational stop signal: Codon with a context, or extended factor recognition element?, *Biochimie.* 78 1996, 945–952.
- [162] Y. Wei, X. Xia, The role of +4U as an extended translation termination signal in bacteria, *Genetics.* 205 2017, 539–549.
- [163] E.S. Poole, L.L. Major, S.A. Mannering, W.P. Tate, Translational termination in *Escherichia coli*: Three bases following the stop codon crosslink to release factor 2 and affect the decoding efficiency of UGA-containing signals, *Nucleic Acids Res.* 26 1998, 954–960.
- [164] E.S. Poole, C.M. Brown, W.P. Tate, The identity of the base following the stop codon determines the efficiency of in vivo translational termination in *Escherichia coli*., *EMBO J.* 14 1995, 151–8.
- [165] W.P. Tate, A.G. Cridge, C.M. Brown, ‘Stop’ in protein synthesis is modulated with exquisite subtlety by an extended RNA translation signal, *Biochem. Soc. Trans.* 46 2018, 1615–1625.
- [166] W. Tate, J. Mansell, S. Mannering, J. Irvine, L. Major, D. Wilson, UGA: a dual signal for “stop” and for recoding in protein synthesis, *Biochem.* 64 1999, 1342–1353.
- [167] W.J. Craigen, R.G. Cook, W.P. Tate, C.T. Caskey, Bacterial peptide chain release factors: Conserved primary structure and possible frameshift regulation of release factor 2, *Biochemistry.* 82 1985, 3616–3620.
- [168] B.C. Donly, C.D. Edgar, F.M. Adamski, W.P. Tate, Frameshift autoregulation in the gene for *Escherichia coli* release factor 2: Partly functional mutants result in frameshift enhancement, *Nucleic Acids Res.* 18 1990, 6517–6522.
- [169] A. Böck, K. Forchhammer, J. Heider, W. Leinfelder, G. Sawers, B. Veprek, F. Zinoni,

- Selenocysteine: the 21st amino acid, *Mol. Microbiol.* 5 1991, 515–520.
- [170] F. Zinoni, A. Birkmann, T.C. Stadtman, A. Bock, Nucleotide sequence and expression of the selenocysteine-containing polypeptide of formate dehydrogenase (formate-hydrogen-lyase-linked) from *Escherichia coli.*, *Proc. Natl. Acad. Sci.* 83 2006, 4650–4654.
- [171] C. M.Brown, P. A.Stockwell, C. N.A.Trotman, W. P.Tate, The signal for the termination of protein, *Nucleic Acids Res.* 18 1990, 2079–2086.
- [172] J.H. Miller, A.M. Albertini, Effects of surrounding sequence on the suppression of nonsense codons, *J. Mol. Biol.* 164 1983, 59–71.
- [173] J. Kopelowitz, C. Hampe, R. Goldman, M. Rechtes, H. Engelberg-Kulka, Influence of codon context on UGA suppression and readthrough, *J. Mol. Biol.* 225 1992, 261–269.
- [174] S. Zhang, M. Rydén-Aulin, L.A. Isaksson, Interaction between a mutant release factor one and P-site peptidyl-tRNA is influenced by the identity of the two bases downstream of the stop codon UAG, *FEBS Lett.* 455 1999, 355–358.
- [175] S. Mottagui-Tabar, A. Björnsson, L.A. Isaksson, The second to last amino acid in the nascent peptide as a codon context determinant., *EMBO J.* 13 1994, 249–57.
- [176] A. Björnsson, S. Mottagui-Tabar, L.A. Isaksson, Structure of the C-terminal end of the nascent peptide influences translation termination., *EMBO J.* 15 1996, 1696–704.
- [177] M. Yarus, Translational Efficiency of Transfer RNA's: Uses of an Extended Anticodon, *Science.* 218 1982, 646–652.
- [178] M. Yarus, S.W. Cline, P. Wier, L. Breeden, R.C. Thompson, Actions of the anticodon arm in translation on the phenotypes of RNA mutants, *J. Mol. Biol.* 192 1986, 235–255.
- [179] L.A. Raftery, M. Yarus, Systematic alterations in the anticodon arm make tRNA^{Glu-Suoc} a more efficient suppressor, *EMBO J.* 6 1987, 1499–1506.
- [180] M. Olejniczak, O.C. Uhlenbeck, tRNA residues that have coevolved with their anticodon to ensure uniform and accurate codon recognition, *Biochimie.* 88 2006, 943–950.

- [181] M. Olejniczak, T. Dale, R.P. Fahlman, O.C. Uhlenbeck, Idiosyncratic tuning of tRNAs to achieve uniform ribosome binding, *Nat. Struct. Mol. Biol.* 12 2005, 788–793.
- [182] S. Nishimura, Minor Components in Transfer RNA: Their Characterization, Location and Function, *Prog. Nucleic Acid Res. Mol. Biol.* 12 1972, 49–85.
- [183] S. Nishimura, Y. Yamada, H. Ishikura, The presence of 2-methylthio-N⁶-(Δ^2 -isopentenyl)adenosine in serine and phenylalanine transfer RNA's from *Escherichia coli*, *Biochim. Biophys. Acta.* 179 1969, 517–520.
- [184] U. Schweizer, S. Bohleber, N. Fradejas-Villar, The modified base isopentenyladenosine and its derivatives in tRNA, *RNA Biol.* 14 2017, 1197–1208.
- [185] A.L. Konevega, N.G. Soboleva, V.I. Makhno, Y.P. Semenov, W. Wintermeyer, M. V Rodnina, V.I. Katunin, A.E. Hesslein, M. Beringer, A.B. Kosek, Purine bases at position 37 of tRNA stabilize codon–anticodon interaction in the ribosomal A site by stacking and Mg²⁺-dependent interactions, *RNA.* 10 2004, 90–101.
- [186] F. V. Murphy, V. Ramakrishnan, A. Malkiewicz, P.F. Agris, The role of modifications in codon discrimination by tRNA^{Lys}UUU, *Nat. Struct. Mol. Biol.* 11 2004, 1186–1191.
- [187] J.W. Stuart, Z. Gdaniec, R. Guenther, M. Marszalek, E. Sochacka, A. Malkiewicz, P.F. Agris, Functional anticodon architecture of human tRNA(Lys³) includes disruption of intraloop hydrogen bonding by the naturally occurring amino acid modification, t₆A, *Biochemistry.* 39 2000, 13396–13404.
- [188] V. Dao, R. Guenther, A. Malkiewicz, B. Nawrot, E. Sochacka, A. Kraszewski, J. Jankowska, K. Everett, P.F. Agris, Ribosome binding of DNA analogs of tRNA requires base modifications and supports the “extended anticodon”, *Proc. Natl. Acad. Sci.* 91 2006, 2125–2129.
- [189] J. Cabello-Villegas, M.E. Winkler, E.P. Nikonowicz, Solution conformations of unmodified and A³⁷N⁶-dimethylallyl modified anticodon stem-loops of *Escherichia coli* tRNA^{phe}, *J. Mol. Biol.* 319 2002, 1015–1034.
- [190] M. Sundaram, P.C. Durant, D.R. Davis, Hypermodified nucleosides in the anticodon of tRNA(Lys) stabilize a canonical U-turn structure, *Biochemistry.* 39 2000, 12575–

- 12584.
- [191] G.R. Björk, T.G. Hagervall, Transfer RNA Modification: Presence, Synthesis, and Function, *EcoSal Plus*. 6 2014,.
- [192] L.A. Petruccio, P.J. Gallagher, D. Elseviers, The role of 2-methylthio-N6-isopentenyladenosine in readthrough and suppression of nonsense codons in *Escherichia coli*, *MGG Mol. Gen. Genet.* 190 1983, 289–294.
- [193] M.L. Gefter, R.L. Russell, Role of modifications in tyrosine transfer RNA: A modified base affecting ribosome binding, *J. Mol. Biol.* 39 2005, 145–157.
- [194] R. Klassen, R. Schaffrath, Collaboration of tRNA modifications and elongation factor eEF1A in decoding and nonsense suppression, *Sci. Rep.* 8 2018, 1–12.
- [195] J.U. Ericson, G.R. Björk, tRNA anticodons with the modified nucleoside 2-methylthio-N6-(4-hydroxyisopentenyl)adenosine distinguish between bases 3' of the codon, *J. Mol. Biol.* 218 1991, 509–516.
- [196] T.G. Hagervall, J.U. Ericson, K.B. Esberg, L. Ji-nong, G.R. Björk, Role of tRNA modification in translational fidelity, *BBA - Gene Struct. Expr.* 1050 1990, 263–266.
- [197] F. Bouadloun, T. Srichaiyo, L.A. Isaksson, G.R. Bjork, Influence of modification next to the anticodon in tRNA on codon context sensitivity of translational suppression and accuracy, *J. Bacteriol.* 166 1986, 1022–1027.
- [198] I.L. Björnsson Asgeir, UGA Codon Context Which Spans Three Codons Reversal by ms2I6A37 in tRNA, *J. Mol. Biol.* 232 1993, 1017–1029.
- [199] D.L. Hatfield, B.J. Lee, R.M. Pirtle, *Transfer RNA in Protein Synthesis*, CRC Press Taylor & Francis Group, 1992.
- [200] A.M.K. Wentzel, M. Stancek, L.A. Isaksson, Growth phase dependent stop codon read through and shift of translation reading frame in *Escherichia coli*, *FEBS Lett.* 421 1998, 237–242.
- [201] H. Bhaskaran, A. Rodriguez-Hernandez, J.J. Perona, Kinetics of tRNA folding monitored by aminoacylation, *RNA*. 18 2012, 569–580.
- [202] I. Ferro, Z. Ignatova, Quantifying the ‘escapers’ among RNA species, *Biochem. Soc.*

- Trans.* 43 2015, 1215–1220.
- [203] L.C. Keffer-Wilkes, G.R. Veerareddygari, U. Kothe, RNA modification enzyme TruB is a tRNA chaperone, *Proc. Natl. Acad. Sci.* 113 2016, 14306–14311.
- [204] D.A. Siegele, J.C. Hu, Gene expression from plasmids containing the araBAD promoter at subsaturating inducer concentrations represents mixed populations, *Proc. Natl. Acad. Sci. USA.* 94 1997, 8168–8172.
- [205] Y. Wei, J. Wang, X. Xia, Coevolution between Stop Codon Usage and Release Factors in Bacterial Species, *Mol. Biol. Evol.* 33 2016, 2357–2367.
- [206] H. Engelberg-Kulka, UGA suppression by normal tRNA^{Trp} in Escherichia coli: Codon context effects, *Nucleic Acids Res.* 9 1981, 983–991.
- [207] J. Parker, Errors and alternatives in reading the universal genetic code., *Microbiol. Rev.* 53 1989, 273–98.
- [208] Y. Mechulam, L. Guillon, L. Yatime, S. Blanquet, E. Schmitt, Protection-Based Assays to Measure Aminoacyl-tRNA Binding to Translation Initiation Factors, *Methods Enzymol.* 430 2007, 265–281.
- [209] M.B. Herrington, Nonsense Mutations and Suppression, *ELS. John Wiley Sons, Ltd Chichester.* 2018,.
- [210] G. Korkmaz, M. Holm, T. Wiens, S. Sanyal, Comprehensive analysis of stop codon usage in bacteria and its correlation with release factor abundance, *J. Biol. Chem.* 289 2014, 30334–30342.
- [211] S. Kimura, M.K. Waldor, The RNA degradosome promotes tRNA quality control through clearance of hypomodified tRNA, *Proc. Natl. Acad. Sci.* 116 2019, 1394–1403.
- [212] S. Kirchner, Z. Ignatova, Emerging roles of tRNA in adaptive translation, signalling dynamics and disease, *Nat. Rev. Genet.* 16 2015, 98–112.
- [213] H.I. S. Nishimura, Y. Yamada, The presence of 2-methylthio-N⁶-(Δ^2 -isopentenyl)adenosine in serine and phenylalanine transfer RNA's from Escherichia coli, *Biochim. Biophys. Acta.* 179 1969, 517–520.

- [214] S. Nishimura, Minor Components in Transfer RNA: Their Characterization, Location and Function, *Prog. Nucleic Acid Res. Mol. Biol.* 12 1972, 49–85.
- [215] M.B. Durand, T.G. Hagervall, G.R. Bjo, H.K. Lundgren, K. Nilsson, P. Chen, Q. Qian, J. Urbonavic, Transfer RNA modification: influence on translational frameshifting and metabolism, *FEBS Lett.* 452 1999, 47–51.
- [216] V. Serebrov, K. Vassilenko, N. Kholod, H.J. Gross, L. Kisselev, Mg²⁺ binding and structural stability of mature and in vitro synthesized unmodified Escherichia coli tRNA(Phe), *Nucleic Acids Res.* 26 1998, 2723–2728.
- [217] N. Kholod, K. Vassilenko, M. Shlyapnikov, V. Ksenzenko, L. Kisselev, Preparation of active tRNA gene transcripts devoid of 3'-extended products and dimers, *Nucleic Acids Res.* 26 1998, 2500–2501.
- [218] N. Kholod, N. Pan'kova, V. Ksenzenko, L. Kisselev, Aminoacylation of tRNA gene transcripts is strongly affected by 3'-extended and dimeric substrate RNAs, *FEBS Lett.* 426 1998, 135–139.
- [219] T. Lindahl, A. Adams, J.R. Fresco, Renaturation of transfer ribonucleic acids through site binding of magnesium., *Proc. Natl. Acad. Sci.* 55 2006, 941–948.
- [220] A. Stein, D.M. Crothers, Conformational Changes of Transfer RNA. The Role of Magnesium(II), *Biochemistry.* 15 1976, 160–168.
- [221] J.S. Loehr, E.B. Keller, Dimers of alanine transfer RNA with acceptor activity., *Proc. Natl. Acad. Sci.* 61 1968, 1115–1122.
- [222] H. Schürer, K. Lang, J. Schuster, M. Mörl, A universal method to produce in vitro transcripts with homogeneous 3' ends., *Nucleic Acids Res.* 30 2002, e56.
- [223] A. Wichlacz, M. Legiewicz, J. Ciesiolka, Generating in vitro transcripts with homogenous 3' ends using trans-acting antigenomic delta ribozyme, *Nucleic Acids Res.* 32 2004, e39.
- [224] B. Singaravelan, B.R. Roshini, M.H. Munavar, Evidence that the supE44 Mutation of Escherichia coli Is an Amber Suppressor Allele of glnX and that It Also Suppresses Ochre and Opal Nonsense Mutations, *J. Bacteriol.* 192 2010, 6039–6044.

- [225] M. Yoshimura, H. Inokuchi, H. Ozeki, Identification of transfer RNA suppressors in *Escherichia coli* I. Amber Suppressor su+2, an Anticodon Mutant of tRNA^{2Gln}, *J. Mol. Biol.* 177 2004, 627–644.
- [226] L. Bossi, Context effects: Translation of UAG codon by suppressor tRNA is affected by the sequence following UAG in the message, *J. Mol. Biol.* 164 1983, 73–87.
- [227] L. Bossi, J.R. Roth, The influence of codon context on genetic code translation, *Nature.* 286 1980, 123–127.
- [228] I.A. Nazarenko, K.M. Harrington, O.C. Uhlenbeck, Many of the conserved nucleotides of tRNA(Phe) are not essential for ternary complex formation and peptide elongation., *EMBO J.* 13 1994, 2464–71.
- [229] T. Samuelsson, T. Boren, T.I. Johansen, F. Lustig, Properties of a transfer RNA lacking modified nucleosides, *J. Biol. Chem.* 263 1988, 13692–13699.
- [230] K. Virumäe, U. Saarma, J. Horowitz, J. Remme, Functional importance of the 3' - terminal adenosine of tRNA in ribosomal translation, *J. Biol. Chem.* 277 2002, 24128–24134.
- [231] C. Claesson, T. Samuelsson, F. Lustig, T. Borén, Codon reading properties of an unmodified transfer RNA, *FEBS Lett.* 273 1990, 173–176.
- [232] S. Yokoyama, S. Nishimura, *Modified Nucleosides and Codon Recognition*, American Society for Microbiology, Washington, DC 20005, 1995.
- [233] P.F. Agris, Decoding the genome: A modified view, *Nucleic Acids Res.* 32 2004, 223–238.
- [234] P.F. Agris, F.A.P. Vendeix, W.D. Graham, tRNA's Wobble Decoding of the Genome: 40 Years of Modification, *J. Mol. Biol.* 366 2007, 1–13.
- [235] M.F. Tuite, tRNA in Decoding and the Wobble Hypothesis, *ELS. John Wiley Sons, Ltd Chichester.* 2001, 1–7.
- [236] H. Tükenmez, H. Xu, A. Esberg, A.S. Byström, The role of wobble uridine modifications in +1 translational frameshifting in eukaryotes, *Nucleic Acids Res.* 43 2015, 9489–9499.

-
- [237] J. Urbonavičius, Q. Qian, J.M.B. Durand, T.G. Hagervall, G.R. Björk, Improvement of reading frame maintenance is a common function for several tRNA modifications, *EMBO J.* 20 2001, 4863–4873.
- [238] E.M. Phizicky, J.D. Alfonzo, Do all modifications benefit all tRNAs?, *FEBS Lett.* 584 2010, 265–271.
- [239] Y. Motorin, M. Helm, tRNA stabilization by modified nucleotides, *Biochemistry.* 49 2010, 4934–4944.
- [240] D.D. Nedialkova, S.A. Leidel, Optimization of Codon Translation Rates via tRNA Modifications Maintains Proteome Integrity, *Cell.* 161 2015, 1606–1618.
- [241] E. Vijgenboom, T. Vink, B. Kraal, L. Bosch, Mutants of the elongation factor EF-Tu, a new class of nonsense suppressors., *EMBO J.* 4 2018, 1049–1052.
- [242] J. Rudinger, R. Hillenbrandt, M. Sprinzl, R. Giegé, Antideterminants present in minihelix(Sec) hinder its recognition by prokaryotic elongation factor Tu., *EMBO J.* 15 2018, 650–657.
- [243] E.J. Murgola, N.E. Prather, F.T. Pagel, B.H. Mims, K.A. Hijazi, Missense and nonsense suppressors derived from a glycine tRNA by nucleotide insertion and deletion in vivo, *MGG Mol. Gen. Genet.* 193 1984, 76–81.
- [244] H. Grosjean, K. Nicoghosian, E. Haumont, D. Söll, R. Cedergren, Nucleotide sequences of two serine tRNAs with a GGA anticodon: the structure-function relationships in the serine family of E. coli tRNAs, *Nucleic Acids Res.* 13 1985, 5697–5706.
- [245] R.G. Panchal, S. Wang, J. Mcdermott, C.J. Link, Partial Functional Correction of Xeroderma Pigmentosum Group A Cells by Suppressor tRNA, *Hum. Gene Ther.* 10 2002, 2209–2219.
- [246] M.C. Matthies, S. Bienert, A.E. Torda, Dynamics in sequence space for RNA secondary structure design, *J. Chem. Theory Comput.* 8 2012, 3663–3670.
- [247] R. Lorenz, S.H. Bernhart, C. Höner zu Siederdisen, H. Tafer, C. Flamm, P.F. Stadler, I.L. Hofacker, ViennaRNA Package 2.0, *Algorithms Mol. Biol.* 6 2011, 1–14.

- [248] X.J. Lu, H.J. Bussemaker, W.K. Olson, DSSR: An integrated software tool for dissecting the spatial structure of RNA, *Nucleic Acids Res.* 43 2015, 1–15.
- [249] http://gestis.itrust.de/nxt/gateway.dll/gestis_de/000000.xml?f=templates&fn=default.htm&vid=gestisde:sdbdeu, 2019.
- [250] <https://www.sigmaaldrich.com/germany.html>, 2019.
- [251] <https://intronbio.com:6001/intronbioen/main/main.php>, 2019.
- [252] <https://www.thermofisher.com/de/de/home.html>, 2019.

10 SUPPLEMENTARY INFORMATION

10.1 Supplementary Figures

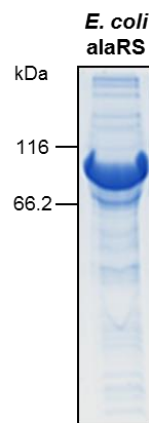


Figure S1: Purification and enrichment of His-tagged *E. coli* AlaRS. pQE30 *E. coli* AlaRS expression in BL21 cells was induced at $OD_{600nm}=0.4-0.6$ with 1 mM IPTG. His-tagged AlaRS was purified using Ni-NTA agarose. Purification and enrichment of *E. coli* AlaRS was assessed using Coomassie-stained SDS-PAA gel.

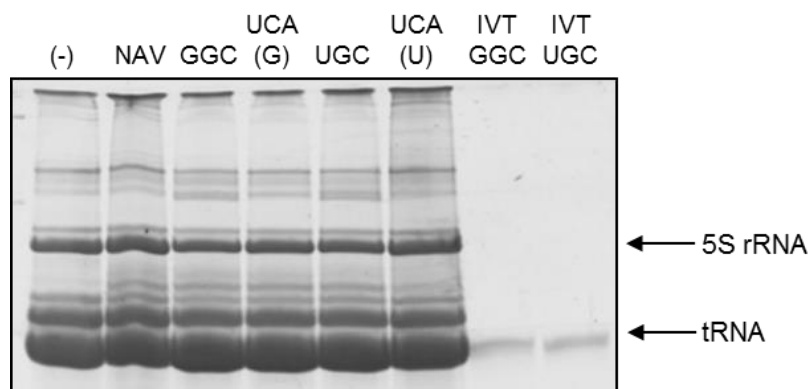


Figure S2: Representative SYBR-gold stained denaturing polyacrylamide gel electrophoresis of total RNA isolated from XL1-blue cells transformed with tRNA-encoding pBST NAV2 vectors (N=3). Expression of $tRNA^{Ala}(GGC)$, $tRNA^{Ala}(UGC)$ and their corresponding opal variants $tRNA^{Ala}(UCA(G))$ and $tRNA^{Ala}(UCA(U))$, respectively, in XL1-blue cells was monitored and compared to untransformed XL1-blue cells (-) and XL1-blue cells expressing the empty vector pBST NAV2 (NAV). *In vitro* transcribed tRNA (IVT) was used as RNA length standard.

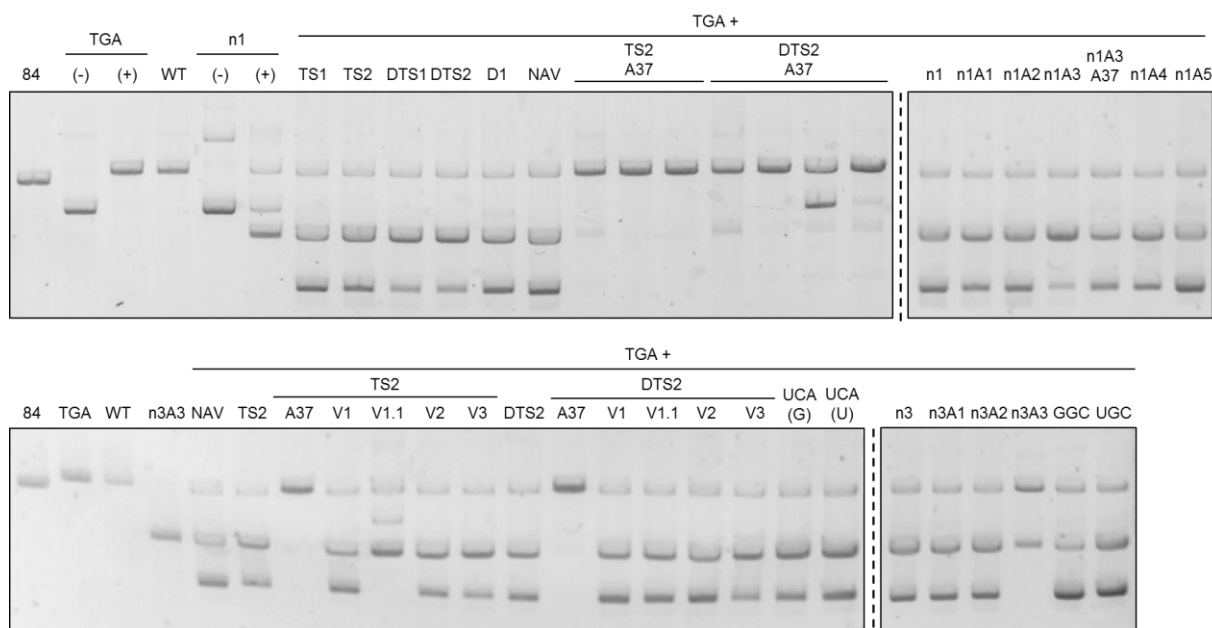


Figure S3: Co-transformation of XL1-blue cells with the eGFP opal construct (TGA) and pBST NAV2 vector coding for different tRNAs. Co-transformation was assessed by double restriction digestion with PstI and XbaI. Empty eGFP vector (84), eGFP opal (TGA) and eGFP wildtype (WT) constructs, empty pBST NAV2 vector (NAV) and XL1-blue cells expressing only tRNAs without eGFP (n1 or n3A3) were used as controls. (+) refers to double restriction digested plasmids, (-) to undigested plasmids. Co-transformed XL1-blue cells reflect the same samples as used for immunoblot.

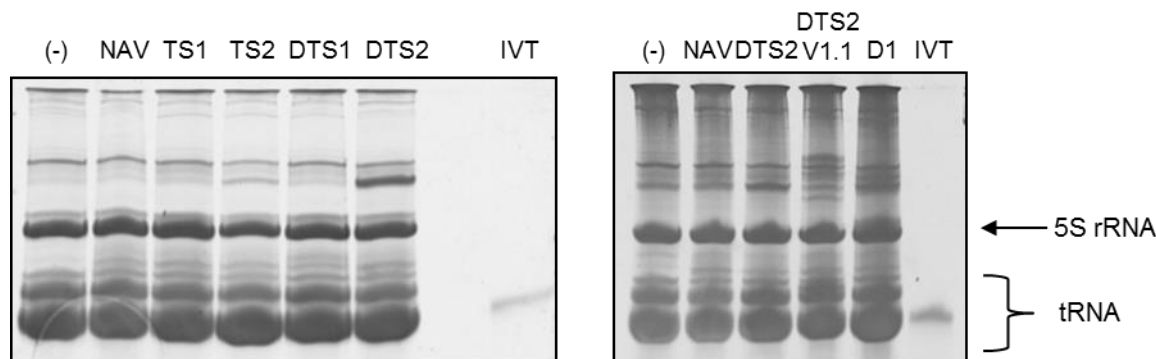




















Figure S4: Representative SYBR-gold stained denaturing polyacrylamide gel electrophoresis of total RNA isolated from XL1-blue cells transformed with tRNA-encoding pBST NAV2 vectors (N=1-3). Expression of nonsense suppressor tRNAs TS1, TS2, D1, DTS1, DTS2 in XL1-blue cells was monitored and compared to untransformed XL1-blue cells (-) and XL1-blue cells expressing the empty vector pBST NAV2 (NAV). *In vitro* transcribed tRNA (IVT) was used as RNA length standard.








10.2 List of substances used in this study

Table 20 provides an overview about the substances which were used during the preparation of this thesis. They are characterized by GHS pictograms, signal words, hazard and precautionary statements [249].




Table 20: Overview about the used substances.

Substance	Pictogram	Signal word	Hazard statements	Precautionary statements
2-[4-(2-hydroxyethyl)piperazin-1-yl]ethane-sulfonic acid (HEPES)			Not a dangerous substance according to GHS	
2-Mercaptoethanol		Danger	301+331, 310, 315, 317, 318, 373, 410	273, 280, 302+352, 304+340, 305+351+338, 308+310
Acetone		Danger	225, 319, 336	201, 305+351+338, 370+378, 403+235
Acrylamide/Bis-acrylamide [250]		Danger	302+332, 315, 317, 319, 340, 350, 361f, 372	201, 261, 280, 304+340+312, 305+351+338, 308+313
Agarose [250]			Not a dangerous substance according to GHS	
Ammonium acetate			Not a dangerous substance according to GHS	
Ammonium persulfate		Danger	272, 302, 315, 317, 319, 334, 335	220, 261, 280, 305+351+338, 342+311
Ampicillin [250]		Danger	315, 317, 319, 334, 335	261, 280, 305+351+338, 342+311
Bromophenol blue			Not a dangerous substance according to GHS	
Chloramphenicol		Warning	351	280
Chloroform		Danger	302, 331, 315, 319, 351, 361d, 336, 372	261, 281, 305+351+338, 311
Creatine phosphate			Not a dangerous substance according to GHS	
D-Glucose			Not a dangerous substance according to GHS	
Dimethyl sulfoxide			Not a dangerous substance according to GHS	

Substance	Pictogram	Signal word	Hazard statements	Precautionary statements
Dimethyl sulfate		Danger	301, 314, 317, 330, 341, 350	201, 280, 301+330+331, 302+352, 304+340, 305+351+338, 308+310
Dithiothreitol		Warning	302, 315, 319, 335	261, 305+351+338
Ethanol		Danger	225, 319	210, 240, 305+351+338, 403+233
Ethylenediamine-tetraacetic acid		Warning	319, 332, 373	280, 304+340, 312, 305+351+338, 337+313
Folinic acid [250]		Danger	315, 317, 319, 334, 335	261, 280, 305+351+338, 342+311
Formamide		Danger	315, 360D, 373	201, 314
Glycerol		Not a dangerous substance according to GHS		
Glycin [250]		Warning	315, 319, 335	261, 305+351+338
Hydrogen peroxide (30%)		Danger	302, 318	280, 305+351+338, 313
Imidazole		Danger	360D, 302, 314	201, 280, 301+330+331, 305+351+338, 308+310
Isopropyl alcohol		Danger	225, 319, 336	210, 233, 240, 305+351+338, 403+235
Isopropyl β -D-thiogalactopyranoside [250]		Warning	319, 351	281, 305+351+338
L-(+)-Arabinose [250]		Not a dangerous substance according to GHS		
LB-Agar [250]		Not a dangerous substance according to GHS		
LB-Medium [250]		Not a dangerous substance according to GHS		
Luminol		Not a dangerous substance according to GHS		
Magnesium acetate		Not a dangerous substance according to GHS		
Magnesium chloride		Not a dangerous substance according to GHS		

Substance	Pictogram	Signal word	Hazard statements	Precautionary statements
Monopotassium glutamate [250]			Not a dangerous substance according to GHS	
Nickel NTA Resin [Thermo Fisher]			Not a dangerous substance according to GHS	
N-Methylisatoic anhydride [250]		Warning	315, 319, 335	261, 305+351+338
p-Coumaric acid [250]		Warning	315, 319, 335	261, 305+351+338
PEG 8000			Not a dangerous substance according to GHS	
Phenol		Danger	301+311+331, 314, 341, 373, 411	260, 280, 301+330+331+310, 303+361+353, 304+340+310, 305+351+338
Phosphoenolpyruvate			Not a dangerous substance according to GHS	
Potassium acetate			Not a dangerous substance according to GHS	
Potassium chloride			Not a dangerous substance according to GHS	
Potassium dihydrogen phosphate			Not a dangerous substance according to GHS	
RedSafe [251]			Not a dangerous substance according to GHS	
Sodium acetate			Not a dangerous substance according to GHS	
Sodium azide		Danger	300+310, 373, 410	273, 280, 301+310+330, 302+352+310, 391, 501
Sodium chloride			Not a dangerous substance according to GHS	
Sodium dodecyl sulfate		Danger	228, 302+332, 315, 318, 335, 412	210, 261, 280, 301+312+330, 305+351+338+310, 370+378
Sodium hydrogen phosphate			Not a dangerous substance according to GHS	
Spermidine [250]		Danger	314	280, 305+351+338, 310
SYBR Gold [252]		Warning	227	210, 280, 370+378

10 SUPPLEMENTARY INFORMATION

Substance	Pictogram	Signal word	Hazard statements	Precautionary statements
Tetramethyl-ethylenediamine		Danger	225, 332, 302, 314	210, 280, 305+351+338, 310
Thiamine [250]		Not a dangerous substance according to GHS		
TRIS acetate [250]		Not a dangerous substance according to GHS		
Trisodium citrate		Not a dangerous substance according to GHS		
TRIZOL [252]		Danger	301+311+331, 314, 335, 341, 373, 412	201, 261, 264, 280, 273, 301+310, 302+352, 303+361+353, 304+340, 305+351+338
Tween 20 [250]		Not a dangerous substance according to GHS		
Urea		Not a dangerous substance according to GHS		
Xylene cyanol FF [250]		Warning	315, 319, 335	261, 305+351+338

11 ACKNOWLEDGEMENTS

Firstly, I would like to express my deep and sincere gratitude to Prof. Zoya Ignatova for the opportunity to work on this interesting project, for her trust in my abilities and her scientific guidance paired with granting me the freedom to allow pursuing my own thoughts throughout this thesis.

I am very thankful to Marco Matthies and Prof. Andrew Torda for the great scientific collaboration and their work on the bioinformatics side of this project.

For reviewing my thesis I am very grateful to Prof. Mario Mörl.

Furthermore, I would like to express my thanks to all former and present members of the working group. Each and every one supported me in their own way. Special thanks to all of my office members and the great technicians Ingrid Goebel and Christine Polte without whom the lab would have fallen into chaos. I would like to especially thank Ingrid Goebel, Dr. Max Anders and Dr. Robert Rauscher with whom I had the joy with to spend most of my time as a PhD and share great memories. I would like to thank Dr. Andreas Czech for his scientific support and experimental help. In addition, I would like to thank all of the students who supported me during this project.

Finally, I would like to express gratitude to my family and friends for their support during the whole time and for accepting every decision I made.

12 EIDESSTATTLICHE VERSICHERUNG

Hiermit erkläre ich an Eides statt, die vorliegende Dissertation selbst verfasst und keine anderen als die angegebenen Hilfsmittel benutzt zu haben sowie diese Arbeit nicht zuvor an anderer Stelle eingereicht zu haben.

Hamburg, den

Suki Albers